UNIVERSIDADE FEDERAL DE SÃO CARLOS
CENTRO DE CIÊNCIAS EXATAS E DE TECNOLOGIA
DEPARTAMENTO DE QUÍMICA
PROGRAMA DE PÓS-GRADUAÇÃO EM QUÍMICA

NITROGEN AND PHOSPHORUS NANOCOMPOSITE FERTILIZERS: SYNTHESIS, PARTICLE SIZE AND MATRIX EFFECTS

Amanda Soares Giroto*

Thesis presented as part of the requirements to obtain the title of DOCTOR IN SCIENCES, concentration area: PHYSICAL-CHEMISTRY.

Advisor: Caue Ribeiro de Oliveira

***scholarship: FAPESP**
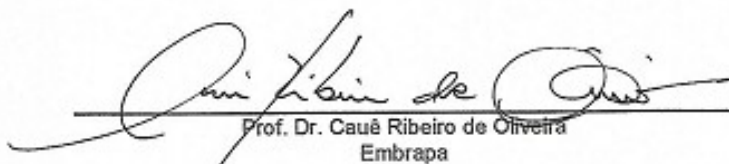
São Carlos - SP
2018

UNIVERSIDADE FEDERAL DE SÃO CARLOS

Centro de Ciências Exatas e de Tecnologia
Programa de Pós-Graduação em Química
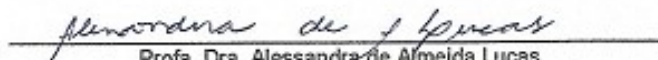
Folha de Aprovação

Assinaturas dos membros da comissão examinadora que avaliou e aprovou a Defesa de Tese de Doutorado da candidata Amanda Soares Giroto, realizada em 26/02/2018:

Prof. Dr. Cauê Ribeiro de Oliveira
Embrapa

Profa. Dra. Ana Rita de Araujo Nogueira
Embrapa

Prof. Dr. Alberto Carlos de Campos Bernardi
Embrapa

Prof. Dr. Vinicius de Melo Benites
Embrapa

Profa. Dra. Alessandra de Almeida Lucas
UFSCar

Todo conhecimento começa com o sonho. O sonho nada mais é que a aventura pelo mar desconhecido, em busca da terra sonhada. Mas sonhar é coisa que não se ensina, brota das profundezas do corpo, como a alegria brota das profundezas da terra. Como mestre só posso então lhe dizer uma coisa. Contem-me os seus sonhos para que sonhemos juntos.

Rubem Alves

Dedico este trabalho a minha família, em especial aos meus pais Jairo e Lena e ao meu irmão Vinícius, por todo amor,apoio e confiança.

Agradecimentos

Gostaria de Agradecer a Deus pela vida, saúde e garra por conseguir chegar até aqui.

Ao Dr. Caue Ribeiro, pela orientação, confiança, amizade e por ser tão atencioso com seus alunos. Sempre digo que quando crescer quero ser como ele.

Ao Dr. Gelton Guimarães pelo suporte, parceria frutífera e amizade.

Aos Prof. Dr. Vinicius Benites, Ana Rita Nogueira, Alberto Bernardi e Alessandra Lucas pelas contribuições e questionamentos durante a minha Defesa.

Ao Prof. Dr. Luiz Conalgo pela parceria incrível no finalzinho do doutorado.

Ao Dr. Gregory Glenn, por ter me recebido com tanto carinho em seu laboratório, durante meu doutorado sanduíche. Assim como o Dr. Artur Klamczynski que teve a maior paciência em me entender e me ensinar. A Dra. Delilah Wood por ter me acolhido em sua família e a Dra. Tina Willians por todo ensinamento.

À dona Pamela e ao Uncle por terem sido minha família em Albany-CA. E aos meus amigos Lorenzo, Francisco, Ramon, Ana, Parham, Maurício e em especial à Rosiane por ter feitos meus dias nos Estados Unidos muito mais felizes.

Ao amigos da sala 89 em especial às amigas Adriana de Campos, Ana Carolina Corrêa por todos os cafezinhos e conversas, obrigada meninas por alegrarem meus dias.

Ao Prof. Dr. Francys, Dra. Elaine Pereira e Suzane Fidélis pela amizade sincera.

A todos do meu grupo de pesquisa, em especial ao Fernando, Osmando, Juliana, Kele, Vagner, Luiz, Paulo, Gelson, Adriel, Vinícius, Fábio, Stella, Marcela, Flávio e Jéssica por tornar o ambiente de trabalho sempre agradável e produtível, acima de tudo pelo companheirismo e amizade.

À Embrapa Instrumentação pela excelente estrutura fornecida para realização deste trabalho. Um agradecimento especial ao pessoal de suporte à pesquisa, Viviane, Adriana, Silviane, Mattêo, Paulinho, Joana, Edilson e Suzane.

Ao Programa de Pós-Graduação em Química da Universidade Federal de São Carlos (PPGQ-UFSCar), pela oportunidade que me foi dada para realizar o doutorado. Às secretárias em especial Cristina e Ariane por toda paciência em nos ajudar sempre.

À FAPESP (Projeto N° 13/11821-5) pela bolsa concedida, pela excelência em todos os quesitos, e por todas as oportunidades que foram possíveis graças ao suporte financeiro.

Aos meus pais, Jairo e Lena, por todo amor, dedicação, luta diária para fazer de mim a pessoa que sou, amo vocês infinitamente. Ao meu irmão, Vi, pelo amor, ciuminho, e por ter se tornado esse homem que eu tanto admiro. À tia Solinda por ter sido minha fonte de inspiração, obrigada por me escutar tantas vezes. Ao meu namorado, André, por ser meu melhor amigo, pela paciência, pela orientação e suporte em todas as horas difíceis.

Sem vocês nada disso seria possível. A todos os outros amigos e familiares que me apoiaram durante toda esta caminhada.

Table List

Figure List

Resumo

Com as altas produtividades agrícolas, há a necessidade da fertilização química do solo, e o nitrogênio e o fósforo estão entre os macronutrientes primários indispensáveis para as plantas. Neste sentido, a demanda atual de uso de fertilizantes obriga que métodos mais racionais de uso destes compostos sejam desenvolvidos, buscando estratégias para aumentar e controlar a solubilidade das fontes utilizadas, além de evitar processos de imobilização, coalescência ou aglomeração, que comprometeriam a disponibilidade durante o processo de aplicação. Portanto, a proposta central deste trabalho foi estudar como a diminuição do tamanho de partículas fosfáticas através da dispersão do seus aglomerados influenciariam na sua cinética de solubilização. Para tanto iniciou-se o trabalho investigando diferentes materiais que poderiam agir como matriz dispersora. Uma das características principais desse trabalho foi trabalhar com matrizes dispersoras que também seriam fonte de nutriente, no caso, nitrogênio. Assim, estudou-se a preparação da matriz ureia:ureia-formaldeído pelo método simples de mistura e fusão dos materiais em fase sólida. De forma a obter materiais com diferentes graus de polimerização da ureia, diferentemente do observado pela literatura, onde só encontram a produção de uma matriz rígida (totalmente polimerizada) de ureia-formaldeído em fase líquida. A partir dos resultados de solubilização em água e até mesmo pelos ensaios de incubação em solo, verificou-se que o grau de polimerização da ureia influenciou fortemente a sua disponibilização em ambos os meios. Uma vez que a ligação entre a ureia e o formaldeído é uma ligação forte, procurou-se outro material para interagir com a ureia, mas fraca que a primeira. Assim, o amido surgiu como um excelente candidato para formação da matriz. Porém, quando se utiliza dessa fonte os teores de N final ficam muito baixo quando se pensa em fertilizante. Com intuito de aumentar o teor final de N na matriz adicionou-se a melamina na estrutura, uma vez que as reações de ureia-melamina já são muito conhecidas na literatura, porém juntamente ao amido, ainda é um material pouco estudado para uso como fertilizante. Interessantemente a melamina mudou a morfologia dos compósitos de TPSUr (amido termoplástico:ureia) deixando-os mais homogêneos e rígidos. E ainda, pelos estudos em casa de vegetação, observou-se que a melamina não teve papel nutricional no período do experimento, porém modificou fortemente a cinética de disponibilização da ureia de forma a ser mais eficiente comparado à ureia pura. Estudada as possíveis matrizes, deu-se inciou ao estudo da

dispersão das partículas fosfáticas em duas diferentes matrizes, recorrendo-se às matrizes mais simples para os primeiros ensaios. Assim a ureia pura e o amido termoplástico:ureia foram utilizados como as duas fontes dispersoras. Os resultados demonstraram que o método de dispersão foi eficiente para manter as partículas na escala nano tendo consequentemente uma maior solubilização em meio aquoso. Nesses ensaios, verificou-se também que a morfologia dos compósitos foi a característica principal para a melhor disponibilização de ambos os nutrientes. Realizou-se ainda os experimentos em solo e partir desses ensaios observou-se que a hidrólise da ureia, modificou o pH local dos compósitos desfavorecendo a complexação do fósforo solúvel e consequentemente deixando-o mais disponível no solo em comparação à fonte de fosfato comercial.

Palavras-chave: Fertilizantes, Nitrogênio, Fósforo, Compósitos, Nanopartículas, Solo.

Abstract

With high agricultural productivity, is necessary a chemical fertilization of soil, and nitrogen and phosphorus are the macronutrients indispensable for plants. In this sense, the current demand for fertilizer requires that more rational methods of using these compounds be developed, seeking strategies to increase and control the solubility of the sources used, as well as avoiding immobilization, coalescence or agglomeration processes, which would compromise availability during the application process. Therefore, the central proposal of this work was to study how the decrease of the size of phosphate particles through the dispersion of their agglomerates would influence their solubilization kinetics. For this, the work was started investigating different materials that could act as dispersing matrix. One of the main characteristics of this work was to work with dispersing matrices that would also be a source of nutrient, in this case, nitrogen. Thus, the preparation of the urea: urea-formaldehyde matrix was studied by the simple method of mixing and melting the solid phase materials. In order to obtain materials with different degrees of polymerization of urea, unlike the literature, where only the production of a rigid (fully polymerized) matrix of urea-formaldehyde in the liquid phase was found. From the results of solubilization in water and even by the incubation tests in the soil, it was verified that the degree of polymerization of the urea strongly influenced its availability in both media. Since the bond between urea and formaldehyde is a strong bond, another material is sought to interact with urea but is poorer than the former. Thus, starch has emerged as an excellent candidate for matrix formation. However, when using this source the final N contents are very low when one thinks of fertilizer. In order to increase the final N content in the matrix melamine was added in the structure since the reactions of urea-melamine are already well known in the literature, but together with the starch, it is still a material little studied for use as fertilizer. Interestingly, melamine changed the morphology of TPSUr (thermoplastic starch: urea) composites, making them more homogeneous and rigid. Also, by greenhouse studies, it was observed that melamine had no nutritional role during the experiment period, but strongly modified the kinetics of urea availability in order to be more efficient than pure urea. Studying the possible matrices, it was begun the study of the dispersion of the phosphate particles in two different matrices, using the simplest matrices for the first tests. Thus pure urea and thermoplastic starch: urea were used as

the two dispersing sources. The results demonstrated that the dispersion method was efficient to maintain the particles at the nanoscale consequently having a higher solubilization in the aqueous medium. In these tests, it was also verified that the morphology of the composites was the main characteristic for the better availability of both nutrients. And to close the work, soil experiments were carried out. From these results it was observed that the hydrolysis of the structural urea, modified the local pH of the composites, disfavoring the complexation of the soluble phosphorus in leaving it more available in the soil compared to the commercial source.

Keywords: Fertilizers, Nitrogen, Phosphorus, Composites, Nanoparticles, Soil.

Summary

1. Introduction

1.1 Motivation

The growth of the world population implies in the increasing search for a highly productive agriculture.[1] Technological advances due to agronomic research have resulted in an increase in agricultural production, mainly due to the development of new sources of fertilizers which, in this way, also contribute to avoiding the deforestation of new areas for food production.[2-5] In Brazil, between 1970 and 2001 there was a 3.5 fold increase of the 16 main agricultural sources, while the use of fertilizers grew 4.4 times and the cultivated area grew only 1.5 times. Therefore, the productivity increase per planted hectare is directly linked to the gain in soil fertilization.[6] In 2010, more than 24.5 million tons of fertilizers were traded in Brazil.[7] Although national fertilizer production grows at an annual rate of more than 8.5%, local capacity is not enough to supply domestic consumption, and imports of approximately 90% of potassium (K), 70% of nitrogen (N) and 50% of the phosphorus (P) used in the fertilization of Brazilian lands.[7,8] Among the three main primary macronutrients (nitrogen, phosphorus, and potassium), phosphorus is the least required (in mass) by plants but whose most limits production and one of the most used in fertilizers in Brazil. This situation results from the generalized lack of phosphorus in the soils of tropical regions, and especially from its strong interaction with the soil, especially in clayey soils or with high concentrations of Fe or Al, which leads to its immobilization and, therefore, unavailability.

Phosphate fertilizers are produced by the chemical processing of phosphate rock, and most of the national phosphate rocks are of low reactivity and present high levels of iron and aluminum in their constitution, which provides low availability of phosphorus to crops if applied directly. In this way, soluble phosphate fertilizers have been used mainly in agricultural crops.[9,10] The main characteristic of these fertilizers is the high solubility in water, however, it presents economic and industrial limitations that involve high energy consumption, high sulfuric acid expenditure and generation of high amount of waste.[11,12] Therefore, the production process of soluble phosphate fertilizers increases their cost, a fact that has induced researchers to study alternative sources for phosphorus supplementation.[13]

Alternative sources are understood to be those with less relative solubility in water and can be exemplified by heat treatment, partial acidification, addition of organic materials to the phosphate sources, or even the use of

microorganisms, in order to increase the solubility of the materials, resulting in higher relative agronomic efficiency and, in most cases, lower costs since it excludes the need to import raw material and formation of industrial waste involved in all the stages of production of this type of source of phosphorus.[10] In recent years, the use of phosphate rock as the main source of supplementation has increased markedly, however, these products have very low solubility in water when compared to all commercial sources of soluble phosphate.[14] However, phosphate rock use in the tropical regions has to be considered.

In this context, nitrogen, the most required macronutrient and consequently applied in larger quantity in the management of the soil in several crops is also observed. Nitrogen fertilizers, especially urea, the main source of nitrogen used worldwide, are characterized as solid granulated fertilizer with concentration around 44 and 46% of nitrogen in the amide form.[15] Besides the high concentration of N, urea has other advantages such as lower manufacturing cost, transport, storage, application, low corrosivity and ease of mixing with other sources. However, as disadvantages, urea is highly susceptible to losses due to its high solubility in water, being lost to the environment by leaching or surface runoff, or by gaseous emissions of ammonia, nitric oxide, and nitrous oxide.[16,17] According to Martha Júnior et. al. (2004),[18] these losses can reach up to 50% of the applied N. Thus, in recent years, the industry has also turned to the production of alternative sources of urea, which are less prone to losses. Some technologies that may contribute to the more efficient use of this fertilizer, and consequently as solutions to the problems mentioned, are the use of slow or controlled release systems, the use of urease inhibitors and nitrification inhibitors, the coating of urea granules with polymer materials, the dispersion of urea in expansive clays and even the partial polymerization of urea.[19-23]

1.2 Solubility and Particle Size

An alternative to increasing the solubility of mineral phosphates or any source of low solubility is by reducing the size of their particles through top-down method or controlled precipitation of the same phases in nanometric sizes (bottom-up method), thereby increasing the contact surface of the substrate with the aqueous solution. The solubility of the particles in the medium is related to their size *(d)* according to the equation of Ostwald-Freundlich:[24]

$$S = S_o \cdot \exp \left(4 \cdot \gamma_{SL} \cdot V_m / RTd \right) \text{ (Equation 1.1)}$$

where S_o is the solubility of the flat surface (minimum energy condition), γ_{SL} is the solid-liquid interfacial energy, V_m is the molar volume of the solid phase, R is the gas constant and T is the temperature. From the analysis of the equation and graph presented in FIGURE 1.1 it is observed that when the term ($4.\gamma_{SL}.V_m/RTd$) tends to zero, the solubility of the particle tends to that of the flat surface, and the particle has minimal solubility. This condition is verified for large particles, where the solubility varies little with the size; conversely, when the term exponential is greater than 1 ($d < 4.\gamma_{SL}.V_m/RT$) the solubility of the particle increases and it tends to dissolve. Since the behavior of the equation is exponential, small variations in particle size may lead to significant increases in solubility.
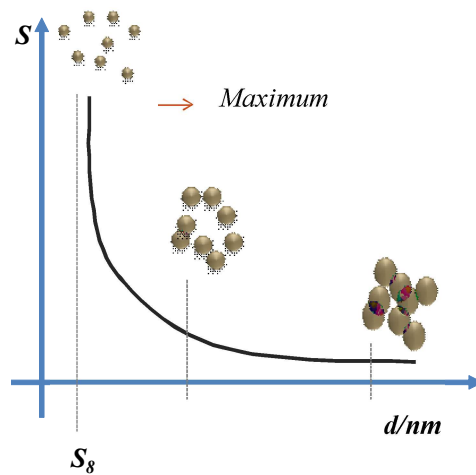
FIGURE 1.1.Graph representing the increase in solubility in water of particles according to the decrease its particles size.

Klaic et. al. (2017)[25] studied a novel combined mechanical-biological approach to synthesize soluble phosphate from rock phosphate (RP) reactive (Bayóvar) having found that RP particle size was a played a key role in phosphate solubilization, with gains of up to 115% for solid-state fermentation. However, in previous experiments in the research group, Plotegher and Ribeiro (2016)[26] showed that short milling times favored the solubilization kinetics, whereas long milling times were deleterious due to agglomeration effects. It was pointed out that agglomeration plays an important role in phosphate availability.

A solution to prevent re-agglomeration of such particles is through their dispersion insoluble matrices so as to avoid agglomeration of the nanoparticles after a certain period of time and yet with the advantage of providing greater control of

solubility due to the gradual exposure of the particles to the medium according to the solubilization of the matrix, as may be exemplified in FIGURE 1.2.
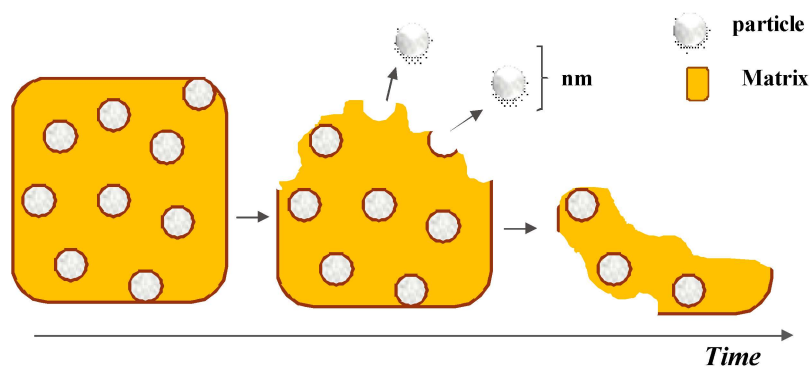
FIGURE 1.2.Demonstration of the gradual release of nanoparticles due to dispersion in a matrix.

On a different approach, Pereira et. al. (2012)[19] produced nanocomposites based on the urea dispersion in montmorillonite clay matrices and verified that the clay acted as a physical barrier within the soluble material and was able to modify significantly its difusional behavior observed by the slow release of urea into water. The authors also concluded that the controlled release of urea from the nanocomposites decreased NH_3 volatilization, resulting in a more homogeneous N availability in the soil and better synchronization with the nutritional demands of the plants. The kind of strategy can offer a practical option for increasing urea-N efficiency, reducing environmental impacts caused by NH_3 loss, and at the same time increases the availability of phosphorus improving the quality of fertilization of both nutrient on low fertility soils such as found in tropical soils. [27]

1.3 Controlling solubility: Nanocomposites

Composite materials are all those in which two distinct materials cooperate in a hybrid structure and the combination of these two component into a hybrid structure gives rise to multifunctional properties due to synergistic effects, arising from particle-particle interactions.[28] Composites are basically composed of a continuous phase (matrix) and a dispersed phase, continuous or not. When the dispersed phase has at least one nanometer size dimension, they are called nanocomposites.[29]

In this work on phosphate particles, the matrices for the formation of nanocomposites must necessarily be compatible with the surface of the nanoparticles -

hence hydrophilic - and it is desirable that they can be continuously processed, for example by extrusion.

Urea presents as an excellent candidate the matrix not only for its nutritional character (source of N)[30] but also for its hydrolysis, which upon release ions to the medium that can inhibit the complexion action of soil colloids. This matrix can be processed by extrusion at low temperatures, and the incorporation of hydrophilic materials such as exfoliated clay at the nanoscale has already been shown to be simple and scalable, as recently seen in a study on the urea/montmorillonite system. Pereira et. al. (2012)[19] verified that the high solubility of urea was controlled by the presence of the exfoliated material, so that nanocomposites urea/nanoscale phosphates could be an interesting strategy for the integrated delivery of two macronutrients.

Another candidate to dispersion the phosphates particles is starch, a polymer derived from agronomic-sources and found naturally in form of granules. In this condition, the starch does not have thermoplastic characteristics.[31] In order to acquire this latter characteristic, is necessary the granular disintegration with consequent formation of a continuous phase due to a combination of mechanical, thermal energy and a plasticizer (water, glycerol, urea, etc.).[32-35] Thereby, the starch becomes known as thermoplastic starch (TPS). TPS are materials that have been extensively studied because they are of renewable, biodegradable, abundant and low-cost sources.[31,36-38]

One good example of starch used as a matrix is observed in Rychter et. al. (2016)[23] where the authors successfully extruded starch-based films plasticizer by urea and used the final material as a fertilizer. Plant growth assessment, including determination of such parameters as fresh and dry matter of plants and their visual evaluation, has proved the stimulating effect of using extruded films on the growth and development of cultivated plants. But the drawback about this material was the low N content into the matrix, around 4.5%, in comparison to the commercial urea (45% of N).

2. Goals and Overview

The hypothesis tested in this thesis was the effect of chemical modifications in polymeric structures (N-source fertilizers), aimed to be used as dispersing matrices for fertilizer nanocomposites, and after analyze the effect of other nutrient source (in nanometric scale) in the total nutrient dynamics (N and P).

The current stage of fertilizer chemistry is based in simple molecules such as urea and NH_4NO_3, providing high N content per gram, but these materials can suffer from volatilization and lixiviation in soil. Tailoring large molecules may reduce these problems by increasing their long-term stability in soil, but at the same time, reducing the total nutrient content. Therefore, the challenge is to identify how to obtain optimum conditions regarding losses and concentration, which may also be balanced by the introduction of other nutrients in the composition – whose could be included as dispersed nanoparticles into the polymeric composition. At the same time, the literature does not provide a consensus about the effect (benefic or not) of reduced particle sizes in fertilizer efficiency. Finally, these fertilizers should be processed as granules for easy application in soil, which is a technical limitation.

Therefore, general goal was to test if the matrix produced by fertilizer precursors, with different polymerization form/degrees (i.e., with high N contents) may be efficient to disperse nanoparticles of a mineral fertilizer to create a nanocomposite structure (i.e., hydroxyapatite, assumed here as a model of different P mineral sources), showing efficiency gains in N and P availability, simultaneously.

Specific goals:

- To test matrices alternatives for a future dispersion of phosphate phase particles;
- To test matrix with higher content of nutrient (N) and with a intermediate solubility in water;
- To test the effect of the mineral phase dispersion on their particle size and solubility;
- To evaluate nanocomposites efficiency in more real conditions: study the dynamic of the soil in presence of nanocomposites.

Summary of each chapter

The main idea of this thesis was to explore the production nanocomposites based on dispersion of phosphate particle in different matrices. For this purpose, new classes of low solubility nitrogen matrices based on melamine, starch intercalated urea/melamine (TPSUr-Mel), and urea-formaldehyde (UF) were developed. Thus, **Chapter I** describes the preparation and characterization of the urea-formaldehyde matrix, which, in addition to the low solubility, is also a N source in contents closely to urea. In this Chapter we verified how the degree of urea polymerization directly influences the solubilization dynamics of the material in aqueous and soil media.

Following these studies, we have proposed to study the correlation in weakly-bonded polymer blends, as the observed in TPSUr (thermoplastic starch plasticized with urea) with melamine - this compound presents 66% N in its constitution but is little studied as fertilizer, despite widely used in other industrial processes. In this way, **Chapter II** presents and describes the preparation of this new matrix based on the interaction of urea + melamine with thermoplastic starch. This chapter also describes the characterization of materials and discussions of the real role of melamine in the formation of composites, as well as the behavior of these materials in soil incubation studies and greenhouse experiments for maize cultivation. From this range of possible matrices for the dispersion of the phosphate particles, the study of multi-nutrient nanocomposites is depicted in **Chapter III**, which describes the process of isolation of nanometer-sized phosphate particles in different matrices with various solubilities and how this dispersion effectively increases the dissolution of mineral sources (hydroxyapatite - Hap), according to the central hypothesis of this work. In this step, pure urea was used as the matrix of high solubility and the thermoplastic starch: urea (TPSUr) as intermediate solubility in relation to the first, as the simpler matrices for the initial tests. Thus, throughout the chapter the role of the matrices in the availability of phosphate in the aqueous medium is described.

Finally **Chapter IV** presents the incubation studies in soils, using the composites produced in the previous chapter, and how the interaction resulting from dispersion of Hap within the urea matrix reduced the phosphorus adsorption and provided higher sustained P availability after incubation in the soil.

3. - Chapter I: Seeking for Adequate Polymeric Fertilizers for Nanocomposites

The content of this chapter is an adaptation of the manuscript entitled **"A Novel, Simple route to produce Urea:Urea-Formaldehyde Composites for Controlled Release of Fertilizers"** by A. S. Giroto, Gelton G. F. Guimarães and Caue Ribeiro, published in Journal of Polymers and the Environment.

Reference: J. Polym. Environ., 2017, DOI 10.1007/s10924-017-1141-z.

ORIGINAL PAPER

CrossMark

A Novel, Simple Route to Produce Urea:Urea–Formaldehyde Composites for Controlled Release of Fertilizers

A. S. Giroto[1,2] · G. G. F. Guimarães[2] · C. Ribeiro[2]

3.1 Abstract

Nitrogen loss through NH_3 volatilization is a primary concern for urea as fertilizer due its fast hydrolysis by soil urease. To minimize this problem herein we developed a partially-polymerized urea-formaldehyde granule as a slow-release fertilizer, by melt stage process as a viable route for large-scale production. In this product the unreacted urea fraction acts as a fast release nutrient source while the polymerized fraction acts in longer times depending on the polymerization degree. This characteristic was analyzed by means of soil incubation experiments (up to 42 days), where the available NH_4^+ contents along time indicated significant lower N losses compared to conventional fertilizer, even for low-polymerized materials. Residual N in the structure was kept stored in the soil for future use by plants, as desired in many agricultural practices, showing that this simple polymerization method provides a smart fertilizer controlled by chemical structure.

3.2 Introduction

Urea is one of the main sources of N used due to its high concentration (46% N) that allows concentrated formulations at lower costs compared to other sources.[39] However, this fertilizer shows less efficiency than other nitrogen sources for a large number of crops in different soils and climates, due to different causes, such as NO_3^- leaching, NH_3 volatilization, and its toxic effect on the plants at the beginning of the vegetative period.[40-42] These factors not only contribute to reducing the efficiency of urea, biomass production, and economic cultivation but also are an important source of environmental pollution.

One of the alternatives to reduce these losses is to reduce urea hydrophilicity, allowing its application as slow release fertilizers. In this scenario, urea formaldehyde (UF) was the first synthetic nitrogen fertilizer produced with low solubility and it belongs to the first group of materials specially developed on a commercial scale for the slow release of nitrogen.[43-45] Studies have verified that N-release from an organic polymer occurs in stages similar to those adopted for urea in agriculture.[46-48] However, most of the research into this polymer synthesis reports the production in the liquid phase, as seen by many patents.[49-53] This process is difficult to control, generally leading to fast polymerization with poor processability. Besides that, the literature does not show strategies for partial polymerization, i.e., all the available products are based on fully-polymerized systems. Therefore, the nutrient release is often

too long for practical application, meaning that the nutrient is available for longer periods than the requested by a plant growth. This fact explains why urea-formaldehyde polymers are not popular as controlled release fertilizers, despite their higher N content compared to other commercial products. In recent research from our group, we proposed a novel nanocomposite material based on the exfoliation of montmorillonite into the matrix of a urea/urea-formaldehyde polymer.[44] A remarkable aspect of this process was the use of a formaldehyde solid precursor instead of the most common formaldehyde solution. Despite its simplicity, this method was limited as to the maximum amount of urea in composition (around 80%), and by the need of partial urea solubilization for a plastic mixture. Considering the basic strategy, herein we propose to investigate the polymerization in the urea melt stage, by also using the formaldehyde precursor previously mixed as powders. The results showed that by this simple method it is possible to obtain dense urea: urea-formaldehyde composites, and with very high N contents (comparable to commercial products), and with nutrient release easily controlled by the composition.

3.3   *Experimental*

Raw materials - used in composite formulations were urea (Synth) and paraformaldehyde (Sigma-Aldrich) with molecular formula showed in FIGURE 3.1. The urea was previously milled to 300 mm in a TE-330 hammer mill (Tecnal, Brazil).
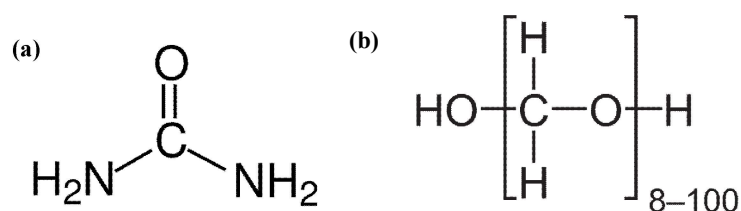
FIGURE 3.1. Molecular structure of urea (a) and (b) paraformaldehyde.

Preparation of Materials - Composites were prepared with different molar ratios of urea and paraformaldehyde (Ur/Pf) as 1:1, 1:0.5 and 0.5:1, respectively. The urea-formaldehyde polymer was formed by reaction of formaldehyde with an excess of urea. In the first stage, urea is hydroxymethylated by the addition of formaldehyde to the amino groups. This reaction actually is a series of reactions that lead to the formation of mono-, di-, and trimethylolureas. The second stage of urea-formaldehyde resin synthesis consists of condensation of the methylolureas to low

molecular weight polymers. The exact ratio, of course, is dependent on the reaction conditions employed in the addition reaction.[44] Paraformaldehyde is a formaldehyde polymer with a polymerization degree between 8 and 100. This polymer de-polymerizes in water and heat.[54] Thus, the use of paraformaldehyde allows control of the urea solubility inside the composite by the extension of the polymerization reaction. The precursor materials (urea and paraformaldehyde) and water (9 wt.%) were pre-homogenized and mixed-melted using a torque rheometer (Polylab RHEODRIVE Rheomix mixer and OS4) under the conditions of 60 rpm for 10 min at 90°C. After mixing, the samples were cured at 80°C in an oven for 12 h and subsequently stored at 90°C until completely dry. The nomenclature given to each composition and the elementary composition is presented in TABLE 3.1.

TABLE 3.1.Nomenclatures of composites, molar ratio, and their total nitrogen %.The raw materials used are indentified by initial Ur for urea and Pf for paraformaldehyde.

Nomenclature	Molar ratio (Ur/Pf)	Total Nitrogen (%)
Urea	-	46.89
Ur/Pf 1:0.5	1:0.5	41.29
Ur/Pf 1:1	1:1	40.33
Ur/Pf 0.5:1	0.5:1	28.21

Characterizations - The materials were initially characterized by scanning electron microscopy (SEM) using a JSM6510 microscope (JEOL). Samples were previously fixed onto carbon tapes and coated with thin layer of gold in an ionization chamber (BALTEC Med. 020).

The imaging by SEM was carried out using the secondary electron mode. The optical image from paraformaldehyde was done using an optical microscopyL2800 Biological Microscope (BEL Photonics, Brazil).

X-ray diffractograms (XRD) were obtained using an XRD 6000 diffractrometer (Shimadzu). The relativeintensity of diffraction was registered in the angular range (2Θ) of 3–40°, using a Cu Ka incident beam (k = 0.1546 nm) and scanning speed of 1° min^{-1} at 30 kV voltage and 30 mA current.

Thermal degradation of samples was evaluated in the 25°C - 600°C range using a Q500 analyzer (TA Instruments, New Castle, DE, USA) under the following conditions: sample size 10.0 ± 0.5 mg, synthetic air atmosphere (80% N_2and20% O_2) with 60 mL min^{-1} flow, heating rate of 10°C min^{-1}.

For differential scanning calorimeter (DSC), samples were heated from 25 to 300°C under a nitrogen flow of 60.0 ml min^{-1}in a DSC Q100 (TA Instruments, USA). The linear heating rate used in both analyses was 10°C min^{-1}.

^{13}C solid-state nuclear magnetic resonance (NMR) measurements were performed on a Bruker (Karlsruhe, Germany) 400 MHz to^{1}H (9.4T) spectrometer using ^{13}C cross polarization magic angle spinning (CPMAS) technique in a 4 mm broad band^{1}H/X MAS probe head. The following parameters and values were used: speed spinning of 8 kHz, 90^{1}H pulse length of 2.3 us, contact time 2 ms, spectral width 50 kHz, 20 Hz of line broadening, and a recycle delay of 3s. Hexamethylbenzene (HMB) was used as external reference standard at 17.2 ppm for methyl-carbons. All the NMR experiments were carried out with 4096 scans.

Fourier Transform Infrared (FT-IR) analyses were performed on a Bucker spectrometer using a spectral resolution of 4 cm^{-1}.

Evaluation of urea release in water - The urea release in water at 25°C and natural pH for each polymer was examined following a method adapted from Tomaszewwska and Jarosiewicz (2002).[55] The total N organic content in each composite formulation was determined by elemental analysis (Thermo Finnigan Model Flash 1112EA). These results (TABLE 3.1) were used to calculate the amount of material used in the release tests. Briefly, samples were soaked in water at 25 °C and were constantly homogenized by gentle stirring using an orbital shaker during 5 days. Pure urea was also tested as a control experiment. The urea concentration in solution was determined by UV–Vis spectrophotometry in a 1601PC spectrophotometer (Shimadzu, Japan) according to the method reported by With et. al. (1961).[56] Curves of the percentage of solubilized urea as a function of time were then obtained. The measurements were replicated three times under identical laboratory conditions for each type of composite formulation.

Release and transformation of N in soils - The release of urea from the composites was also evaluated in two Oxisols, both were collected in the surface (0-20 cm) in an area with agricultural activity in the municipality of São Carlos, Brazil. Before use, the soil samples were air-dry and crushed to pass through a 2 mm screen. The soil chemical and physical properties are reported in TABLE 3.2. The pH (H_2O) was determined with a glass electrode (soil:water ratio, 1:1); organic C by the Walkley-Black method;[57] cation-exchange capacity (CEC);[58] soil texture analysis was determined

by the pipette method;[59] water-holding capacity (WHC);[58] and urease activity using the buffer method of Tabatabai and Bremner (1972).[60]

To compare the urea release and N transformations, soil samples were incubated with urea or composites at a ratio of soil:N (1000:1 $g.g^{-1}$) placed in 125 mL polyethylene screw-cap bottles as Urea, Ur/Pf 1:1, 1:0.5 and 0.5:1. The samples were incorporated into the soils and soil moisture content was standardized at 80% WHC with the addition of deionized water. A container with 5 ml of 4% boric acid (Sigma-Aldrich) was added in the polyethylene bottles, to capture the volatilized ammonia (NH_3) during the incubation period. Samples were incubated for 0, 1, 3, 7, 14, 21 and 42 days under controlled air temperature and humidity. Analyzes were performed after each incubation period. Determinations were carried out via volatilization of boric acid by titration with HCl 0.01 mol L^{-1} (Synth) and then the soil mineral N was extracted by KCl 1 mol L^{-1} (Vetec) at the extractant:soil ratio (10:1). In order to paralyze the urease activity, 5 mg L^{-1} of phenyl mercuric acetate (Sigma-Aldrich) from the extraction stage was added to the extraction solution. The suspension remained under stirring for 1 hour and was then filtered with the use of as low filter with a diameter of 12.5 cm (Nalgon). The extract was stored in a polyethylene bottle with a volume of 100 mL at 5°C in a refrigerator.

The ammonium (NH_4^+) and nitrate (NO_3^-) levels in the extracted soil were analyzed by the colorimetric method.[61,62] The contents recovered in each N fraction were expressed as percentages referring to the N applied as urea or composites. The profile of the volatilization of ammonia (NH_3) and the formation of NH_4^+ in soil was presented by the average values accompanied by their respective standard deviations. Differences among treatments by total recovery as NH_3 volatilized and exchangeable NH_4^+ and NO_3^- after aerobic incubation were assessed by analysis of variance (ANOVA) and when the F test was significant, differences among treatments were compared by the Tukey test (P <0.05).

TABLE 3.2.Chemical and physical properties of the studied soils.

Oxisol	Red-Yellow	Red
pH (H_2O)	5.4	5.0
Organic C (g kg^{-1})	7.6	7.0
CEC^a(cmol$_c$ kg^{-1})	4.8	4.2
Sand (g kg^{-1})	667	433
Silt (g kg^{-1})	19	35
Clay (g kg^{-1})	314	532
WHC^b(g kg^{-1})	140	200
Urease activity (mg N kg^{-1} h^{-1})	9.7	7.1

[a]CEC, cation exchange capacity
[b]WHC, water-holding capacity

3.4   *Results and discussion*

In previous works urea and formaldehyde were used to synthesize UF (urea-formaldehyde) resins and the reaction was always performed in aqueous solution.[49-51] Here, in order to improve the yield and stabilization of UF resins, paraformaldehyde was used as the raw material and the reaction was performed in urea melt. This work proposes using just the mixing-melting between urea and paraformaldehyde follow by cure and drying of materials, avoiding large amounts of water in addition to acids and basic reagents used to control the reaction medium. Therefore, the data for characterization of formed polymers are presented below.
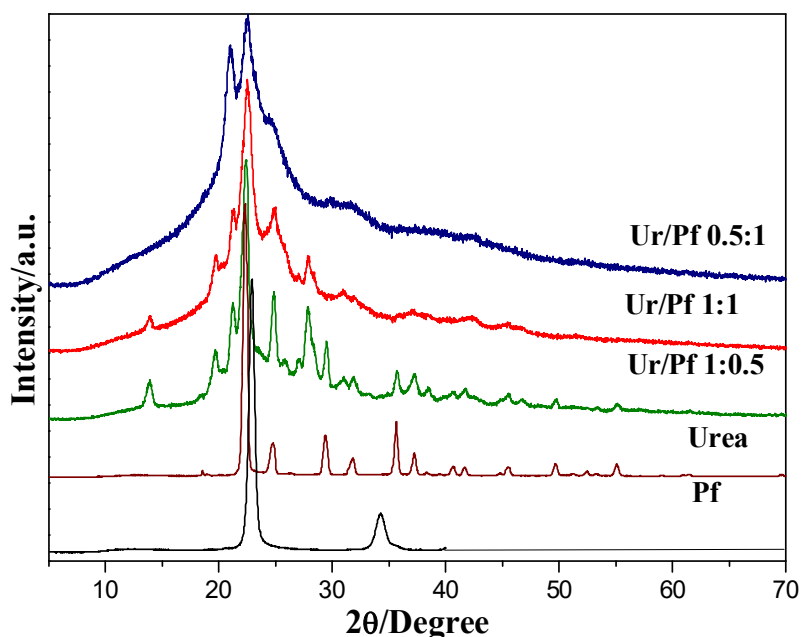
FIGURE 3.2.XRD patterns for neat urea, paraformaldehyde, and formulations of urea/paraformaldehyde at different molar ratios.

FIGURE 3.2 shows XRD patterns of the pure urea and paraformaldehyde and composites with different compositions. The pattern of neat urea and paraformaldehyde showed typical peaks at $2\theta=22.5°$, $24.7°$, $29.3°$, $31.8°$, $35.5°$, $37.3°$ and $22.9°$, $34.3°$ for the precursor materials, respectively. By the XRD patterns of samples, it was possible to verify the polymerization by a wide band in the reacted samples, which is characteristic of a semi-crystalline material. This band is proportional to the molar ratio of paraformaldehyde in mixtures, i.e., the polymerization is directly influenced by the amount of this compound, as expected. This is consistent with the findings for Roumeli et. al. (2012),[63] who observed the highest amorphous proportion in urea: formaldehyde composites at a ratio of 0.5:1 (Ur/Pf), i.e., excess formaldehyde.
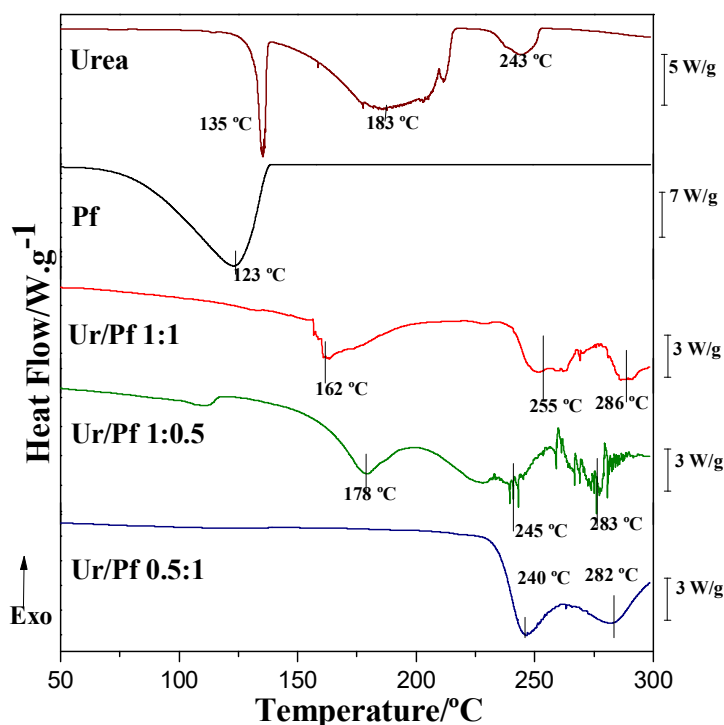
FIGURE 3.3.DSC curves for neat urea, paraformaldehyde and polymers.

DSC experiments were used to confirm the thermal behavior of the polymerization reaction among components. FIGURE 3.3 shows DSC profiles for neat components and mixtures, where the endothermic peak of paraformaldehyde at 123 ºC is absent in any of the mixtures – which is an indicator that this component was totally consumed during the polymerization step, as reported by Yamamoto et. al. (2016)[44] Regarding urea, melting at 135 °C and decomposition between 150<T<210°C are clearly seen.[64] As presented in FIGURE 3.2 for the Ur/Pf0.5:1 polymer (which is supposed to be a fully polymerized material, since paraformaldehyde is in stoichiometric excess), the shift to 246°C and 286°C is confirming the complete polymerization (probably associated with degradation steps). For the other samples, peaks suggesting to free urea degradation were still present (162°C and 178°C).
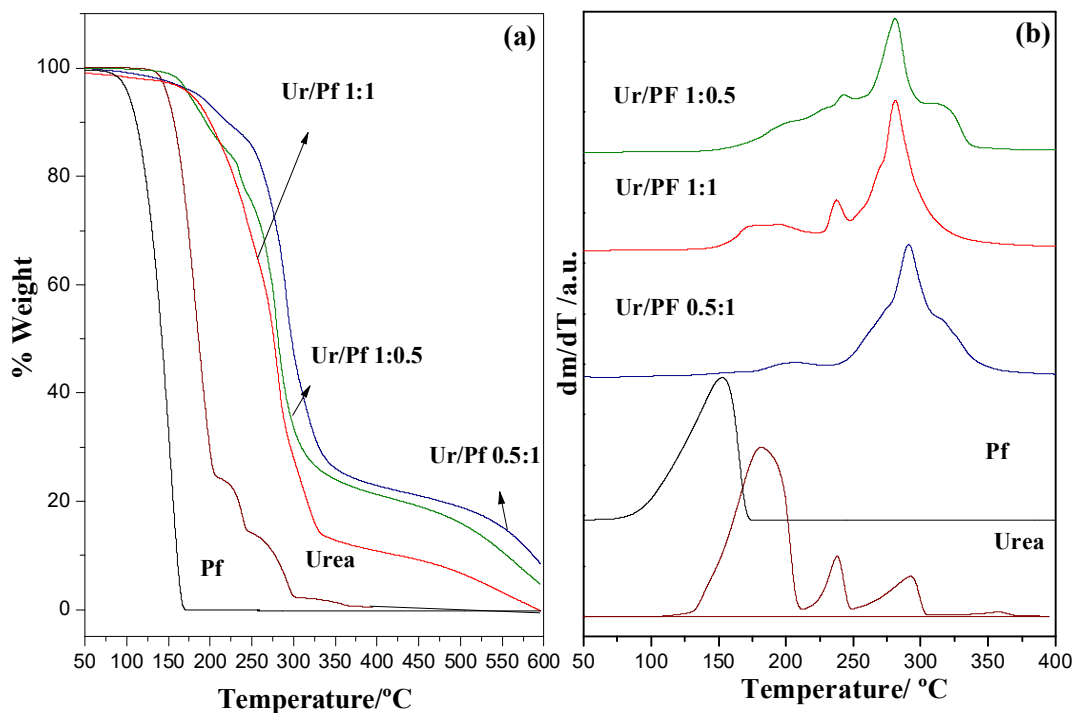
FIGURE 3.4.TGA (a) curves and DTG (b) of Ur/Pf formulations and their neat precursors.

FIGURE 3.4 shows the TGA/DTG curves for neat precursors and polymers. This analysis confirms the polymerization degree of different samples. In the urea TGA curve, three distinct thermal events are visible, urea decomposition onset 160 ºC<T<210 °C and degradation around 237 °C (loss of amine groups) and around 292 °C degradation of polymerized fractions.[64] It was also observed that paraformaldehyde shows a single mass loss step at 150 °C, which is related to a direct volatilization process – confirming that the peak at 123°C in DSC (FIGURE 3.3) is associated with this process. For Ur/Pf 0.5:1 sample a significant (68%) mass loss at the range 174 – 384 °C corresponding to depolymerization/volatilization/decomposition of Ur/Pf polymer followed by a second mass loss around 20% due to an initial degradation of the polymer chain. Considering that the proportion 0.5:1 is relative to the material more polymerized a residual of 8.54% is observed after 600 ºC probably due to strong crosslinking formed between urea and formaldehyde groups in the final material. The thermal profile of sample 0.5:1 shows consequently more degradation peaks in the DTG curve, related to the presence of the urea-formaldehyde polymer. This was also seen in the Ur/Pf 1:1 sample but with a less amount of residual material (5.43%) probably owing a lower amount of urea polymerized in comparison to the previous material with a higher proportion of paraformaldehyde (0.5:1). While the material Ur/Pf 1:0.5 had no

weight left after 600 ºC. This was expected since Ur/Pf stoichiometry for full polymerization is at least 0.5:1, thus the others materials should be classified as urea:UF composites due to free urea still presented. However, even in these materials, DTG data reveal that the majority of the material is polymerized since the main peak weight loss is at 280 °C for all polymers. These results showed that the 0.5:1 ratio is necessary if complete urea polymerization is desired.[65] Furthermore, the results showed that Ur/Pf polymers synthesized by melt condensation polymerization have lower free formaldehyde content, high thermal stability, and better stability during storage.[66]
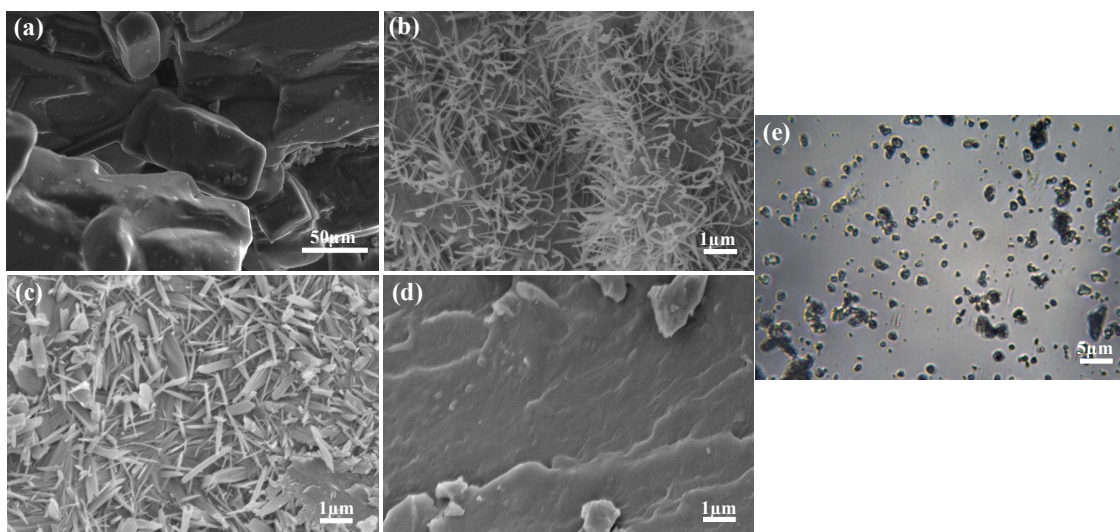
FIGURE 3.5.SEM micrographs for (a) pure urea, (b) Ur/Pf 1:0.5, (c) Ur/Pf 1:1, (d) Ur/Pf 0.5:1 and (e) optical image from paraformaldehyde.

FIGURE 3.5 shows SEM micrographs of the pure urea and obtained polymers and paraformaldehyde optical image. The urea shows regular size particles larger than 50µm.The morphology of the Ur/Pf 1:0.5 (FIGURE 3.5b) shows that the surface is composed of rod-shaped and fibrous crystals formed above a homogenous surface, referred to as unreacted urea. For the sample Ur/Pf 1:1, the reaction leads to large amounts of thicker needle-shaped particles, indicating the higher polymerization degree, as supposed. Finally, Ur/Pf 0.5:1 showed a smooth and homogeneous surface, which indicates the change in morphological evolution during polymerization – since previous results show the complete urea polymerization in this material. As observed by the optical image, the paraformaldehyde resembles small granular, near-spherical particles, whose morphology is not seen in the polymerized samples. This indicates that the needle-shaped structures are resultant of the polymerization reaction, by a re-

crystallization mechanism, and are not remnants of the precursor materials. This needle-shaped structures tend to coalesce to larger rods, leading to almost continuous phases, as seen in Ur/Pf 0.5:1 sample. Therefore, it may be proposed that this shape results from the formation of small seeds in liquid/dissolved phase, precipitating over urea granules. Following, the growth of needle-shape structure is defined by the preferential growth in high-energy planes, which is surpassed by isotropic growth in high crystallization extension, leading to bigger crystals by classical growth or coalescence. This is almost similar to the crystal growth from melt, typically seen for metals and many other polymers crystallized from solution.[65]
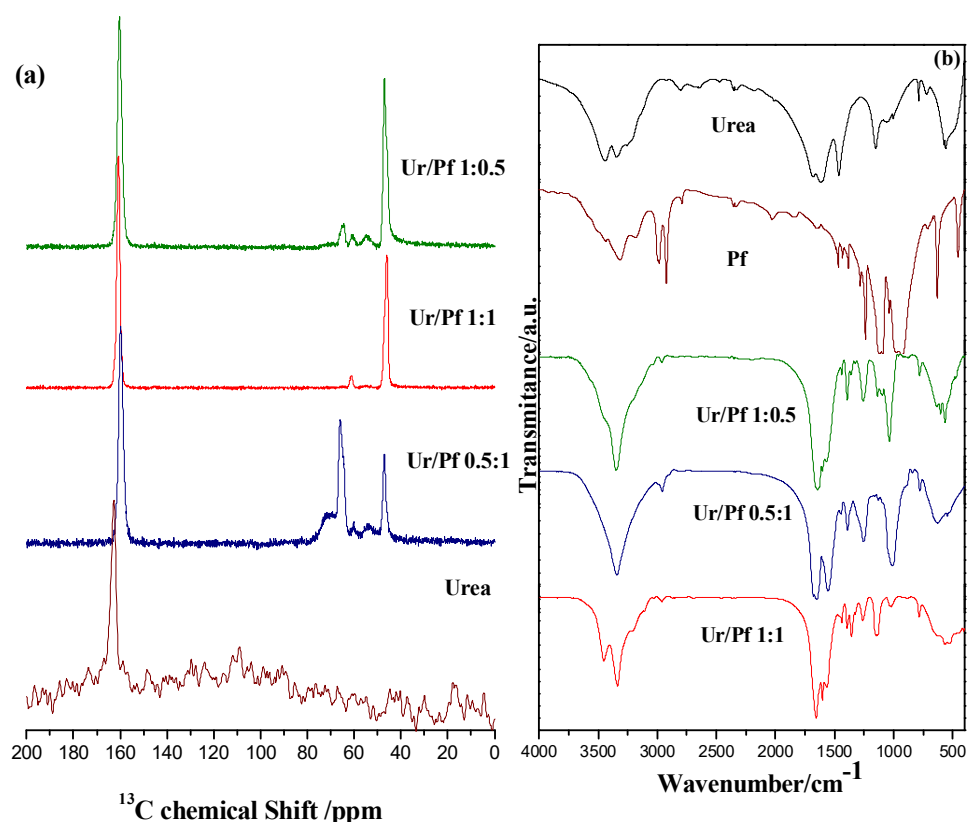
FIGURE 3.6.The spectrogram of ^{13}C NMR of urea and polymers, (b) FTIR transmittance spectra of pure urea, neat paraformaldehyde, Ur/Pf 1:0.5, Ur/Pf 0.5:1 and Ur/Pf 1:1.

The ^{13}C NMR analyses were performed upon the synthesis of polymers in order to better understand the chemical structure formed after curing process, as seen in FIGURE 3.5a. Based on ^{13}C chemical shifts it is possible to evaluate the presence of various functional groups on the polymers. TABLE 3.3 summarizes the chemical shifts confirming the proposed reactions as showed in FIGURE 3.7. In the first step, the hydroxymethylation refers to the addition of up to three formaldehyde molecules with a

urea bi-functional molecule thereby producing hydroxymethyl ureas, as noted by the chemical shift around 65-66 ppm and 71-72 ppm. In some cases, hydroxymethylation conditions (slightly alkaline pH and temperatures around 70 °C) also favor the formation of methylene ether bridges between hydroxymethyl urea as observed for the polymer Ur/Pf 1:1 at 76 ppm. These ether bridges may later undergo rearrangement to form methylene bridges (-CH$_2$-), thereby releasing formaldehyde molecules.
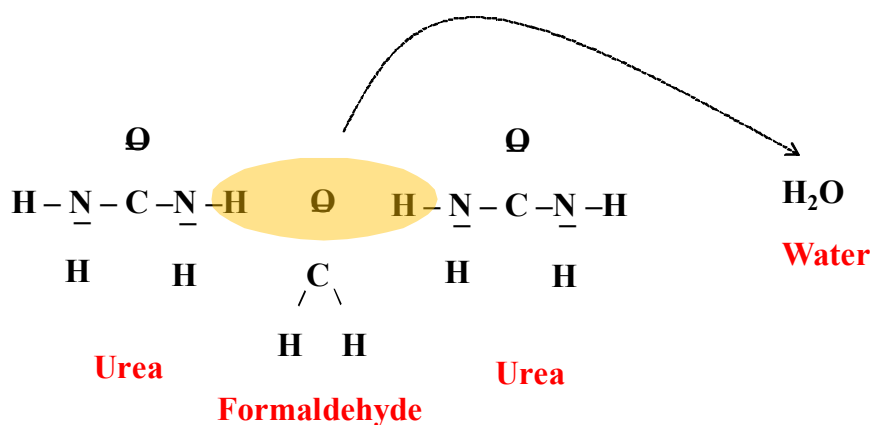
FIGURE 3.7.Polymerization reaction of the urea-formaldehyde polymer.

The second stage, acid condensation, prevails oligomer Ur/Pf conformation. The hydroxymethyl ureas, the free urea, and free formaldehyde react to form linear or partially branched molecules with average or high molecular weights. The type of bridge predominantly formed at this stage is the methylene bridge with chemical shifts around 47-48ppm, 53-54 and 60-61ppm as observed for all materials. In the third synthesis step, the second portion of urea reacts with the free formaldehyde producing more hydroxymethyl ureas. It was possible to verify the formation of species with different degrees of free urea substitution.

For the chemical shifts shown there is a priority formation of mono-substituted urea for materials with the 1:1 and 1:0.5, materials with lower polymerization degrees and the formation of di-substituted urea for the polymer Ur/Pf 0.5:1, the polymer with the highest polymerization degree. This material also exhibited chemical shifts regarding branched chemical groups.[65-68] It was not observed any paraformaldehyde band left (in the region of 80–90 ppm) which is attributed to single carbon present (reactive formaldehyde oligomer) as also observed by Hoong et. al. (2015)[69]; Fan et. al. (2009)[70] and Tomita et. al. (1994)[71] showing that all paraformaldehyde was polymerized.

TABLE 3.3. ^{13}C NMR solid chemical shifts of some of the structural fragments that appear in the Ur/Pf resins showed in FIGURE 3.5.

Structural fragment	Name of group/ Typical signal (ppm)	Chemical shift/ppm		
		Samples (Ur/Pf)		
		1:0.5	1:1	0.5:1
-C(=O)-NH-CH$_2$-NH-C(=O)-	**Methylenes** 47-48	46.9	47.02	47.0
-C(=O)-N-CH$_2$-NH-C(=O)-	53-54	-	-	54.0
-C(=O)-N-CH$_2$-N-C(=O)-	60-61	61.0	60.82	60.1
-C(=O)-NH-CH$_2$-OH	**Hydroxymethyls** 65-66	-	65.12	65.8
-C(=O)-N-CH$_2$-OH / CH$_2$	71-72	-	-	71.0
-C(=O)-N-CH$_2$-OH / CH$_2$-OH				
-C(=O)-NH-CH$_2$-O-CH$_2$-N-C(=O)- (R = H or -CH$_2$-) R	**Dimethylene ethers** 74.4-75.5	-	76.0	-
>N-C(=O)-N< Free urea / Monosubstituted urea / Disubstituted urea / Trisubstituted urea	**Carbonyl regions** 162 / 160-161 / 159-160 / 158.5-159.0	160.8	160.3	159.8

FIGURE 5.6b shows a comparison of FT-IR spectra from 4000 to 400 cm^{-1} between pure urea, neat paraformaldehyde, and Ur/Pf polymers. All the changes of amine stretching vibration frequency indicate the formation of Ur/Pf polymer, which was consistent with previous work.[63,65,72] It was possible to see that multiple and broad peaks in the Ur/Pf resin spectra are mainly due to the polymer structure complexity. The bands at 3439 and 3336 cm^{-1} correspond to N–H asymmetric and symmetric stretching of urea as shown for pure urea and Ur/Pf 1:0.5 clearly exhibit that the same stretching frequency disappears and shifts to higher regions (3422 cm^{-1}) after the reaction for Ur/Pf 1:1 and Ur/Pf 0.5:1.[73] The broad peak around 3350–3450 cm^{-1} can be also

attributed to the hydrogen bonded O–H and N–H. The fact that this band is rather broad may be attributed to monomers such as water and formaldehyde, whose O–H group may form hydrogen bonds with reactive functional groups such as CH_2OH, NH_2, and N-H, as observed by Jada (1988).[74] But no band was found in the regions of 1097 to 905 cm^{-1} (C-O aliphatic ether) referent to paraformaldehyde indicating that no residue of this material was presented in final polymers.[75] Also, it is important to mention that the free –NH_2 group has a characteristic peak at 3440 cm^{-1}, while the bonded –NH group at 3340 cm^{-1}.[62] In spectra for urea, the characteristic bands of amide I, II, and III are around 1680, 1612 and 1463 cm^{-1}, respectively. These peaks are assigned to the C–O stretching of amide I and II, as well as the –N–H scissors of amide I. The multiple peaks at 1460–1470 cm^{-1} may be attributed to C–H bending vibrations of the CH_2–N group, while the small peaks in the area of 1320–1450 cm^{-1} can be assigned stretching of groups like CH_2OH, CH_3, and CN as observed also by Zhong et. al. (2017)[76] The shift has also been assigned to C–H stretching and –O–H bending vibrations of alcohol, but in Ur/Pf 1:1 theses peaks almost disappear. The fact that in the pure UF resin spectrum, the peak is centered at the area of 3410 cm^{-1} in the space of Ur/Pf 0.5:1, indicates that the amount of bonded –NH is higher compared to the free –NH_2. The 1255 cm^{-1} peak is attributed to both the asymmetric stretch of N–CH_2–N and the asymmetric stretch of –C–O–C– of ether linkages.[73] Also, the peak at 2958 cm^{-1} becomes sharper and more distinct, which along with the absence of the 2900 cm^{-1} peak of the asymmetric C–H alcohol stretches, indicates that quantity of ether and methylene linkages is increased in the cured resin and thus, a cross-linking process has evolved.
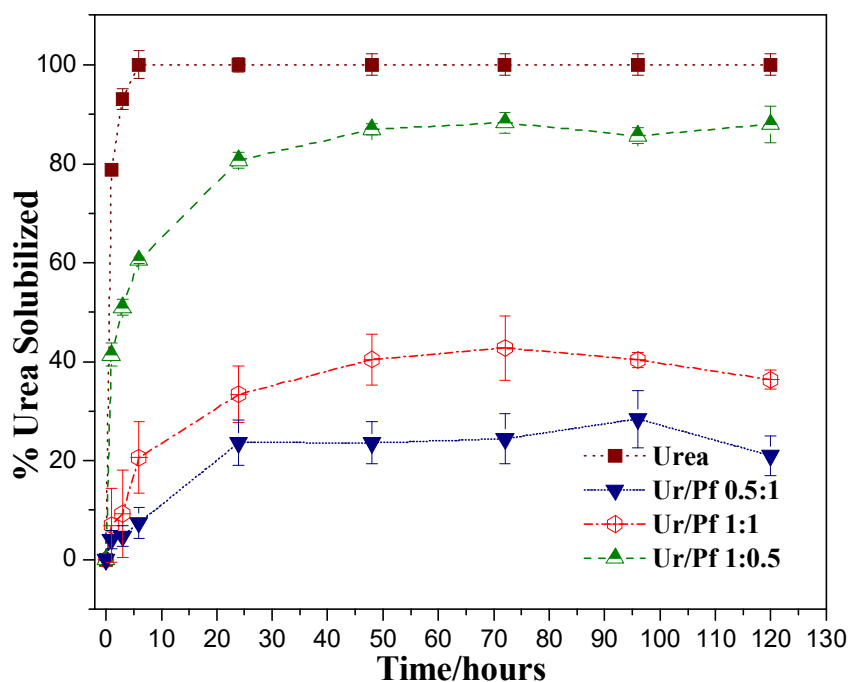
FIGURE 3.8.Kinetics of urea release at 25ºC in an aqueous medium (neutral pH) for commercial urea and Ur/Pf polymers.

FIGURE 3.8 shows the urea release profile in water (full immersion) for all samples. It is noteworthy that all materials had a slowed behavior in the urea release, even the non-completely polymerized sample (Ur/Pf 1:0.5) when compared to urea. The degree of polymerization plays a key role in this process since the release time and the equilibrium value over 50 hours was directly dependent on the polymer content. It was observed that Ur/Pf 1:0.5 showed a behavior very close to pure urea. Considering that this sample is characterized by a partially polymerized structure, this release may correspond to the solubilization of that unreacted urea, but also to the polymer itself – since this is probably a low molecular weight polymer, it is possible that the structure presents some solubility and then, part of the solute correspond to oligomers or soluble polymeric chains. However, this suggests that the time for total urea release for this polymer may be greater than 120 h, i.e., 5 days of complete immersion in water. For other materials, urea releases of only 30% and 20% for Ur/Pf 1:1 and 0.5:1 were observed, respectively, at the end of 50 hours (equilibrium time). This value is almost constant until the end of the experiment, suggesting that the maximum solubilization degree was attained. Altogether, this full immersion test is very aggressive and may not correspond to real conditions in the field, where the moisture level is limited by the soil uptake capacity.
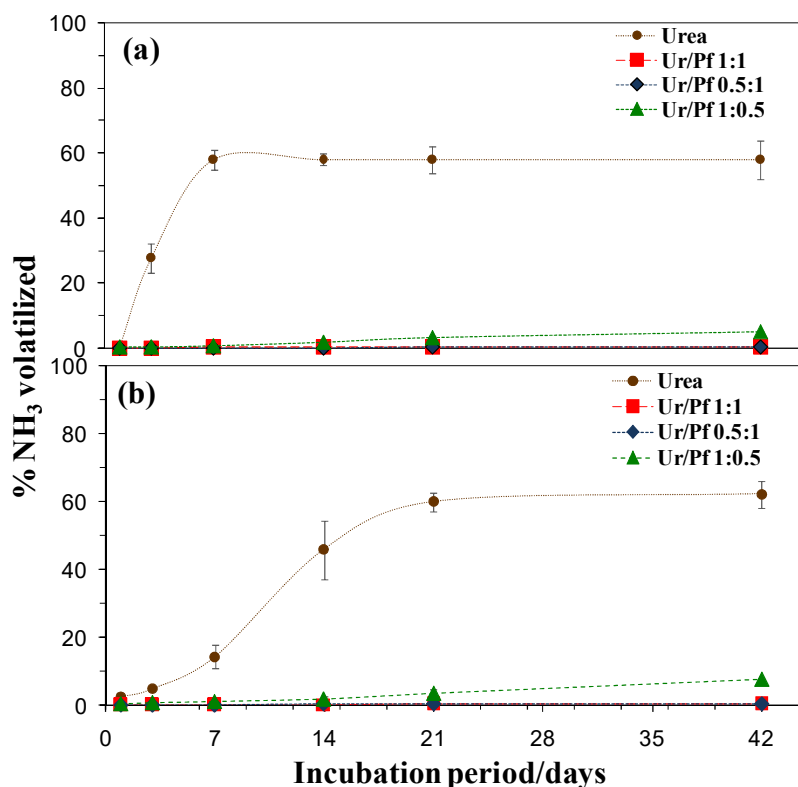
FIGURE 3.9.Fertilizer N recovery as NH_3 volatilized during the aerobic incubation of urea (Ur), or polymers (Ur/Pf) applied to the (a) Red-Yellow Oxisol and (b) Red Oxisol. Data are shown as a mean of triplicate incubations with bars to indicate the standard mean error.

Therefore, in order to analyze the release of nitrogen for the prepared materials in near-real conditions, incubation experiments were performed, and the influence of soil moisture and temperature on the volatilization of NH_3 and formation of NH_4^+ and NO_3^- were analyzed – as seen in FIGURE 3.9, 3.10 and TABLE 3.4, respectively. The samples behavior was clearly influenced by the polymerization extent.

FIGURE 3.9 shows the N recovery as NH_3 volatilized during aerobic incubation of Ur or polymers (Ur/Pf) applied in both type soils studied. The rapid urea release from the Ur treatment demonstrated the high NH_3 volatilization exceeded 60%, an amount poorly affected by the soil type (Red-Yellow or Red Oxisol). However, the hydrolysis of urea was faster in the Red-Yellow than Red, which can be observed by the over 50% ammonia volatilization until the first week for the Red-Yellow soil, while Red soil attained this level only at the third week. This result can be attributed the much higher urease activity and higher sand content of the Red-Yellow soil, as reported in TABLE 3.2, which intensifies the NH_3 volatilization trend. The high NH_3losses from

urea in the incubation experiment can be attributed to low CEC of both soils (TABLE 3.2) agreeing with Guimarães et. al. (2016).[77]

The polymerization of urea with paraformaldehyde provided control of urea release, even in the partially polymerized sample (Ur/Pf 1:0.5) in both soils and inhibited the N losses (FIGURE 3.9). This sample was characterized by a reduced polymerization degree evidenced by structural analysis (TABLE 3.3) which intensified the release of urea during the incubation period. Before urea hydrolysis, the breaking of the fragment structure and release of the urea molecule into the soil is necessary. This breaking can be attributed to the microbial activity in soil that was faster for the treatment with low rate paraformaldehyde. It is important to notice that, even with this sample presenting a possible significant amount of low molecular weight polymers, by the synthesis conditions, these soluble molecules were also effective to reduce the total NH_3 volatilization.
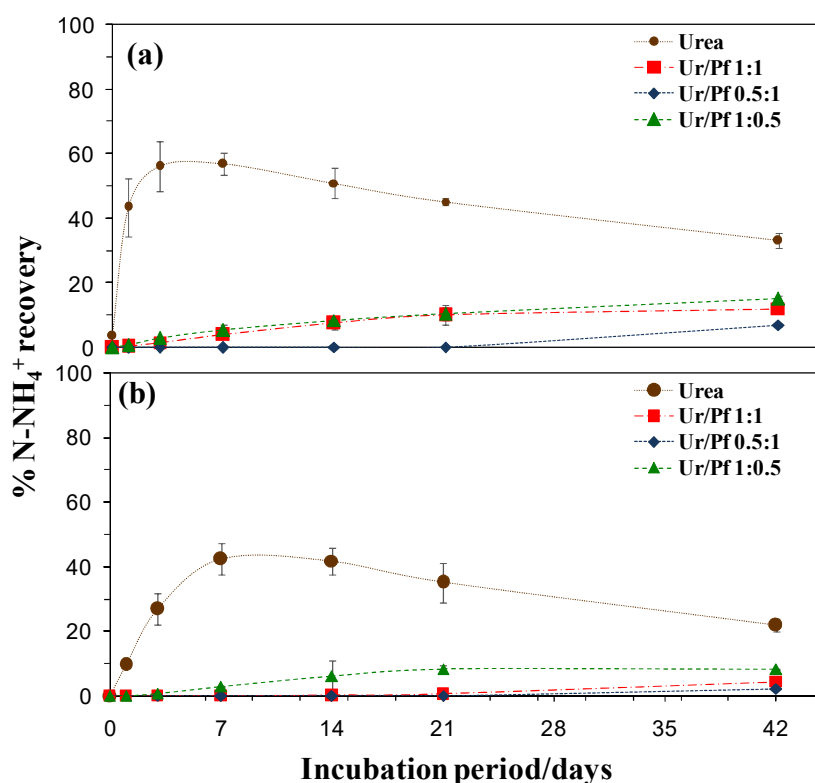
FIGURE 3.10. Fertilizer N recovery as ammonium (NH_4^+) during the aerobic incubation of urea, or polymers (Ur/Pf) applied to the (a) Red-Yellow Oxisol and (b) Red Oxisol. Data are shown as an average of triplicate incubations with bars to indicate the standard mean error.

FIGURE 3.10 shows recovery of exchangeable NH_4^+ during the incubation period in the Oxisols. The NH_4^+ content reflects production through urea hydrolysis, primarily consumption via NH_3 volatilization and low effect of nitrification. For both soils, the unamended urea shows a fast NH_4^+ content increase until the first week after application in the soil, however, it is followed by a decrease provided by the loss of N from ammonia volatilization. The polymers provide a more constant and homogeneous NH_4^+ release during the incubation period. Unfortunately, the content of NH_4^+ from Ur/Pf composites was low during the six-week study attributed to high control urea release, which is consistent with the evidence of the increase rate of paraformaldehyde in the treatments. The smallest polymerization of Ur/Pf 1:1 and Ur/Pf 1:0.5 provided higher of NH_4^+ release than Ur/Pf 0.5:1 during incubation in Red-Yellow and more consistent for Ur/Pf 1:0.5 than other treatments in Red Oxisol. No definite explanation can be offered for low nitrification, which remained lower than 3.5% during the incubation period for both soils.

TABLE 3.4 compares the fertilizer N recovery as total volatilized NH_3, and total exchangeable NH_4^+ and NO_3^- after aerobic incubation intervals of urea and composites (Ur/Pf) in two Oxisols. In both soils, the total N losses from urea alone showed similar behavior exceeding 60%. In contrast, the Ur/Pf 1:0.5 treatment did not exceed 8%, while the treatment with the highest polymerization degree showed insignificant N losses. This advantage evidences the efficiency of the paraformaldehyde to control urea release and N losses. Similarly, the lower total NH_4^+ content of composites compared to the Ur treatment can be attributed to the more gradual release of urea. Therefore, the increase of the polymerization paraformaldehyde percentage decreases NH_4^+ content in the soil. However, the Ur/Pf polymers present high urea content without release to the soil after six weeks of incubation, which could be released in the longer period.

TABLE 3.4.Fertilizer N recovery as NH_3 volatilized and exchangeable NH_4^+ and NO_3^- after aerobic incubation of Red-Yellow or Red Oxisol.

	Treatment	Total NH_3	Total NH_4^+	Total NO_3^-	Residual N
		%	%	%	%
Red-Yellow	Ur	60.4 a[1]	33.2 a	3.24 a	3.16
	Ur/Pf 1:0.5	5.02 b	15.5 b	3.51 a	75.97
	Ur/Pf 1:1	0.35 c	12.2 c	3.38 a	84.07
	Ur/Pf 0.5:1	0.35 c	7.1 d	2.84 a	89.71
Red	Ur	62.16 a	27.26 a	2.75 a	7.83
	Ur/Pf 1:0.5	7.51 b	8.47 b	1.86 a	82.16
	Ur/Pf 1:1	0.28 c	4.33 c	2.80 a	92.59
	Ur/Pf 0.5:1	0.28 c	2.06 c	2.30 a	95.36

[1]Mean values reported from triplicate incubations. Values within a column followed by the same letter do not differ significantly by the Duncan test at $P < 0.05$.

The total N recovery as NH_3, NH_4^+, and NO_3^- from unamended urea was 96% for Red-Yellow and 92% for Red Oxisol (TABLE 3.4). In contrast, the total N recovery of composites does not exceed 24%, which demonstrates that these compounds have more than 75% N to be released after 42 days. The N recovery as exchangeable NO_3^- did not show differences between the treatments, with values not exceeding 3.5% for Red-Yellow and 2.8 for Red Oxisol.

3.5   *Conclusions*

The results showed a simple method, based on mixing- melt of urea with different amounts of paraformaldehyde, that was effective to produce N controlled release materials. The composition plays a key role in the release profiles since the polymerization extent was shown as the mechanism needed to delay N solubilization. This was only possible by controlling the in-situ production of formaldehyde through the degradation of a solid precursor, paraformaldehyde, in processing conditions comparable to the expected for melt extrusion. It is worthy to mention that, in this strategy, the conventional setup for polymer extrusion processing may be easily adapted to produce this kind of fertilizer, which is an important technological advance compared to the conventional fertilizing products. This also influences on the actual chain length, i.e., the partial polymerization was shown as an effective strategy to produce oligomers and low-molecular-weight polymers, which will interact faster to the soil biota –

releasing the nutrient. Also, the soil profile, analyzed in two Oxisol, was seen as an important factor for release: soils with higher urease activity induced higher polymer solubility, however at low levels – indicating that these materials can avoid volatilization effects, even in the low-polymerized materials (with higher free urea contents). Finally, considering that the polymers are expected to continue their degradation behavior, the residual N in the structure is maintained for further use in the soil, as desired in many agricultural practices.

4. - Chapter II: Increasing the N content in Polymeric Matrices

The content of this chapter is an adaptation of the manuscript entitled **"Modification of Thermoplastic Starch used as a Matrix for N Fertilizers"** by Amanda S. Giroto, Gelton G. F. Guimarães, Rodrigo Garcia, Luiz A. Conalgo, Artur Klamczynski, Greg M. Glenn and Caue Ribeiro, under preparation.

4.1. Abstract

Nitrogen is an essential element for plant growth. Among of all nitrogen fertilizers urea is considered the most widely used due its high N content but its potential is limited by its high solubility in water and losses up to 50% is related. To overcome this problems a range of technologies have been developed with the aim of improving the urea efficiency. All alternatives imply in reducing final N content. In this sense, this work describes a study a one-step method to prepare slow-release nitrogen fertilizer through the modification of thermoplastic starch by blending with melamine. Therefore, characterizations and release kinetics was done for the composite as well as the greenhouse experiments to show how the true role of melamine in the composites fertilizers.

4.2. Introduction

Nitrogen (N) is an essential element for plant growth, and N deficiency has been considered as the most important limiting factor for crop yield.[78] Urea is considered the most widely used N fertilizer due its high N content but its potential is limited by its high solubility in water and losses related to leaching out and run offs, while fixing by soil particles as a neutral organic molecule is limited. To overcome this problems a range of technologies have been developed as slow or controlled release systems, use of urease enzyme inhibitors and nitrification inhibitors, coating with polymeric materials, the dispersion of urea in expansive clays and even the partial polymerization of urea, with the aim of improving the urea efficiency.[79,80]

An interesting and new solution is the urea intercalation within matrices constituted by chemically or physically cross-linked polymers, which retards its release to water or soil.[81-85] In this sense natural hydrophilic polymers as cross-linkers or blends, such as starch, are preferred to synthetic polymers because of their nontoxic, low cost, renewable and biodegradable characteristics.[23,81,86-89] However, all these modifications imply in reducing final N content, indicating that the total nutrient availability is compromised by the application technology. On the other hand, other N-based molecules are poorly studied compared to urea, despite having higher N contents. A typical example is melamine ($C_3N_6H_6$), a trimer of triazine, which is composed by 66% of N. This molecule also interacts to urea by hydrogen bonds in amine groups, but its biodegradability is much slower than urea, despite complete.[90] The application of

melamine-intercalated blends may increase the total N content but also contribute to stronger interactions among urea and starch, leading a novel class of fertilizer products.

Therefore in this present study a one-step method to prepare slow release nitrogen fertilizer has been proposed. In our approach, extrusion process was used to incorporate N into a thermoplastic starch with a modifier agent, melamine, that was responsible for blending between urea and starch. However, the relationship between the reaction conditions, material structure and long-term release behavior of fertilizer-loaded by this composite has not been thoroughly investigated.

4.3. Experimental

Materials - The corn starch Melojel (30% amylose and 70% amylopectin) containing 12% moisture was purchased from National Starch and Chemical Company (Bridgewater, New Jersey). Urea reagent grade 98% and melamine 99% were purchased from Sigma-Aldrich (St. Louis, Missouri). Urea was milled using a Willey mill equipped with 1mm screen, other materials were used as received.

Samples preparation - The starch-based material has been prepared as follows: 66% of starch (as is) was mixed with 34% of urea (w.w^{-1}), and then suitable amount of melamine, as given in TABLE 4.1. All components were mixed for 10 min in plastics bags until homogenization was achieved. The extrusion of materials was performed using co-rotating twin screw extruder (model Micro 18 Leistritz, Germany) with L/D = 30:1 and equipped with driving and mixing elements. The extruder was setup with 6 heating zones at temperatures of 70, 80, 90, 105, 105 and 105 °C, and rotating speed of 150 rpm to obtain the materials in fast condition of processing and 80 rpm for the materials with a slower processing conditions. Feed rate was kept at 23-25 g.min^{-1} while water was pumped directly into the extrusion chamber on the first temperature zone at a rate of 4 g min^{-1}. After the processing the materials were left at room temperature and after drying were cut into small pellets. Thus, the materials were designed in according their mass ratio between urea and melamine amount and the processing speed (fast or slow), respectively as shown in TABLE 4.1.

TABLE 4.1.Nomenclature, mass ratio of urea (Ur) and melamine (Mel), used in the composites production, percentage of urea and the percentage of nitrogen (N) and carbon (C) total present in the raw materials and composites.

Materials	Ur/Mel ratio	% Urea	% N Total	% C total
Urea	-	100	46.41	19.09
Melamine	-	-	67.10	27.43
TPSUr	-	34	16.46	29.87
1:2 *Fast*	1:2	11	23.28	34.90
2:1 *Fast*	2:1	22	19.05	33.35
1:2 *Slow*	1:2	11	20.65	35.41
2:1 *Slow*	2:1	22	18.81	34.13

The total nitrogen and carbon organic content in each composite formulation was determined byy elemental analysis (model 2400, PerkinElmer, Massachusetts, USA) in order to quantify the actual mass fraction of N in each material. The nitrogen results obtained were used to calculate the amount of material used in the release tests (TABLE 4.1).

Characterizations

Scanning electron microscopy - Samples were mounted onto aluminum specimen stubs using double-sided adhesive carbon tabs (Ted Pella, Redding, CA). All specimens were coated with gold–palladium for 90 s in a Denton Desk II sputter coating unit (Denton Vacuum U.S.A, Moorestown, NJ). Specimens were viewed in a Hitachi S4700 field emission scanning electron microscope (Hitachi HTA, Japan) at 5 kV.

Thermogravimetric analysis (TGA) - The thermal analyses of the composites and the precursors was measured in a PerkinElmer Pyris1 TGA Thermogravimetric Analyzer (Norwalk, CT). The samples (10 mg± 0.2) were heated from 35 to 600 °C at a rate of 10 °C min^{-1} under nitrogen atmosphere at a flow rate of 20 mL min^{-1}.

X-Ray diffraction (XRD) - A Shimadzu XRD6000 diffractometer was used to conduct X-ray diffraction analyses (XRD) of the nanocomposites. The relative intensity was registered in a diffraction range (2θ) of 3-40°, using a Cu-Kα incident beam (λ=0.1546 nm). The scanning speed was 1° min^{-1}, the voltage and current of the X-ray tube were 30 kV and 30 mA, respectively.

FT-Raman Spectroscopy - Raman spectroscopy measurements were performed in a FT-Raman spectrometer (Bruker RAM II with a Ge detector), equipped with a Nd:YAG laser with wavelength centered at 1064 nm. Ultraviolet–visible diffuse

reflectance spectroscopy (DRS) was carried out with a Cary 5G spectrometer in the total reflection mode with an integration cell and scanned wavelength range of 200-800 nm.

^{13}C *Nuclear magnetic resonance* - ^{13}C solid-state NMR measurements were performed in a 9.4 T (400 MHz for 1H) Avance III NMR Bruker spectrometer (Karlsruhe, Germany). The ^{13}C spectra were acquired with cross-polarization magic angle spinning (CPMAS) technique in a 4 mm MAS probe. The acquisition parameters were: Spinning rate of 8 kHz, ^{1}H 90° pulse of 2.3 us, contact time of 2 ms, spectral width of 250 ppm, and recycle delay of 3 s. Hexamethylbenzene (HMB) was used as external reference standard at 17.2 ppm for methyl carbons. All the NMR experiments were carried out with4096 scans.

Tests

Evaluation of nitrogen releases in water - The nitrogen release in water at 25 °C and neutral pH for each composite were examined using the same initial amount of nitrogen for each material in according to the total nitrogen from each composite. Briefly, samples were soaked in water at 25 °C and were uniformly homogenized by gentle stirring using an orbital shaker (Thermo scientific) for 5 days. Pure urea was also tested as a control and in this case to calculate the amount of urea solubilized the solution was analyzed using the method adapted from Tomaszewska and Jarosiewicz (2002)[55]. Curves of the nitrogen-released (%) as a function of time were then, calculated using the analyses of nitrogen residual after each time of experiment. The measurements were performed in three replications under identical laboratory conditions for each type of composite formulation.

Carbon Mineralization - Composites were analyzed for degradation in soil conditions using Microoxymax respirometer equipped with CO_2 sensor (Columbus Instruments, Columbus, US). Soil was purchased from local hardware store and screened to obtain particles smaller than 1.4 mm. The samples were ground to pass 100 micrometer screen and analyzed for Carbon and Nitrogen content (ALS International, Tucson, US). Samples (0.20 g) were loaded to the chambers containing 20 g of soil hydrated to 58% moisture and kept at 30 ºC. Chambers were connected to the CO_2 sensor and the CO_2 emission was recorded in 2 hours intervals over three weeks period. All samples were run in triplicates. Percentages of carbon mineralization based on total carbon content obtained from elemental analyses were calculated.

Release and transformation of N in soils - The release of nitrogen from the composites was evaluated in an Oxisol soil, collected in the surface (0-20 cm) in an

area with agricultural activity in Brazil. Before use, the soil samples were air-dry and crushed to pass through a 2 mm screen. The chemical and physical properties of soils are reported in TABLE 4.2. The pH was determined with a glass electrode (soil:water ratio, 1:1); organic C by the method of Walkley-Black;[57] cation-exchange capacity (CEC) by Embrapa (1979);[58] soil texture analysis was determined by pipette method;[59] water-holding capacity (WHC) by Embrapa (1979)[58].

TABLE 4.2.Chemical and physical properties of soils used.

Soil	pH	CEC[a]	Ca^{2+}	Organic C	Sand	Silt	Clay	WHC[b]
		(cmol$_c$ kg^{-1})	(cmol$_c$ dm^3)			(g kg^{-1})		
Red Yellow	5.4	4.8	234	7.6	667	19	314	140
Loam Sandy	7.2	5.4	591	2.3	880	40	80	120

[a]CEC, cationexchange capacity
[b]WHC, water-holding capacity

To compare the N release and its transformations, soil was incubated with urea or urea/melamine composites on the ratio of soil:N (1000:1 g g^{-1}) and placed in 125 mL polyethylene screw-cap bottles. The samples were incorporated into the soils with moisture content standardized in 80% WHC with the addition of de-ionized water. A container with 5 ml of 4% boric acid (Sigma-Aldrich) was added in the polyethylene bottles, to capture the volatilized ammonia (NH_3) during the incubation period. Samples were incubated for 0, 1, 3, 7, 14, 25 e 42 days under controlled temperature (25 ºC).

Nitrogen release was determined by N remaining in the composites after each incubation period, which was quantified by elemental analysis (CHN). The NH_3 volatilization was determined by titration of boric acid with HCl 0.01 mol L^{-1} (Synth) and then the N mineral soil was extracted by KCl 1 mol L^{-1} (Synth) in the ratio extractant:soil (10:1). In order to inactivate the urease enzyme, a solution of 5 mg L^{-1} of phenyl-mercuric acetate (Sigma-Aldrich) was added to the extraction stage. The suspension was stirred for 1 h, then it was filtered using filter with diameter 12.5 cm (Nalgon). The extract was stored in a polyethylene bottle with a volume of 100 mL at 5 °C in a refrigerator.

The levels of ammonium (NH_4^+) in the extracted soil were analyzed by the colorimetric method proposed by Kempers and Zweers (1986).[61] The contents recovered in each N fraction were expressed as percentages referring to the N applied as

urea or composites. The profile of the volatilization of ammonia (NH_3) and the formation of NH_4^+ in soil is presented by the average values accompanied by their respective standard deviations. Differences among treatments by total recovery as NH_3 volatilized and exchangeable NH_4^+ after aerobic incubation were assessed by analysis of variance (ANOVA) and when the F test was significant, differences between treatments were compared by Tukey test (P <0.05).

    Dry matter production and N recovery efficiency - For the greenhouse experiment a low-fertility soil was used. Sandy-Loam soil was collected from Lathrop area California, United States sampled to a depth of 20 cm from a pasture site. Before use, the soil was air-dried and crushed to pass through a 2 mm screen. The soil physicochemical characterizations were done and the results could be observed in TABLE 4.2.

    The efficiency of the fertilizers was analyzed by N uptake seeds from sweet corn greenhouse experiment. Plastic pots with approximately 3.5 kg of the soil used. A completely randomized design with seven treatments: control (without fertilization), pure urea, melamine, and composites (1:2 *Fast*; 2:1 *Fast*; 1:2 *Slow*; 2:1 *Slow*) and four replications for each treatments. The soil in each pot was treated with a solution (50 mL) containing supplying 2.91 g of P and K (as K_3PO_4), 0.5207 g of S (as $(NH_4)_2SO_4$), 0.103 g of B (as H_3BO_3), 0.0168 g of Cu (as $CuSO_4$), 0.0280 g of Mn (as $MnSO_4$), 0.0716g Zn (as $ZnSO_4$), and 0.0013 g Mo (as Na_2MoO_4), which was prepared according to Novais et. al. (1991).[91] The soil was then moistened with distilled water to 70% of water-holding capacity. Ten seeds were planted per pot, and thinning was done four days later to obtain a final stand of five plants per pot. Soil moisture content was maintained by applying water once a day. The composites were applied to the surface of moist soil among plants, which supplied 700 mg of N (as urea or urea + melamine) to each of 28 pots. After 60 days the aerial parts were cut above the soil and placed in paper bags. The aerial parts were put to dry in a forced-air oven at 70 °C for 24 h, and the dry matter was then weighed and ground to < 1 mm with a Wiley mill, for determining the total dry matter content. The N recovery by all plants was evaluated using a CHN elemental analyzer (model 2400, PerkinElmer, Massachusetts, USA) to measure the recovery of N from fertilizers. These parameters were analyzed statistically by ANOVA using Tukey´s honest with significant difference at P < 0.05.

4.4.   *Results and Discussion*

The extruded composites processed with different ratio of Ur/Mel did not show any visual difference. The differences were observed in the composites extruded at different speeds. The composites extruded at lower velocity produced flexible materials, which can be easily bend whereas the materials processed at higher velocity became more brittle. The visual differences between materials can be observed by FIGURE 4.1. To understand the difference in the composites they were analyzed by SEM, TGA, XRD and Raman vibrational spectroscopies, and ^{13}C high resolution solid state NMR spectroscopy.

FIGURE 4.1.Images of composites after pelletized and dried.

FIGURE 4.2 shows SEM images of the surfaces and cross-sections of native maize starch and the composites. FIGURES 4.2a and a' show the images of native maize starch granules in two different magnifications. These FIGURES show spheroid shapes with diameters ranging from 1 to 15 μm, similar to starch structures reported by Chen et al. (2017).[92] FIGURES 4.2b and b' show the SEM images of composite formed by the extrusion of starch and urea (Ur) that is known as thermoplastic starch-Ur (TPSUr).To obtain the TPSUr composite it was necessary to destroy the original structure of starch granules by heating it in the presence of water and urea, at temperatures over 80 °C. FIGURE 4.2b' show needle like structures in TPSUr composite that is different than the ones observed for pure starch. It seems that urea disrupt intermolecular and intermolecular hydrogen bonds of the native starch and transforming it in plastic like structure.[34,35,93-95] However, in this case a low compatibility between the materials was observed. Melamine was added to improve the mechanical properties and the amount of nitrogen in TPSUr fertilizer and its effect is demonstrated in the SEM images of FIGURE 4.2c to 4.2f.
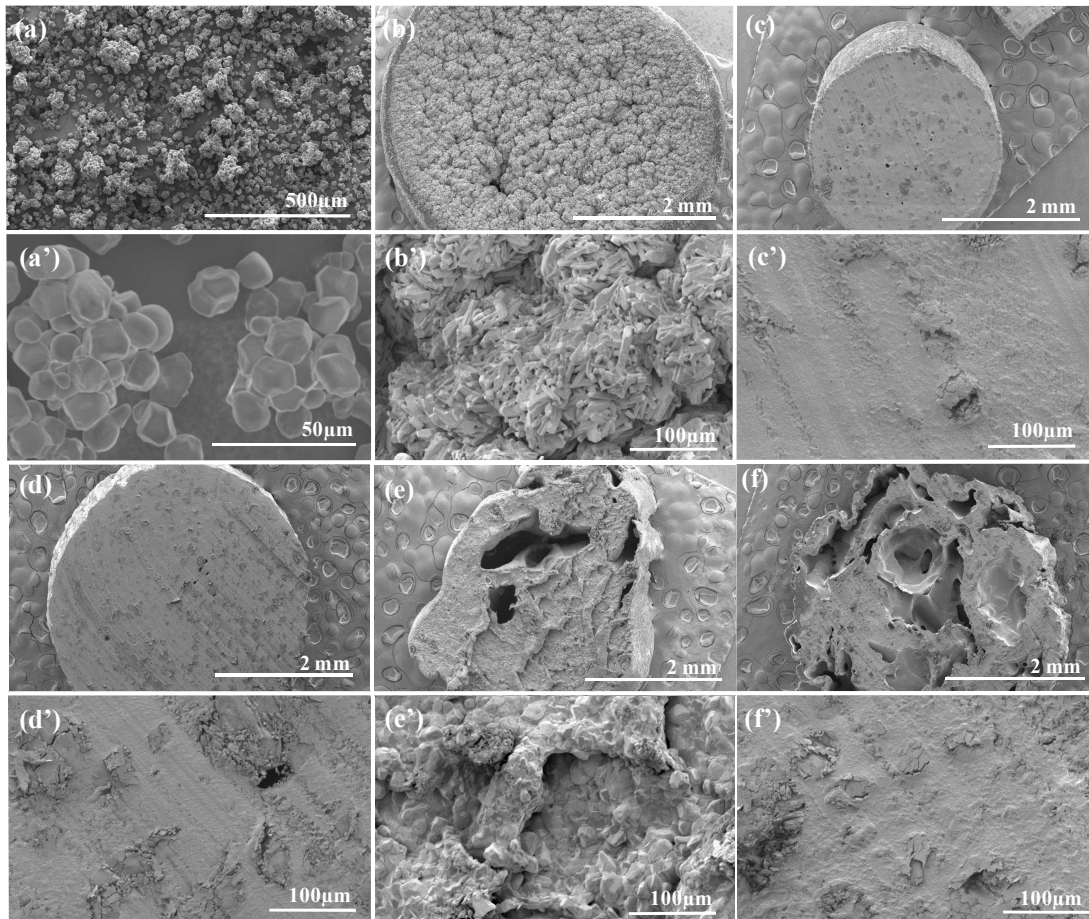
FIGURE 4.2.SEM images obtained from surface of composites: (a) native corn starch (b) TPSUr, (c) 2:1 *Slow*, (d) 1:2 *Slow*, (e) 2:1 *Fast* and (f) 1:2 *Fast*.

FIGURE 4.2c and 4.2d presents the images of the composites produced by the addition of melamine (Mel) to starch/urea matrix at extrusion rates slow and with different proportion of Ur-Mel (2-1 FIGURE 4.2c, c' and 1-2 FIGURE 4.2d, d') and fast extrusion rates (2-1 - FIGURE 4.2c, e' and 1-2 -FIGURE 4.2d f,f'). These Figures (2c to 2f) showed that Mel cause an effective change in TPSUr-Mel structure, with a much more plastic structure, independent of the Ur/Mel ratio or extrusion speed. However, the images of FIGURES 4.2e and 2f show that the extrusion at higher speed (80 rpm) affected the macroscopic structures of the composites with large pore than the composites processed at slower speed that is a much more compact materials (FIGURES 4.2c and 2d). These larger pores can be related to the formation of gas bubbles (water evaporation) during extrusion and reducing the water content and consequently producing a less flexible material. To the best of our knowledge, this is the first time that melamine was used to improve starch with urea compatibilization in extrusion process.
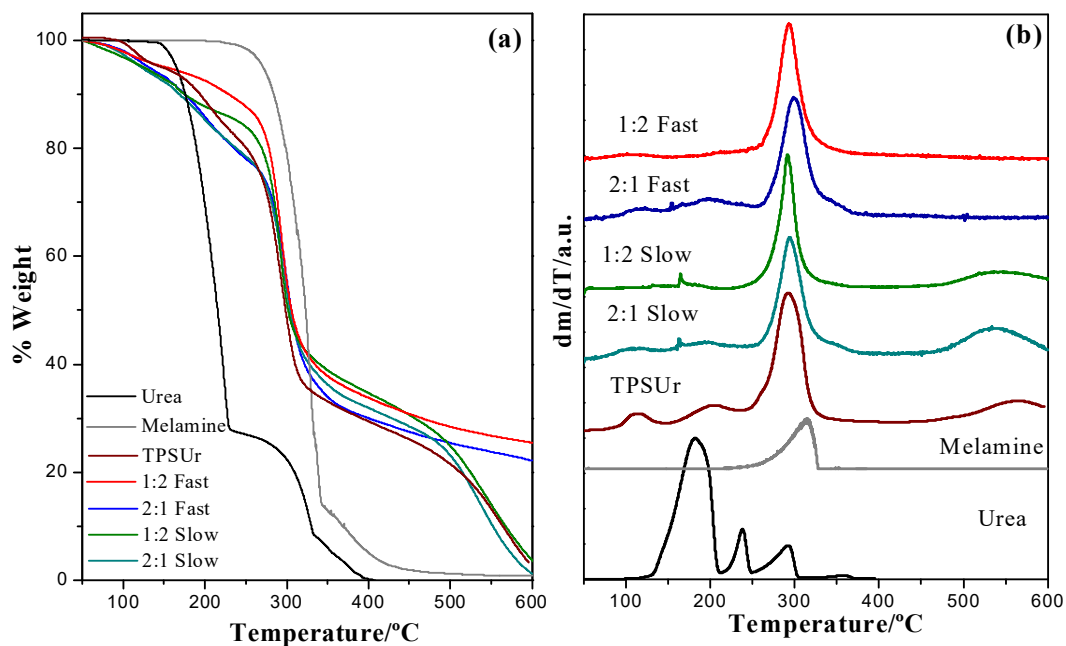
FIGURE 4.3.Comparison between (a) TGA and (b) DTG profiles for the precursors and composites.

FIGURE 4.3 presents the TGA and DTG curves of urea, melamine, TPSUr and TPSUr-Mel composites. The degradation of the melamine occurs in one step between 260 and 330 ºC with a maximum rate loss at 312 ºC. A low residual weight (around 2 wt. %) is obtained at high-temperature. Urea melts at 133 ºC and first mass loss was observed between 133 ºC and 190 ºC, refereeing to the decomposition of urea.[96] The mass loss stage with a maximal peak in 238 ºC is relative to urea decomposition followed to the third stage (270–302 ºC), where the mass loss became much gentler than that in the first and second stages with complete degradation at after 450 ºC.[97,98] TPSUr showed a behavior between of native starch and urea. Three regions were also verified for this material, peaks in around 113 ºC shows a beginning decomposition of urea excess, followed by urea decomposition into the structure (205 ºC) and the break and degradation of chain polymeric of starch in 292 ºC.

TGA curves of composites demonstrate that the two components react together leading to a thermal stabilization of the system for a temperature higher than 400 ºC especially, for the fast treatments. Decomposition curves of materials with an excess of urea are similar to a pure urea, with initial weight loss in the same temperatures that for TPSUr curves. The presence of melamine in the composites increases the thermal degradation temperature by approximately 10 ºC with respect to samples without a starch chain. Moreover, whereas urea, starch and melamine are

totally degraded at 600 ºC, the 1:2 and 2:1 *Fast* materials still exhibit a residual weight around 20 wt.% at this temperature, due possibly by formation of graphitic carbon nitride (g-C_3N_4) as observed by Carvalho et. al. (2017),[99] produced above 560 ºC, by condensation of melamine or melon as reported by Jurgens et.al. (2003).[100] The TGA/DTG results also show that the fast extrusion process has more influence in the composite than the Ur/Mel ratio.
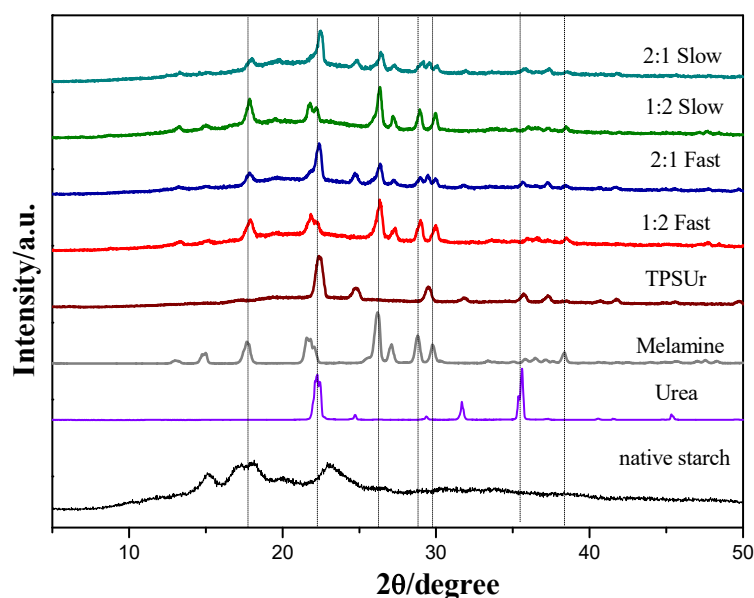
FIGURE 4.4.X-ray diffractograms of starch, TPS-Ur, Ur and Mel and the composites.

FIGURE 4.4 shows the typical A-type diffractograms of maize with 30% amylose. The A polymorph has signature doublet at $2\theta = 17.1º$ and $18.1º$ in addition to strong reflections at $2\theta = 15.1$ and $23º$. The broad peak from 10 to 60º that has been assigned to amorphous amylopectin. On the other hand all the extrudes starch materials did not shows the A-type amylose peaks only a broad signal from 10 to 60º that is typical of the amorphous materials. The sharp peaks in the diffractograms have been assigned to Urea (TPSUr sample) and melamine in 1:2 samples. Although the urea and melamine reflections overlap most amylose peaks, the composites diffractograms clear show that the extrusion process destroy the crystalline structure of the native maize starch. Therefore, XRD method, which reflects the presence of long-range crystalline structures,[101] did not give much information about the influence of the Ur-Mel ratio and extrusion process.
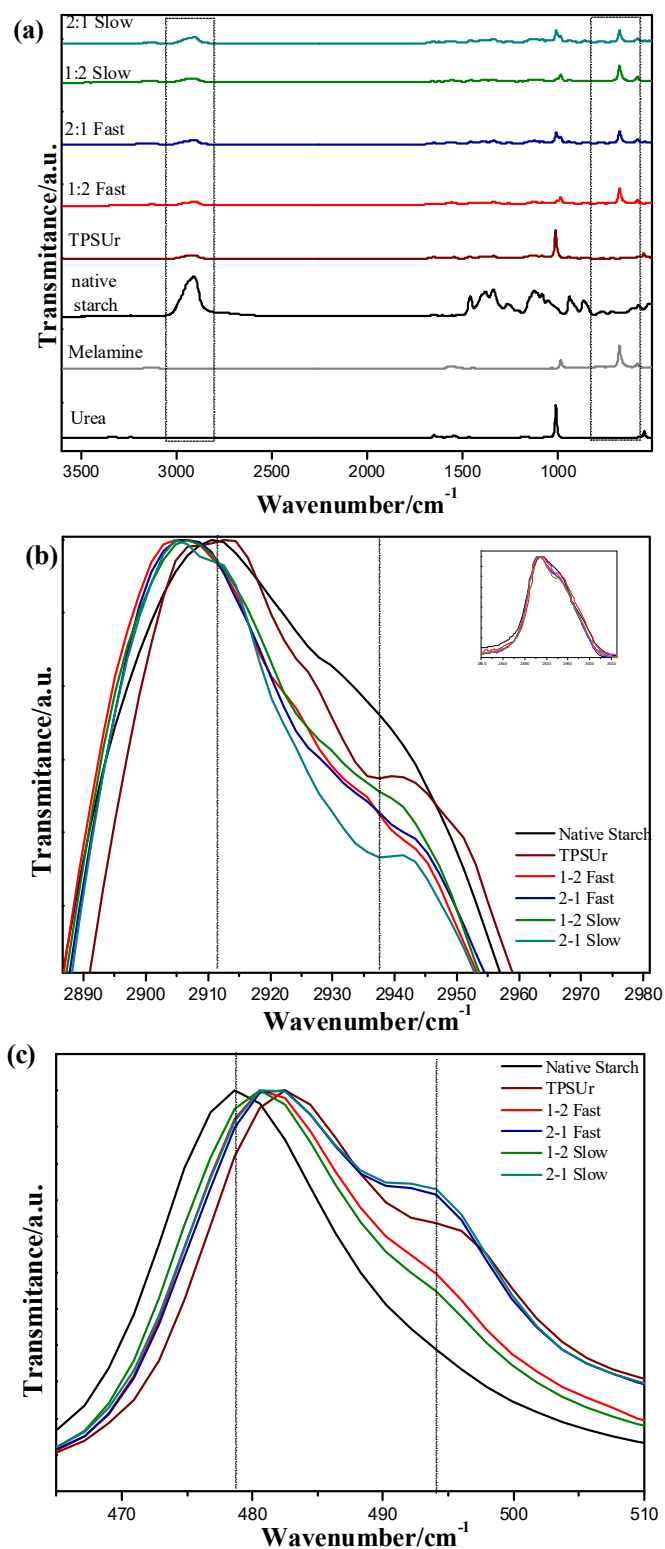
FIGURE 4.5.(a) FT-Raman spectroscopy of native starch, urea, melamine, TPSUr and composites, (b) details of the region between 2890 to 2980 cm^{-1} and (c) expansion of the region between 465 to 510 cm^{-1}.

The samples were analyzed by FTIR spectroscopy, which detects vibration of the chemical bonds that change the bond dipole moment, showing a strong

overlap between the starch, urea and melamine peaks. Therefore this technique was not efficient to study the influence of Ur/Mel ratio and extrusion procedure in the TPSUr composites. FT-Raman spectroscopy detects the vibration that does not change bonds dipole moments, that is less common that the vibrations detected by FTIR. The FT-Raman spectra for starch, urea, melamine, and the TPSUr composites are shown in FIGURE 4.5. The assignments of starch bands have been published elsewhere.[102] The strongest peaks are the C-H signal at approximately 2910 and 480 cm^{-1}, that have been assigned to C-H symmetric and asymmetric stretching modes and to skeletal modes of pyranose ring (C–C–O) modes, respectively. These two bands do not overlap urea or melamine peaks and were used to monitor starch crystallinity (FIGURE 4.4). Mutungi et. al. (2012)[102] used these two peaks and the signal at 865 cm^{-1}, as an internal reference, to measured the crystallinity of cassava starches. The peak at 2910 cm^{-1}, shows a strong correlation (r= 0.93) band width measured as FWHM and crystallinity, indicating that that the C-H are sensitive to conformation and packing of polymer chains. The peak at 480 cm^{-1} shows band shift to lower values and band sharpening have been correlated to starch crystallinity, with correlation coefficient r=0.95 and 0.98 respectively.
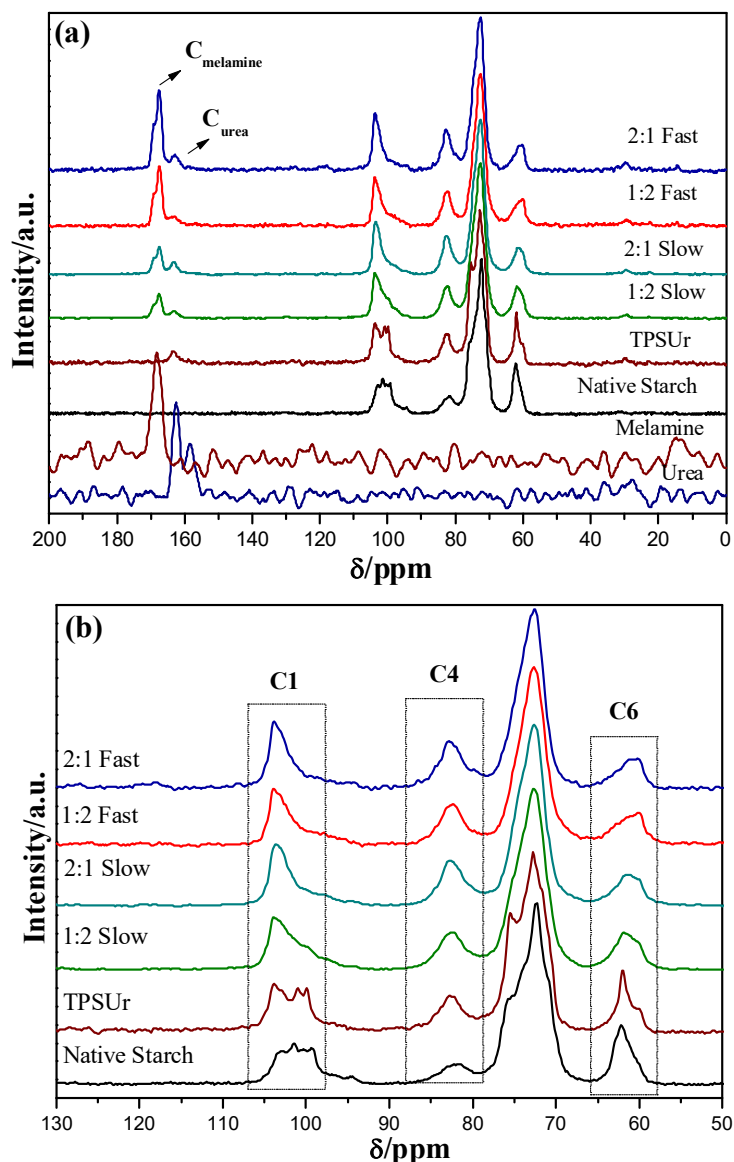
FIGURE 4.6.Solid state ^{13}C NMR spectrum of (a) TPSUr, native corn starch and urea, (b) composites with *Fast* treatment and (c) composites with *Slow* treatment spectrums.

High resolution nuclear magnetic resonance (HRNMR) is more sensitive to interactions among organic structures, giving detailed information for local interactions. FIGURE 4.6 shows the cross polarization magic angle sample spinning (CPMAS) high-resolution solid-state ^{13}C NMR spectra of TPSUr, native maize starch and urea and composites with and slow treatment. Both starch and urea/melamine signals can be used to evaluate the effects of the processing in the composites. The starch spectra show C1 carbon peak at approximately 100 ppm, C4 at 83 ppm, C2, C3 and C5 at approximately 73 ppm and C6 at 62 ppm.[103] The precise chemical shift values in the different starch samples present in FIGURE 4.6a depend on water content and presence of crystalline and non-crystalline structures. These shifts depend on local

electron densities around carbon atoms due to conformational effects.[104] Therefore, different conformational populations due different crystalline structure and amorphous structures can be measured using solid-state ^{13}C CP/MAS spectra. Tan et. al. (2007)[105] shows that here is a high correlation between all for starch carbons peaks and starch crystallinity.[106]

The crystallinity of the native starch can be observed by the multiple C1 peaks of starch that reflects different conformations of crystalline and non-crystalline chains. In TPSUr spectrum the C1 carbon shows a peak at 103 ppm that is typical of no crystalline starch indicating that the preparation procedure is reducing the crystallinity. The C1 peak became featureless in the TPS-Ur-Mel composites indicating that the procedure destroys most of the starch crystallinity. The intensity C4 peat at 83 ppm has also been used to monitor starch crystallinity. C4 intensity is normally inverse correlated to crystallinity. FIGURE 4.6b spectrum shows that C4 intensity increases from starch to TPSUr and to the other composites. The effect of crystallinity of C2, C3 and C5 peak ~73 ppm direct correlates with peak resolution, i.e. starch>TPSUr> others starches composites. The C6 is also correlated to crystallinity. The more crystalline starch shows sharp peak at 62 ppm and it shift to low chemical shift and lower intensity in amorphous one. Therefore the CP/MAS solid-state ^{13}C NMR show that crystallinity was larger in starch>TPSUr> TPS-Ur-Mel *Slow* >TPS-Ur-Mel *Fast*. Therefore ^{13}C CPMAS NMR spectra, that depend on the local environment of the nucleus, was more useful than XRD for these samples, which depends on long-range order to show the microscopic difference between the formulations and extrusion process. The ^{13}C MAS NMR spectra of TPS-Ur-Mel composites also show two signals at 167.5 and 169.2 ppm, with relative intensity of 1.5:1, that have been assigned to melamine and a small peak at 162 that has been assigned to urea carbon. The two melamine peaks have been reported in literature and indicates that there is two not magnetic equivalent carbons in solid state. The detailed analysis of chemical shifts and line width did not show strong interaction between melamine, urea and starch, suggesting that the material have a blend (instead of a real cross linked) structure. The intensities of the carbonyl ^{13}C signal of the urea, in all samples are very low compared with the urea concentration in the samples, varying from 34 to 11% (w.w^{-1}) in TPSUr to TPS-Ur-Mel 1:2. The first hypothesis for the small urea ^{13}C signal was the weak dipolar interaction of the urea carbonyl group with the hydrogen of the amino groups, that is necessary to enhance carbon signal via cross polarization. However, the weak dipolar interactions of carbonyl groups have been

enough to enhance ^{13}C carbonyl signal of proteins and other organic molecules and therefore it cannot be the only factor for the weak urea signal.

The explanation of the very low ^{13}C intensity of the carbonyl group is very long ^{1}H spin-lattice relaxation times (T_1) in crystalline urea. The $T_1$of ^{1}H in crystalline urea, at approximately 300 k is in the order of 1 hour that means that is necessary about 5 hours for 99.33% recovery of the ^{1}H magnetization.[107] Therefore, the transition of the ^{1}H of urea in crystalline state is almost totally saturated, in the recycle delays of 5s, used in the CPMAS experiments. Consequently there is very low ^{1}H magnetization to be transfer to ^{13}C, via cross polarization and the process is very inefficient.

Kristensen et. al. (2004)[108] pointed out that the long ^{1}H relaxation time and inefficient cross polarization difficult the record of the ^{13}C signal of crystalline urea. They also pointed out that this long relaxation times make urea an excellent probe for cellulose surface investigation. They demonstrate that the urea ^{13}C signal obtained by CPMAS is only related to the mobile urea molecules interacting to the cellulose surface. If the urea was deposited, as microcrystal, rather than interacting to cellulose surface, the ^{13}C carbonyl signal is expected to be insignificant. These considerations lead that only urea interacting with other polymers are actually observed in CPMAS experiments, using short recycle time, also true for the ^{13}C signal of urea in TPSUr composites. Therefore, the small urea peak in FIGURE 4.6a may come only from the mobile urea molecules that interact with starch and is not due to the crystalline urea with very long T_1.

The kinetic study of nitrogen release was performed to understand the different releases behavior of each nitrogen source on water (TABLE 4.3 and FIGURE 4.7).
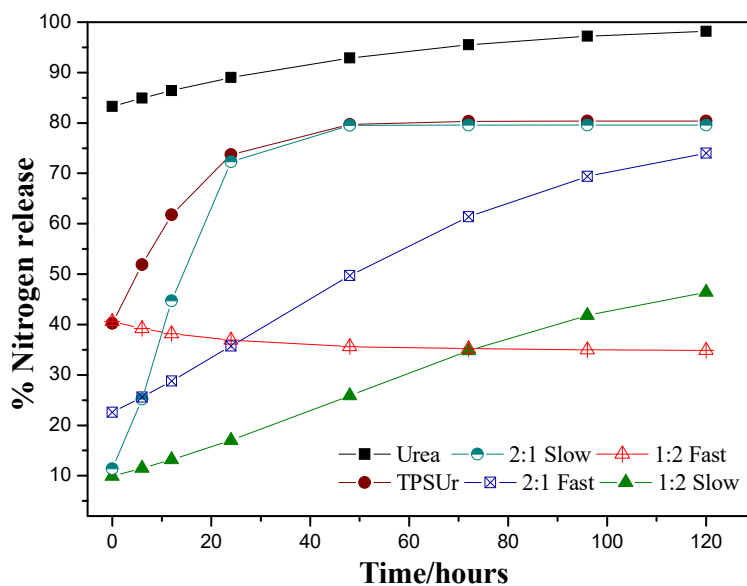
FIGURE 4.7.Urea release rate as a function of time for pure urea and each of the composites at pH 7 and 25 ºC in water.

As observed by FIGURE 4.7 urea had a quickly solubilization in the early experiments hours. All composites had a lower solubilization in comparison to urea. TPSUr showed a behavior more controlled, releasing 75% until 24 hours. After this point the release rate becomes constant. This was due to the fast solubilization of urea weakly interacted with starch and the rest will be available during the polymer degradation. This behavior was also identified for the composites. 2:1 *Slow* had a fast release of urea but more controlled than the TPSUr. During materials processing, in the condition slow, both composites became more plastic due to a greater dispersion of the urea into the polymer. While in the fast condition the composites had a lower dispersion of the urea and a porous structure. As expected, the 2:1 *Fast* material was to have a faster release but the poor dispersion created regions with large amounts of agglomerated material, which hindered the diffusion of water and consequently the lower release of urea.. It was clearly observed that materials with higher melamine contents had a longer availability of urea due to higher interactions between the amine groups of urea, melamine and starch. The final of N released for 1:2 *Fast* at the end of the experiment has the same level of release as the 1:2 *Slow* even though the materials had a different morphology. It is worth remembering that the percentage of N residual not released until 120 hours are strongly bound in the polymer matrix, and can be released in longer periods of experiments or in conditions related to the degradation of the polymer matrix of the starch.

TABLE 4.3. Statistical parameters for nitrogen release in water for each composite.

Samples	Adjusted parameters			R²	Initial Release a/(1+b)
	a	b	c		
Urea	100 (93.6; 110.8)***	0.2 (0.1; 0.3)**	0.02 (-0.004; 0.05).	0.94	83.3
TPSUr	80.4 (76.7; 84.1)***	1 (0.7; 1.3)***	0.1 (0.04; 0.2)**	0.98	40.2
1:2 *Slow*	51.7 (30.1; 73.3)**	4.2 (1.9; 6.5)**	0.03 (0.01;0.05)*	0.96	9.9
2:1 *Slow*	79.6 (67; 86.3) ***	6 (-0.6; 12.7).	0.17 (0.02; 0.31)*	0.96	11.4
1:2 *Fast*	34.9 (21.8; 48)**	-0.14 (-0.5; 0.2)	0.04 (-0.3; 0.4)	0.16	40.6
2:1 *Fast*	79.1 (20.9; 137.2)*	2.5 (-0.04; 5).	0.03 (-0.01; 0.1)	0.85	22.6

Logistic model: y=a/(1+b*exp(-c*time)). t-test signif. codes: *** 0.001; ** 0.01; * 0.05; ¨ 0.1

The behaviors of the composite fertilizers in terms of nitrogen release in solution to evaluation of the controlled release behavior of the materials tested. The profiles N releases (% N release) are shown in FIGURE 4.7. The mathematical model (Equation 2) was fitted to the experimental values for N released (FIGURE 4.7).

$$\hat{y} = (a/(1+b*exp(-c*t)))$$ (Equation 4.1)

where $a/(1+b)$ is the initial response for the nitrogen release; b is the induction time or period required for the system to reach steady-state release; c is the kinetic order of the response with respect to rate. The significance level for all analyses was 5%.[109]

As can be observed by TABLE 4.3, urea has an instant release of 83.3% in only 2 hours of contact with water. The 1:2 *Fast* composite had an initial release behavior very close to the TPSUr around 40%. However, the TPSUr releases 80% of the total N while the 1:2 *Fast* still retains 65% of the N structure at the end of the experiment. It is also noted that 2: 1 Fast had an initial release 2 times higher than 2:1 *Slow*. In this case, the porosity of the material was the key to the higher solubilization rate. It can be said that the porosity was responsible for the faster release of urea in the first periods of time, and after the release of the free and weakly interacted urea, the dispersion became responsible for the greater availability of the urea that was trapped in the polymer network.
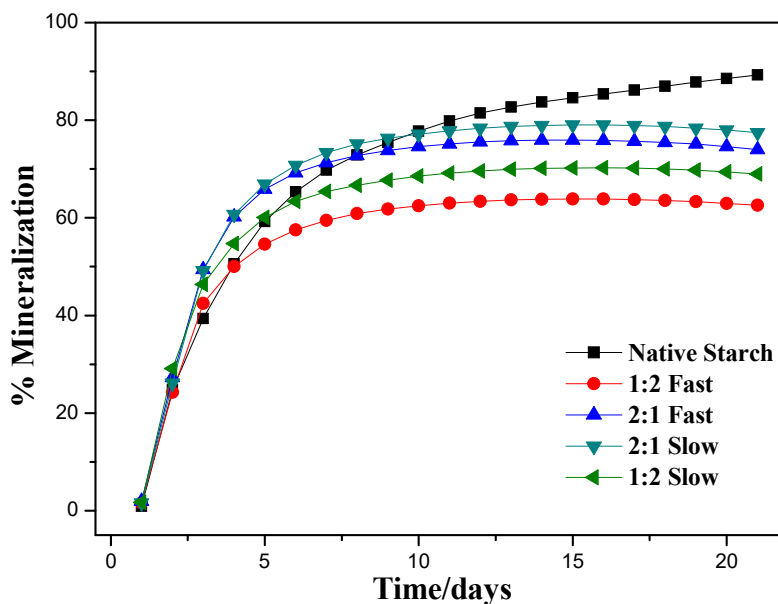
FIGURE 4.8.Mineralization of native starch and composites during first 21 days.

The respirometry test was employed to study biodegradation of composites with different urea/melamine ratios. Results of biodegradation of native starch and composites are shown in FIGURE 4.8. Composites contained between 33.78 and 35.45%carbon and 18.74 and 20.9% of nitrogen (TABLE 4.1). The total degradation calculated on the basis of carbon ranged from 62.6% in 1:2 Fast to 77.2% in 2:1 Slow. In general, although the differences are small, samples containing 1:2 urea/melamine ratio the mineralization percentage was lower than in samples where the ratio between urea-melamine was 2:1. One could argue that this result indicates that samples containing more urea were more available to soil organisms than those with more melamine. Also, there was no statistical difference between slow and fast treatments within given urea/melamine ratio.

A study of the release and transformation of N in soil from urea or composites in a soil incubation was done to verify the role of these composites in a more real conditions. FIGURE 4.9 shows the profile of the release and transformation of N in soil from urea or composites in different period of incubation.

The pure urea was solubilized in the first few hours after application to the soil. On the other hand, the composites presented high residual N content after the incubation period (FIGURE 4.9a). The N source (urea or melamine) and the processing condition (*Slow* or *Fast*) influenced the release of N in the soil. The treatments with higher proportions of urea (2: 1) presented a higher N release and consequently a lower

N content than treatments with proportions (1:2). Similarly, the *Fast* processing condition contributed to the higher release of N relative to the *Slow* condition due to the higher porosity of the 1: 2 *Fast* and 2:1 *Fast* composites presented in FIGURE 4.2 (d) and (f). The formation of pores or channels in these composites increased the percolation of water in the composite and favored the release of N-urea by diffusion. Thus, the 1:2 *Slow* composite, which contains a lower proportion of urea and less pore/channel formation, had a lower release of N and consequently a higher residual N content after incubation of the composites to the soil. In contrast, the 2:1 *Fast* composite, which contains a higher proportion of urea and increased pore/channel formation, had higher N-urea release reflecting the lower residual N content.

FIGURE 4.9b shows the percentage of N lost by NH_3 volatilization after incubation of urea or composites applied to the soil. The NH_3 volatilization profile is influenced by the release rate of N-urea in the soil. Urea, due to its rapid solubilization / release in the soil, showed the highest NH_3 volatilization with values close to 50% after 14 days of incubation. The processing condition (Slow and Fast) did not influence NH_3 volatilization, regardless of urea/melamine ratio used in the composition. The 2:1 *Slow* and *Fast* composites presented low volatilization up to 14 days, but the N losses were increasing reaching values close to 25% at the end of the incubation period. On the other hand, composites with a higher proportion of melamine (1:2 *Fast* and *Slow*) presented insignificant losses of N by volatilization. This result can be attributed to two factors: the higher proportion of N in the form of melamine and the interaction between urea-starch-melamine that delays the release of urea in the soil. Thus, the lower N loss by NH_3 volatilization of the composites can be attributed to a lower proportion of N in the urea form and to the release control provided by melamine/starch.

FIGURE 4.9c shows the fraction of mineral N available in the soil, in the form of NH_4^+, during the incubation period of urea or composites. Under the conditions under which the experiment was evaluated, the availability of $N-NH_4^+$ in the soil results from the N-release profile and the loss of $N-NH_3$. Urea due to rapid release/solubilization showed a high availability of $N-NH_4^+$ ($\sim 45\%$) between 7 and 14 days of incubation, however, this availability have reduced due to intense N loss by NH_3 volatilization. On the other hand, the availability of $N-NH_4^+$ from the composites presented increasing increments after the first days of incubation, reaching values between 17 to 26% from the 28th day of incubation, from 1:2 and 2:1 composites, respectively. It should be noted that the availability of $N-NH_4^+$ from the 2:1 *Slow* and

Fast composites was similar to urea availability from the 28th day of incubation, although these composites still presented around 60 and 53% residual N (remaining N in the pellet after incubation period), respectively. Thus, in addition to the same N content in the soil provided by urea during 42 days of incubation, the composites present high residual N content, attributing to these composites potential for soil N fertilization in medium and long periods.
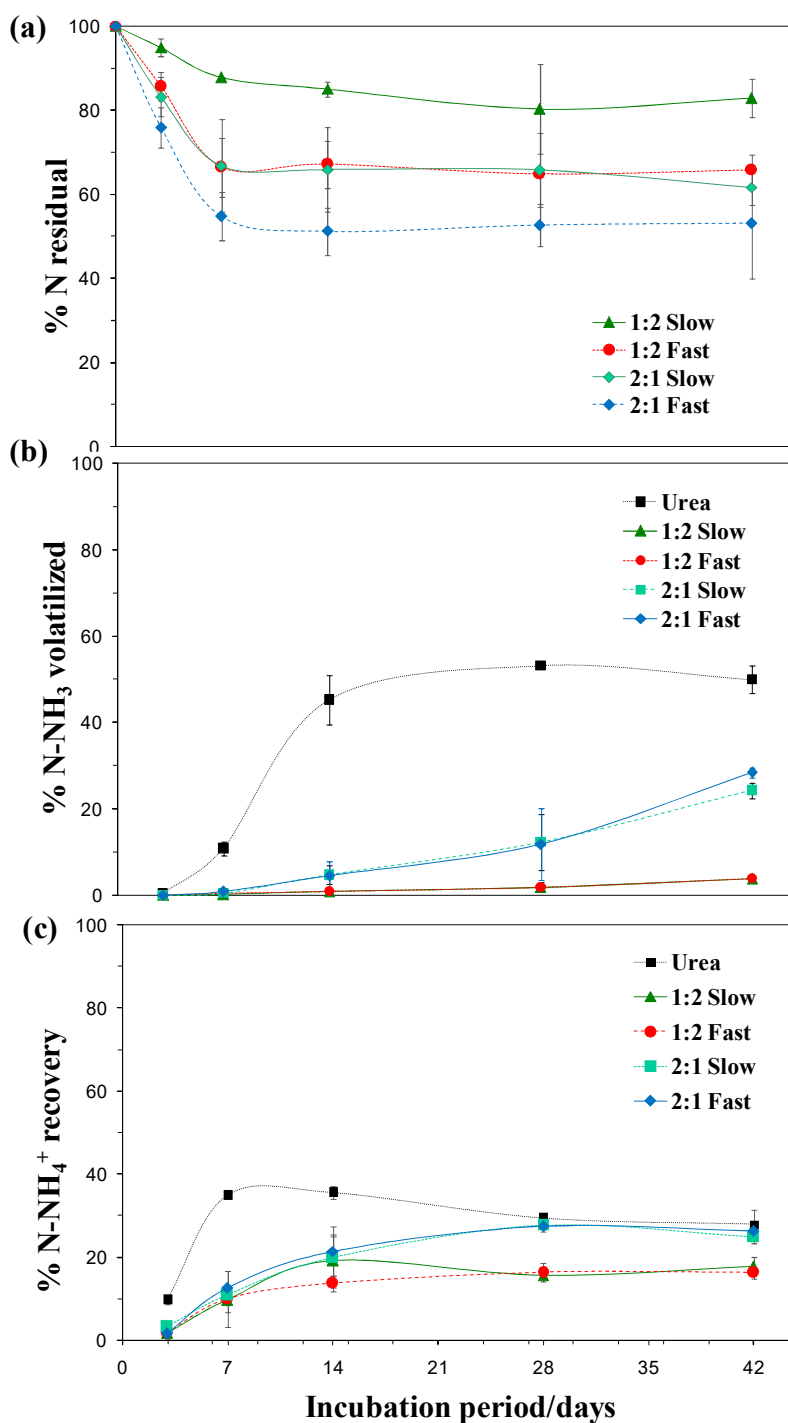
FIGURE 4.9.(a) Percentage of Nitrogen recovery from the composites after the incubation period and (b) Percentage of volatilized ammonia (NH_3) during the aerobic incubation of urea or composites applied to the soil and (c) N recovery as ammonium (NH_4^+) during the aerobic incubation of urea or nanocomposites applied to the soil. Data shown as a mean of triplicate incubations with bars to indicate the standard deviation of means.

FIGURE 4.10 shows the results of dry matter production by corn plants and N recovery efficiency (RE) from urea and composites fertilization. The dry matter content by corn fertilized with urea, TPSUr and composites 2:1 Slow or Fast were similar and presented values above 20 g pot^{-1} FIGURE 4.10a. This result reflects the availability of $N-NH_4^+$ from the 2:1 and urea composites that were similar after 28 days of incubation and higher than the observed availability for the 1:2 composites. Probably the smaller release of N in a short period of time, provided by 1:2 composites did not allow the adequate development of maize plants, reflecting four times smaller dry matter yield in relation to corn plants fertilized with urea or composites 2:1. In addition, melamine-only fertilization did not alter dry matter production in relation to unfertilized plants (Control), where low yield (1.5 g pot^{-1}) corresponded to the low natural availability of N from Loamy Sandy Soil.

FIGURE 4.10b shows the apparent recovery efficiency of N (RE) relative to the total nutrient applied to the soil in the form of urea and/or melamine. As observed in the dry matter production, the RE of the 2:1 composites were similar to the efficiency of urea with values greater than 30%. In contrast, 1:2 composites presented RE values close to 5%, confirming the low N release from these composites during the period evaluated. In addition, the low RE value of 1:2 composites can be attributed to a higher proportion of N in the form of melamine (66%) since this source has the low release of its structural N in short time interval.[90] Confirmation of this information can be confirmed by the low RE (close to 1%) for maize plants fertilized with melamine alone. Unlike the urea that is rapidly converted to mineral N in the soil, after its hydrolysis by the enzyme urease present in the soil, the structural N present in the melamine molecule is converted to $N-NH_3$ after its biodegradation.[90] Thus, the release of N is favored and occurs more rapidly in soils with greater microbial activity. However, the low organic C content of Loamy Sandy soil (TABLE 4.2) is indicative of low microbial activity and, consequently, of the slow mineralization of the melamine molecule and the supply of N.
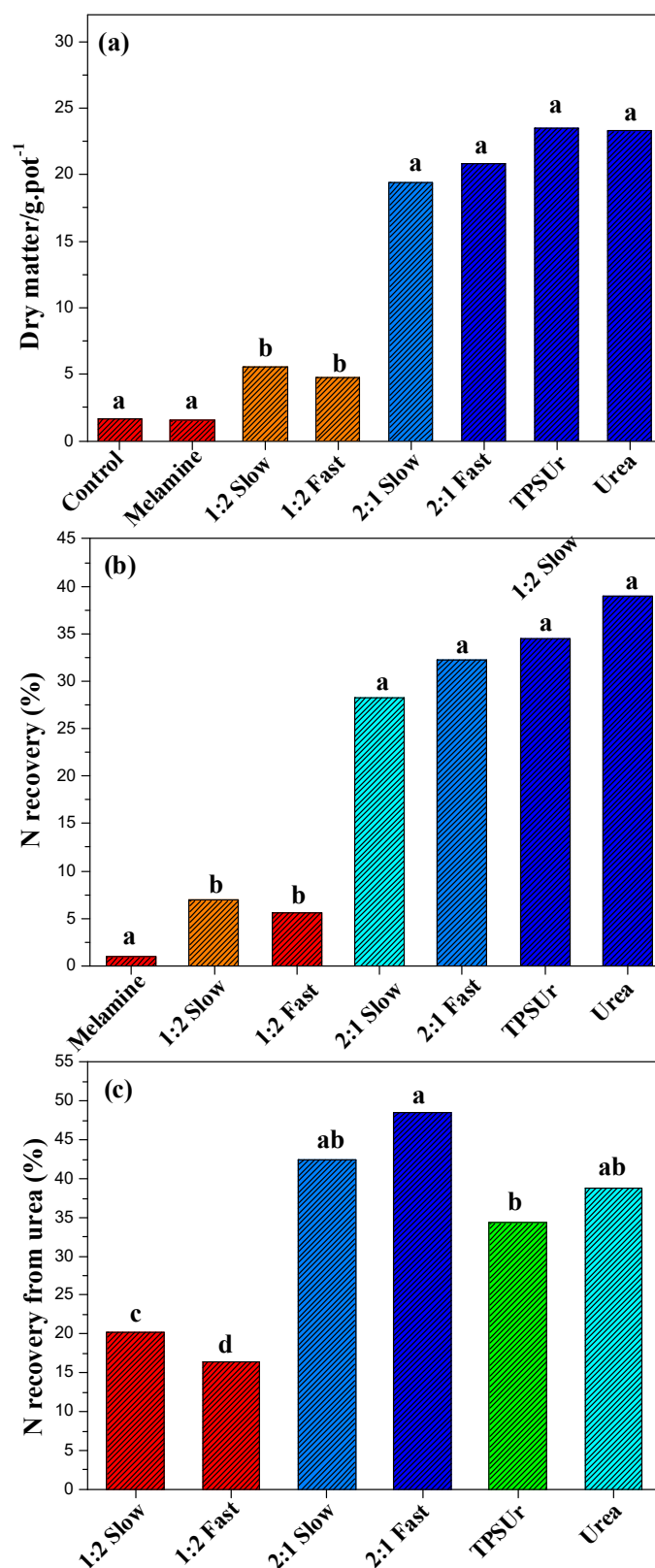
FIGURE 4.10.(a) Accumulation of above ground dry matter and (b) N recovery by corn plants with fertilized with melamine, TPSUr, pure urea or composites, and (c) N recovery considering only the N applied in the urea form. Treatments having the same letter do not differ significantly (P < 0.05) by Tukey test.

Another factor that can be attributed to the low RE value of 1:2 composites is the higher urea dispersion (between the starch chains, in the form of blends - it controls/reduces the release of urea). The results observed so far indicate that the effect of melamine present in the composites (1:2 and 2:1) was more expressive in the control of urea release rather than the source of N for plants grown in a short period of time. Thus, a new RE calculation was performed considering only the N from urea.

FIGURE 4.10c shows the RE in relation to N applied to the soil only in the form of urea. In this condition, the RE from the 2:1 composites were higher than 40%, but similar efficiency was observed for pure urea. However, it is noteworthy that the mass of N in the form of urea provided by the 2:1 composites was 33% smaller in relation to the urea treatment. This result suggests that the N-urea provided by the composites was better utilized by corn plants, with a saving of 33% of N-urea which was replaced by N as melamine. In addition to acting in the control of urea release, melamine present in the composites is expected to supply N to the plants in longer periods of cultivation or in new cycles. The low dose of N-urea provided by the composites 1:2, 66% lower relative to the urea treatment, may have compromised the development of the plants leading to a lower use of N. Finally, the results indicated that the urea-melamine interaction controlled the release of N-urea and consequently increased the efficiency of N from urea. However, melamine did not present potential as a source of N to plants in a short time interval.

4.5.   Conclusions

In conclusion, the extrusion process was successfully used to incorporate N-melamine into a thermoplastic starch with a modifier agent. The results indicated that the processing conditions was the key role to obtain more homogeneous materials due to more dispersion of urea. Characterization demonstrated the formation of a structure of the type blend between urea-melamine-starch, responsible for retard the urea solubilization and consequently its hydrolysis. This means that the availability of N-NH_4^+ from composites was similar to urea after the 28th day of incubation. Furthermore, composites still presented a percentage residual of N around 60 and 53% available to be used in longer periods. Finally, the results indicated that the urea-melamine interaction controlled the release of N-urea and increase the efficiency of use of N from urea.

5. - Chapter III: A Nanocomposite – How the dispersion affects the total Nutrient Availability

The content of this chapter is an adaptation of the article entitled **"Controlled Phosphate Release From Hydroxyapatite Nanoparticles Incorporated into Biodegradable, Soluble host matrices"** by Amanda S. Giroto, Suzane C. Fidélis and Caue Ribeiro, published in RSC Advances.

Reference: RSC Adv., 2015, 5, 104179.

Controlled release from hydroxyapatite nanoparticles incorporated into biodegradable, soluble host matrixes

A. S. Giroto,[ab] S. C. Fidélis[ab] and C. Ribeiro*[b]

5.1. *Abstract*

We report in this paper a strategy to prepare nanocomposite fertilizers based on the dispersion of hydroxyapatite (Hap) into urea and thermoplastic starch at nanoscale, where Hap was assumed as a model for poorly soluble phosphate phases, such as phosphate rocks. Our experiments revealed the role of particle agglomeration on the effective phosphate release, showing that Hap dispersion within two water-soluble matrices (urea and thermoplastic starch/urea) is an effective strategy to increase Hap solubility. Aspects such as matrix solubility, morphology and Hap loading were detailed studied. Also, these structures showed an interesting slow-release of urea, i.e., the materials were at the same time a system for faster release of poorly soluble phosphate phases and slow release of very soluble nitrogen source (urea). Our results support the development of a new class of smart fertilizers, with release properties tailored by nanostructure.

5.2. *Introduction*

Fertilizers supply is one of the key aspects of high productivity in agriculture, chiefly for the macronutrients nitrogen (N), phosphorus (P) and potassium (K). Among NPK, Phosphorus is the least macro element required by plants, however this nutrient has limited the agricultural production due to its low availability in soils, especially in tropical areas.[110] Unfortunately, the low solubility of phosphate rocks limits their direct application as a fertilizer. As a consequence, phosphate rocks have been converted into soluble phosphate fertilizers by using chemical means.[111] An alternative to this issue would be increasing the solubility of phosphate minerals by the aid of nanotechnology. This technology has been proposed as an emerging approach with enormous potential to improve the effectiveness of agricultural fertilizer.[112] Due to the very small size and high surface to volume ratio, nanoparticles are expected to dissolve faster than their bulk counterparts.[113,114] The distinctive properties of nanoparticles could be used to design more efficient P fertilizers as well.[6] Some works have shown that the reduction of the particle size of soluble phosphate rocks improves their agronomic effectiveness[115] because of the increase in the dissolution rate and higher probability of the nanoparticles to interact with the roots.[116,117] This concept was also recently used by Montalvo et. al. (2015)[118] who evaluated the use of hydroxyapatite

nanoparticles as a potential P-fertilizer with improved efficiency based on the hypothesis that nano-sized particles can diffuse more easily through the soil to reach the plants. The dispersion of P-fertilizers within organic matrices could also be combined with the particle size reduction approach as well as techniques that avoid particle re-agglomeration. Recently, Liu and Lal (2014)[119] investigated the use of hydroxyapatite nanoparticles (15 nm) dispersed into carboxymethyl cellulose as a novel P-fertilizer which exhibited enhanced efficiency and lower eutrophication risk than conventional water-soluble calcium phosphate. Therefore the organic matrix could also serve as an electrostatic barrier to hinder the fixation of phosphate nanoparticles in soil, principally in those with higher contents of humic acid as reported by Wang et. al. (2012).[120]

Organic matrices used in the formation of nanocomposites must necessarily be compatible with the hydrophilic surface of the phosphate nanoparticles, and it is also desirable that the matrix/phosphate nanoparticles formulation could be continuously processed, e.g. by extrusion. Two interesting candidates to be used as a matrix are urea and thermoplastic starch. Urea is a water soluble compound and the main N-fertilizer used for agricultural crops, while thermoplastic starch has lower solubility and has been extensively studied as a polymer matrix of nanocomposites due to its renewable, biodegradable, plentiful and inexpensive aspects.

Hence, the objective of this work was to examine the solubility in water of nano-scaled inorganic phosphate particles and their interactions with matrices of different solubility: urea and thermoplastic starch (TPS). This works further describes how the release process of PO_4^{3-} ions can be tailored by nanocomposite production strategies. The use of nanocomposites could support the further development of a new class of smart fertilizers, which will permit new applications for poorly soluble phosphate mineral phases.

5.3. *Experimental*

Preparation of Nanocomposites Ur/Hap - The nanocomposites were prepared by mixing urea (Ur) and hydroxyapatite (Hap) at different urea/Hap ratios (w.w^{-1} basis) of 1:1 (50% Hap), 2:1 (33% Hap), and 4:1 (20% Hap) according to a urea melt processing method adapted from the method used by Pereira et. al. (2012).[19] The nanocomposite samples were produced using a torque rheometer (Polylab RHEODRIVE Rheomix mixer and OS4) under the conditions of 60 rpm for 10 min at 100 °C. The materials were dried at room temperature for 24 hours. The

nanocomposites were designated as Ur/Hap 1:1, Ur/Hap 2:1, Ur/Hap 4:1 with respect to the urea/Hap mass ratio, respectively.

Preparation of Nanocomposites TPS:Ur/Hap - The thermoplastic starch (TPS) was obtained by a physical mixture of corn starch, urea (Ur) and distilled water at a mass proportion of 56/24/20, respectively. To this blend there was added 1% (w.w^{-1}) of stearic acid and 1% (w.w^{-1}) of citric acid. This final TPS:Ur formulation was processed in a co-rotating double screw extruder (L/D = 40, ZSK-18 Coperion model) equipped with driving and mixing elements. The extruded was setup with 6 heating zones at temperatures of 100, 110, 115, 120 at 130 °C to 120 °C, and rotating speed of 150 rpm to obtain TPS:Ur blends in the form of pellets. The TPS:Ur/Hap nanocomposites with Hap mass contents of 50, 30 and 20% were synthesized by premixing and processing the powders (starch, urea, stearic acid, citric acid, and Hap) by extrusion under the same processing conditions used for the pure TPS:Ur blend. The samples were named as TPS:Ur/Hap 1:1, TPS:Ur/Hap 2:1 and TPS:Ur/Hap 4:1, respectively.

Characterizations

Size measurements - Dynamic light scattering (DLS) analyses were carried out on a High Performance Particle Zeta Sizer (Malvern Instruments) to obtain the average particle sizes. 1 mg of Ur/Hap nanocomposite sample was transferred to a 25 ml glass bottle, which contained 10 ml of distilled water. Before the DLS measurements, the solution was sonicated (Bransom 450 W) for 10 min in order to disperse the Hap particles within the solution. For the TPS-based nanocomposites, the samples were kept in liquid nitrogen until complete freezing, and then ground with the aid of a mortar and pestle. About 1 mg of sample powder was placed into 10 ml of acetone and sonicated under equal conditions prior to the DLS measurements.

X-ray diffraction - A Shimadzu XRD6000 diffractometer was used to conduct X-ray diffraction analyses (XRD) of the nanocomposites. The relative intensity was registered in a diffraction range (2θ) of 3-40°, using a Cu-Kα incident beam (λ=0.1546 nm). The scanning speed was 1° min^{-1}, the voltage and current of the X-ray tube were 30 kV and 30 mA, respectively.

Scanning electron microscopy - The morphology of the samples was analyzed by means of scanning electron microscopy (SEM) using a JEOL microscope model JSM 6510. The samples were dispersed over a carbon tape pasted on the surface

of a metallic disc (stub). Then, the disc was coated with carbon in a Leica EM SCD050 chamber and imaged using the secondary electron mode.

X-ray Computed Micro-tomography - A pellet of each sample was placed in a rotating steel support and analyzed on a micro-tomography scanner (model 1172, SkyScan). The image acquisition process was conducted using the following parameters: unfiltered, spatial resolution (voxel size) of 2 μm, 0.3° step rotation, 180° rotation and 6 frames for average process (averaging).The image reconstruction process of the tomographic sections was done by using the NRecon software (SkyScan) in which the following parameters were used: smoothing -5; ring artifact correction -5, and beam hardening correction of 60%.

Solubility Tests

Phosphate release rate in acid solution - Previously, an apparatus was arranged by placing a known mass of each sample inside dialysis membranes (Sigma-Aldrich, St. Louis, MO, USA) with dimensions of 15 cm x 7.5 cm which were immersed into a becker (500 mL) with citric acid solution 2% (w.w^{-1}), incubated and kept in a chamber at controlled temperature of 25 °C (347 Fanem CD). Aliquot parts (1 mL) were collected at different time intervals up to 144 hours. The phosphate quantifications were performed in triplicate. Concomitantly, it was also performed a test using only pure hydroxyapatite as a control experiment. The determination of phosphorus was based on the method reported by Murphy and Riley (1962)[121] which consists of an acidified solution of ammonium molybdate (Synth, Diadema, SP, Brazil) containing ascorbic acid (Synth, Diadema, SP, Brazil) and a small amount of antimony, which causes the formation and reduction of phosphomolybdic acid. The maximum absorption of the phosphomolybdenum blue formed in the presence of antimony occurs at a wavelength of 880 nm.

Urea release rate in acid solution - Urea solubilization experiments were performed simultaneously with the phosphorus solubilization tests, according to a method adapted from Tomaszewska and Jarosiewicz (2002).[55] The concentration of urea in solution was determined by UV-Vis spectrophotometer (Shimadzu-1601PC).[56] Each measurement was done in triplicate under identical experimental conditions for each sample.

5.4. *Results and discussion*

X-ray diffraction (XRD) results for pure Hap and Ur, and their corresponding nanocomposites are shown in FIGURE 5.1. The XRD patterns of all Ur/Hap nanocomposites displayed peaks ascribed to the Hap nanoparticles.[122] It can be seen the presence of a peak at 11 of 2ɵ in the pure Hap pattern which is related to the Hap lamellar phase.[123–126] This peak was absent in the nanocomposite patterns probably due to intercalation of urea into the lamellar space of Hap. As showed by Zuo et. al. (2009)[126] the intercalation with DNA resulted in a remarkable reduction of this peak, with some displacement. This strategy is the same used to analyze polymer clay nanocomposites, where the (001) space in clay is analyzed through XRD.[127,128] The XRD pattern of pure Ur exhibited a set of peaks at 23, 25, 29, 32, 36, 37 of 2ɵ, which were still present, even showing lower intensity, in the XRD patterns of the nanocomposites. The decrease of the urea peak intensity can be explained by the chemical interactions between Ur and Hap as previously reported by Kottegoda et. al. (2011)[129] The further analysis of the peak at 22 of 2ɵ strongly indicates the breakdown of the urea crystalline structure due to strong interactions with the Hap nanoparticles (FIGURE 5.1b). Then, one can expect that the XRD patterns, as well as other characterizations, are very influenced by this urea domains, which have the same features of pristine urea. Since the patterns reveal some small modifications in peak at 22–22.5º, this notices that the urea crystallization process was affected by Hap addition, but probably only in the interfaces. In Ur/Hap 4:1, better Hap dispersion probably affected by the higher interface area, as seen by the relative Hap size (as seen in FIGURE. 5.3). In Ur/Hap 1:1, Hap agglomeration indicated lower interface areas, which is consistent to the other characterizations.
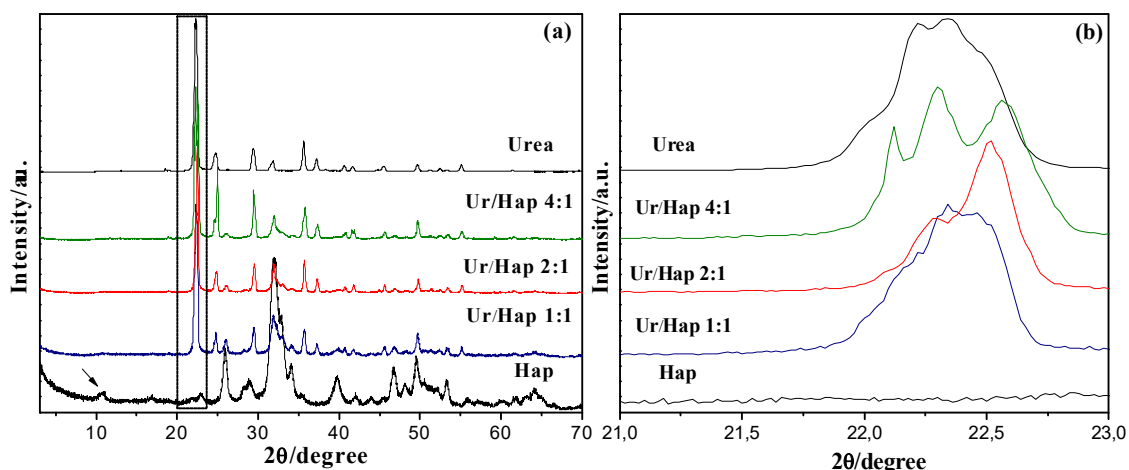
FIGURE 5.1.(a) XRD patterns of pure Hap, pure Urea and Ur/Hap nanocomposites; (b)expanded region of the peak at 22° relating to urea in the Ur/Hap nanocomposites.

Scanning electron microscopy (SEM) was applied to characterize the morphology of the pure Hap and Ur/Hap nanocomposites (FIGURE 5.2). The Hap nanoparticles (FIGURE 5.2a were seen as solid agglomerates of very small nanoparticles (smaller than 100 nm) with atypical round-like morphology. The morphology of the Hap nanoparticles remarkably changed for each nanocomposite sample (FIGURE 5.2b-d), which may be a result of the urea intercalation process as observed by Pereira et. al. (2002).[19] In fact, the best dispersed structure was observed for the Ur/Hap 4:1 nanocomposite sample, which consisted of Hap nanoparticles separated by large domains of Ur. The Ur domains was found to be crystallized in the nanocomposite structure which supports the hypothesis that urea acted as a host matrix for the Hap nanoparticles. These results are concordance with the more intense Ur peaks in the Ur/Hap nanocomposites observed by XRD (FIGURE 5.1).
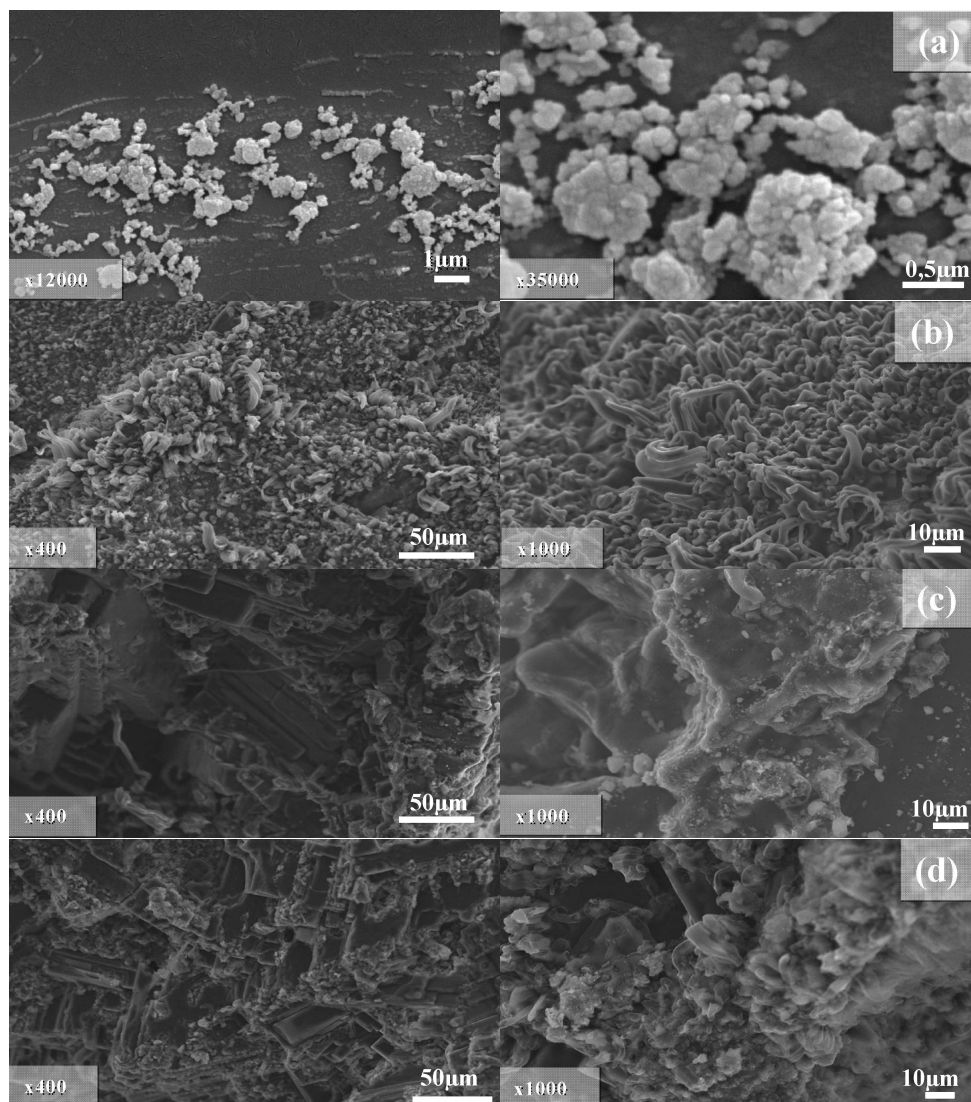
FIGURE 5.2.SEM images of (a) pure Hap and the Ur/Hap nanocomposites (b) Ur/ Hap 1:1, (c) Ur/Hap 2:1, and (d) Ur/Hap 4:1.

The phosphate solubility could be potentially increased by diminishing the size of its particles or by improving the dispersion of the particles, since the particle solubility of the particles depends on its size.[130] Since mineral phosphates have low solubility in water, turning them into very well dispersed small particles could promote an increase of surface area to interface the soil, consequently increasing the phosphate release rate. Complete solubilization of Ur was observed when the Ur/Hap nanocomposites were immersed into water, finely dispersing the Hap nanoparticles to the aqueous medium. Accordingly, it was possible to verify the influence of the Hap agglomeration concerning the different degrees of dispersion of the Hap nanoparticles within the nanocomposites matrix. The size of the Hap nanoparticles was determined by DLS for all nanocomposites samples after dissolution in water (FIGURE 5.3). It can be

observed that the original agglomerates in pure Hap exhibited an average size of 618 nm. This is the largest size of agglomerates of Hap nanoparticles that could be found in the nanocomposite samples, as earlier observed by SEM (FIGURE 5.2).
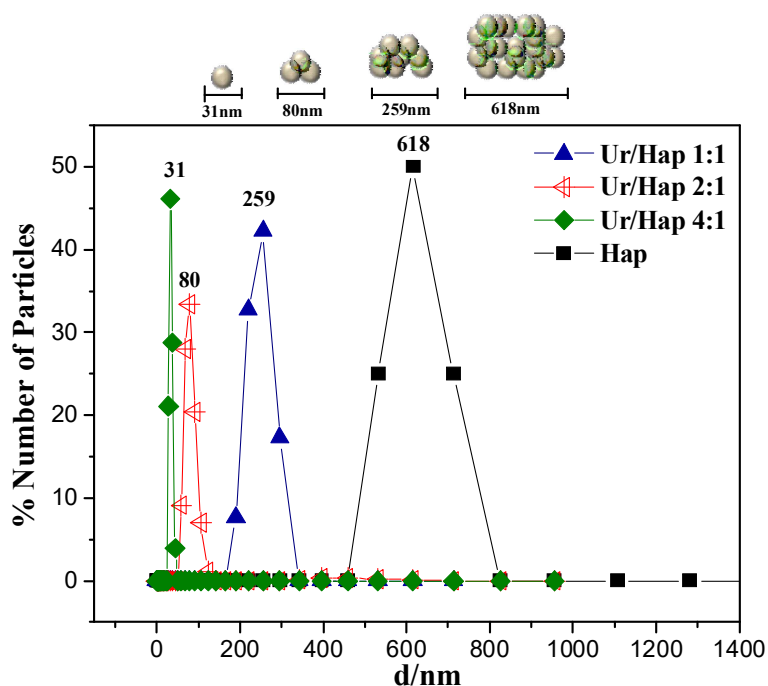
FIGURE 5.3.Influence of the Ur content on the Hap particle size. The scheme shows the state of aggregation of the Hap nanoparticles in the Ur/Hap nanocomposites.

It was also suggested by SEM that the Ur matrix was able to reduce the Hap agglomeration because of the dispersion and immobilization of the Hap nanoparticles over its surface. DLS measurements further confirms this observation as the average Hap particle sizes for the nanocomposite samples Ur/Hap 1:1, Ur/Hap 2:1 and Ur/Hap 4:1 were found to be 249, 80, and 31 nm, respectively. Thus, the size of the Hap nanoparticles may be directly related to the content of Ur in the Ur/Hap nanocomposites, that is, the larger the urea content the smaller the Hap nanoparticles size. Possibly, the Hap nanoparticles were separated from each other by the continuous Ur domains, which ultimately prevented re-agglomeration of Hap in the nanocomposite, as illustrated in the scheme of FIGURE 5.3.
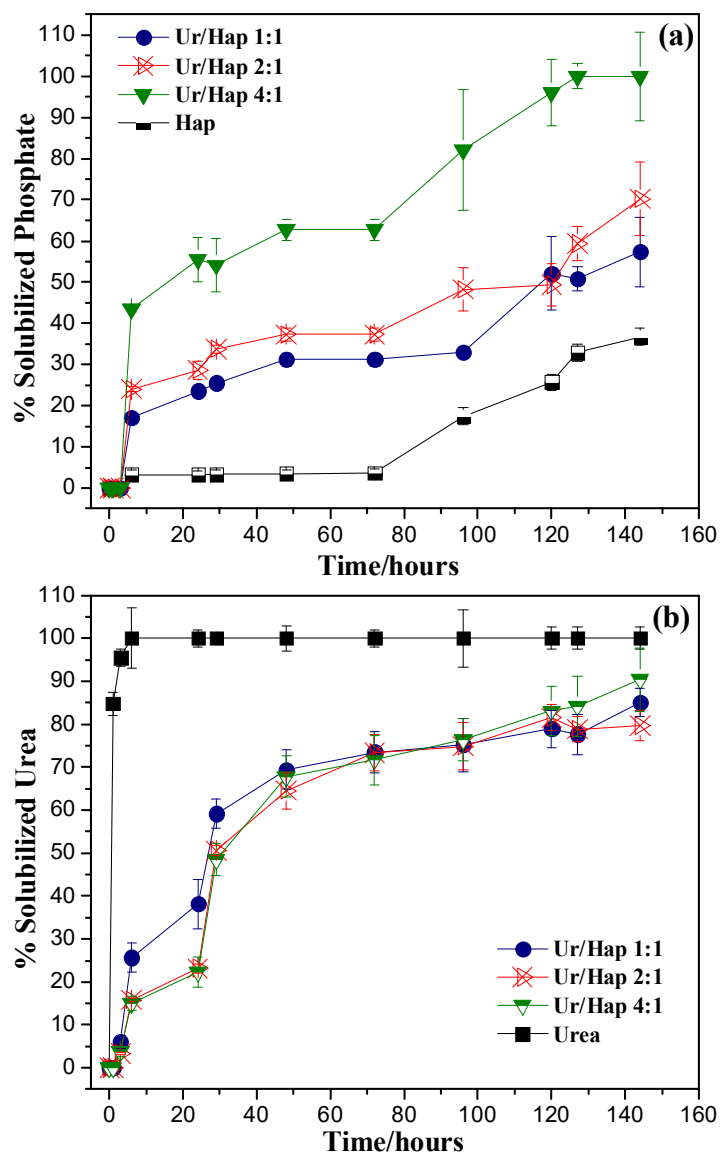
FIGURE 5.4.Solubilization rate of phosphate and urea as a function of time for pure Hap, pure Ur and Ur/Hap nanocomposites. Tests were done at pH 2 and temperature of 25 °C.

FIGURE 5.4a shows the phosphate release trend for the produced Ur/Hap nanocomposites in comparison with pure Hap. It can be noted that pure Hap has a low solubilization rate in acid medium, reaching only 37 % of solubilized phosphate over 144 hours. By analyzing the nanocomposite behavior, it may be noted that all formulations showed higher phosphate release rates compared with pure Hap, for example 60 % for Ur/Hap 4:1. A particular aspect is the kinetics observed for each system. It can be observed that there was a clear correlation between the agglomeration degree of the Hap nanoparticles and the percentage of released phosphate. The sample

with smallest Hap particle size (Ur/Hap 4:1) exhibited the highest phosphate solubilization extent (100%). This result was clearly followed in extent by those found for the Ur/Hap 2:1 and Ur/Hap 1:1 nanocomposite samples, which displayed Hap particles sizes gradually larger, and consequently released 70 % and 50 %, respectively, of their total phosphate content.

The use of urea as a host matrix for Hap was interesting because of its high solubility in water and high commercial importance in agriculture. Thus urea release tests were also done for the Ur/Hap nanocomposites, as depicted in FIGURE 5.4b. The total dissolution of pure Ur occurred within 3 hours due to the saturation of the solution around the urea granule surface. However, it can notice that all nanocomposite samples presented a delayed urea solubilization of up to 144 hours. It may be suggested that the interfacial chemical interactions between Ur and Hap (urea adsorption) are responsible for the delayed dissolution of the Ur matrix, considering the fact that urea was not totally free to react with water.

It is worth mentioning that the urea dissolution tests (complete immersion) were performed under very aggressive conditions. Even so the Ur release rates were comparable to values found for other controlled release systems designed with basis on different concepts, as observed by Wu and Liu (2008)[131] for polymeric coatings in NPK granules. This denotes that the values found for the Ur/Hap are promising. In conventional application conditions, the samples would be exposed to low water contents, and one can expect a better urea retention effect for the Ur/Hap nanocomposites.

In order to analyze the influence of the matrix solubility on the phosphate release rate, similar amounts of Hap were dispersed in a TPS:Ur blend matrix. FIGURE 5.5 shows the XRD patterns of the pure components (TPS, Hap, Ur) and TPS:Ur/Hap nanocomposites containing different contents of Hap.
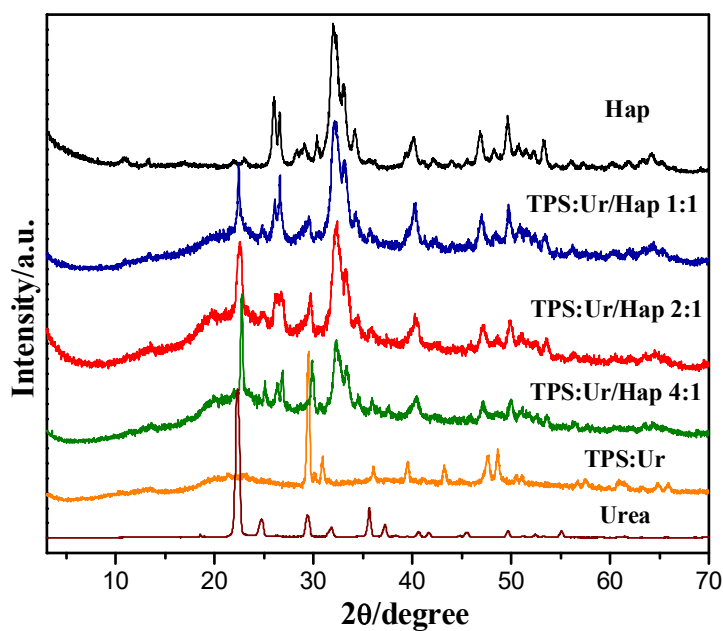
FIGURE 5.5.XRD patterns of Hap, pure TPS:Ur blend and nanocomposites TPS:Ur/Hap 1:1, TPS:Ur/Hap 2:1, and TPS:Ur/Hap 4:1.

Peaks associated with the granular native starch were not observed in the XRD pattern of the pure TPS:Ur blend, indicating that the extrusion process successfully produced a continuous matrix. Only peaks related to the presence of urea crystals can be seen in the XRD pattern of the pure blend. Furthermore, peaks related to the presence of Ur and Hap were notice able in the XRD patterns of the TPS:Ur/Hap nanocomposites. There was also a halo between 5 and 20° of 2θ which is related to the amorphous TPS portion of the nanocomposites. It is also observed a peak at approximately 22° of 2θ which can be ascribed to the presence of free urea domains in the polymeric network of TPS.[132]
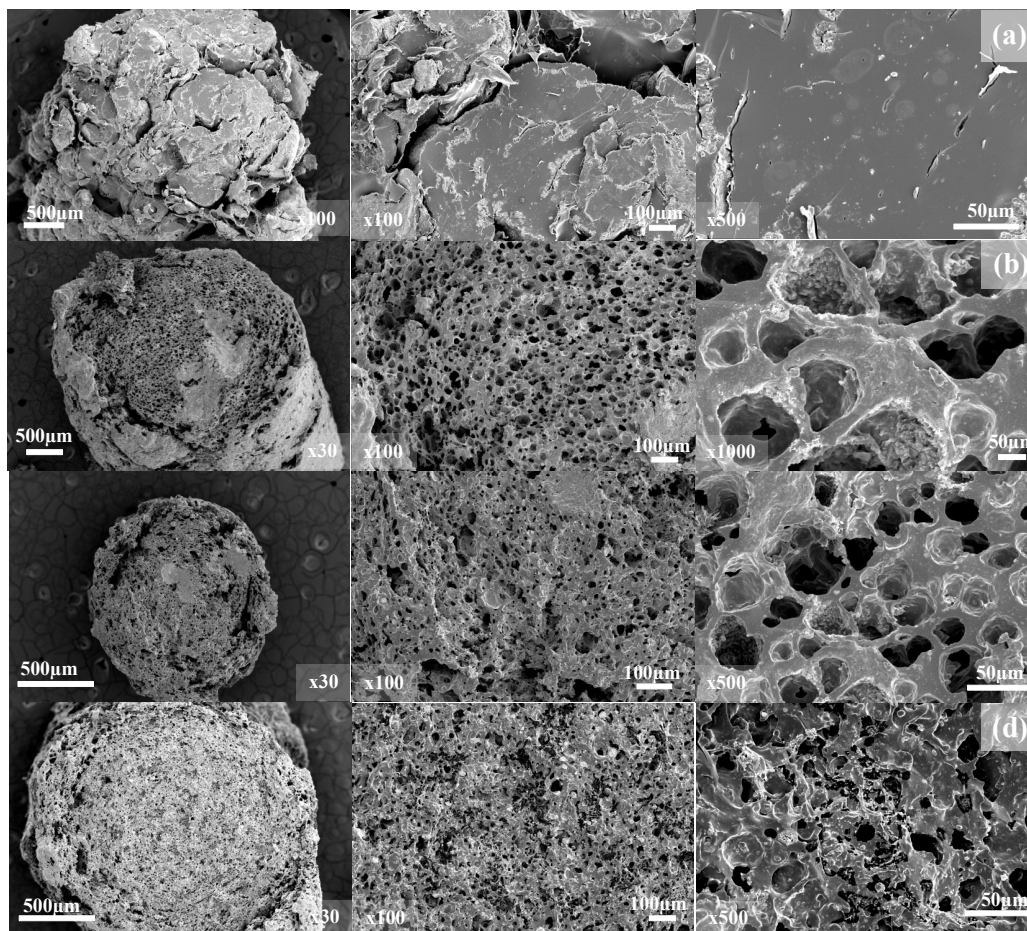
FIGURE 5.6.SEM images of pure TPS:Ur (a), nanocomposites TPS:Ur/Hap 1:1 (b), TPS:Ur/Hap 2:1 (c), and TPS:Ur/Hap 4:1 (d).

The complete disruption of starch is verified in FIGURE 6a by the occurrence of a continuous material with smoothed surface.[94] Large Ur crystals were not observed in the SEM image of the TPS:Ur blend, indicating that they were well embedded into the TPS structure. It was visibly observed that Hap played an important role on the TPS:Ur/Hap nanocomposite morphology evolution: all nanocomposites showed a porous architecture (FIGURE 5.6b-d), which is probably because of the release of moisture from starch during the extrusion process, generating structural voids controlled by the nanocomposite mechanical resistance – which is possibly related to different Hap amount. A good chemical compatibility between the TPS and Hap is suggested by the homogeneous phase material resulting from the mixture between TPS (matrix) and the Hap nanoparticles.

In order to examine the porous structure of the TPS:Ur/Hap nanocomposites, a non-destructive X-ray tomography analysis was carried out. In this

case, a full 3D image of internal structure of the samples was generated, which was useful to analyze the internal porosity resulting from the extrusion process.
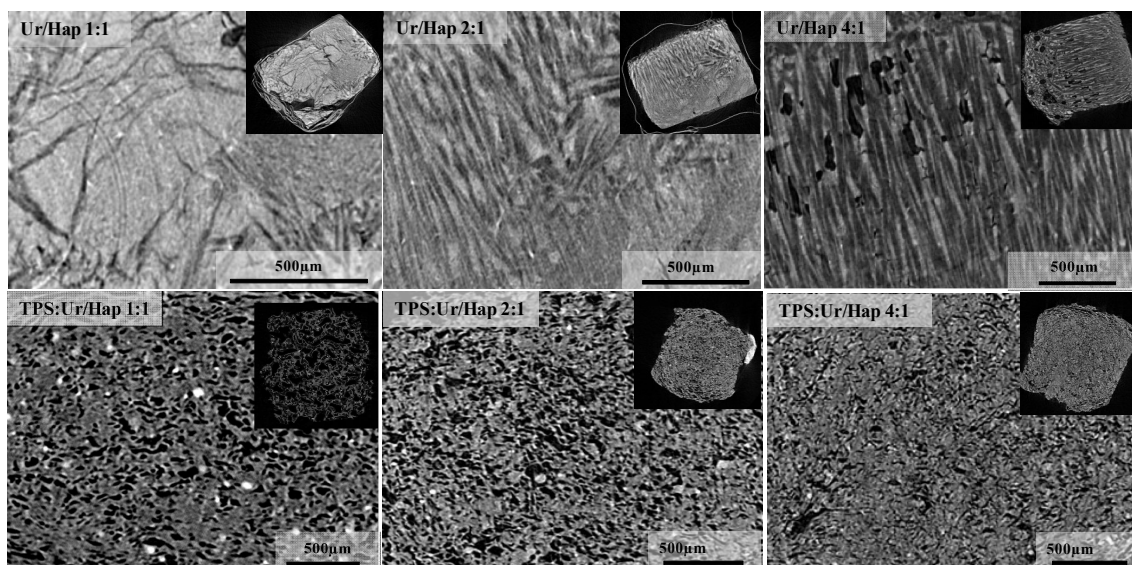
FIGURE 5.7.Cross-sectional images of the nanocomposites Ur/Hap and TPS:Ur/Hap/ obtained by X-ray micro-tomography.

Typical cross-sectional views shown in FIGURE 5.7 revealed that the presence of Hap was responsible for the formation of large porous in the structure of the TPS:Ur/Hap nanocomposites. The Ur/Hap nanocomposites were found to possess a dense microstructure, which was in accordance with the processing conditions used (Hap incorporation from melted urea). It is then expected that the large porosity of the TPS:Ur/Hap nanocomposites will facilitate the release of phosphate, since this will increase the total surface area accessible for dissolution. On the other hand, the compact structure of the Ur/Hap nanocomposites confirms that the Hap dissolution is driven by a previous dissolution of the Ur matrix.

FIGURE 5.8 displays the particle size distribution of Hap present in the TPS:Ur/Hap nanocomposite after complete dissolution in water. It is verified that the pure TPS:Ur matrix imparted a similar dispersion effect on Hap as that found in the case of the pure Ur host matrix. The Hap particle size decreased by approximately 85 % in comparison with pure Hap. There was no significant difference between the average size values found for the TPS:Ur/Hap nanocomposites. The result can be explained by re-agglomeration of small portions of Hap particles after dissolution of the nanocomposites, as illustrated by the drawing in FIGURE 5.8.
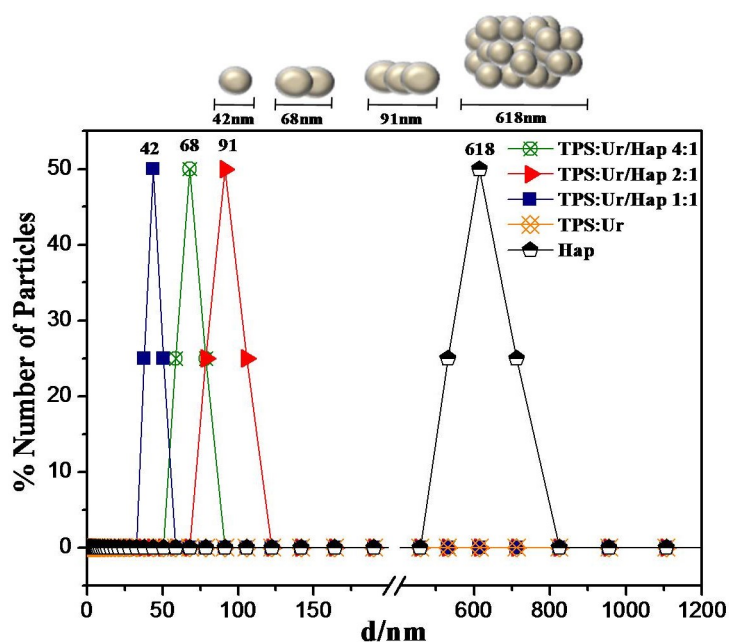
FIGURE 5.8.Distribution of Hap particle size of Hap occurring in the TPS:Ur/Hap nanocomposites.

The phosphate release evolution for the TPS:Ur/Hap nanocomposites in acid solution over time is presented in FIGURE 5.9a. All the TPS:Ur/Hap nanocomposites exhibited initial phosphate release faster than that observed for the Ur/Hap nanocomposites. The samples TPS:Ur/Hap 4:1, 2:1 and 1:1 presented phosphate release percentages of 90, 57 and 32 % after 24 hours, respectively. The largest phosphate percentage released both at initial and equilibrium point was noted for the nanocomposite containing the lowest content of Hap nanoparticles, probably due to the high hydrophilicity of the TPS:Ur matrix.

The different values found for the solubilization of phosphate are related to strong interactions between the TPS and Hap, and the high dispersion degree of the Hap nanoparticles within the TPS:Ur matrix. These interactions could have acted as a chemical barrier against the phosphate solubilization. It can also be observed that the TPS:Ur/Hap 1:1 sample presented a phosphate release similar to that of pure Hap. Furthermore, it is also noted the physical barrier effect imposed by the Hap nanoparticles, since the phosphate release rate was fully related to the swelling degree of the starch granules.

Urea release experiments were further conducted for the TPS:Ur/Hap nanocomposites (FIGURE 5.9b). All nanocomposites released Ur in a manner slower than the Ur solubilization. Additionally, it is verified that the nanocomposites

containing high Hap contents presented a delayed urea release at same time, suggesting that the Hap nanoparticles acted as a physical barrier against the Ur solubilization.
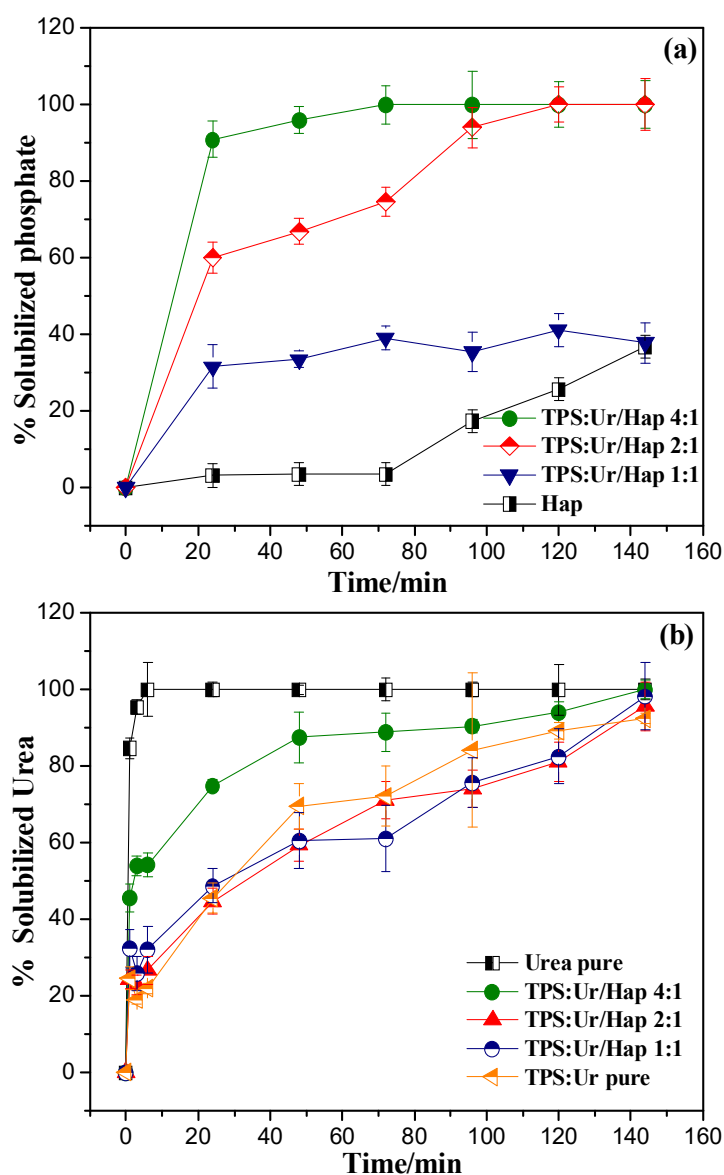
FIGURE 5.9.Phosphate solubilization rate (a) and urea solubilization rate (b) at 25 °C and pH 2 as a function of time for pure Hap, pure Ur, and TPS:Ur/Hap nanocomposites.

A comparison between both types of nanocomposites developed in this study revealed that the TPS:Ur/Hap nanocomposites presented faster releases of phosphate and urea than the Ur/Hap nanocomposites, which are probably due to the water accessibility through their highly porous matrices. Also, the TPS:Ur/Hap nanocomposites depicted a matrix less hydrosoluble and more rigid than Ur, meaning that the Hap nanoparticles were probably better isolated within their structure. Observing the release behaviors, one can notice different trends of diffusion between

the Ur/Hap and TPS:Ur/Hap nanocomposites. A comparison between the phosphate release curves also allowed ascertaining which diffusion model driven the solubility of each nanocomposite. The release involves several mechanisms, including desorption from the surface of the polymeric matrix, diffusion of the active compound through the pores of the polymer matrix or the polymer wall, the disintegration of the nanoparticles and subsequent release of the active compound, and dissolution and erosion of the matrix or wall. TABLE 5.1 shows the constant values obtained according to the equation proposed by Rigter and Peppas (1987),[134] whose the kinetic parameter settings are given by Equation 1:

$$M_t/M_{eq}=Kt^n \qquad \text{(Equation 5.1)}$$

where t is the time, K is the diffusion constant that depends on the type of material and the permeation medium, n is the difusional exponent which gives information about the type of transport mechanism for a given solute, and M_t and M_{eq} are the phosphorous concentration released at a time t and at the steady state, respectively. The parameter n values typically range from zero to one, where values of 0.5 correspond to a typical difusional release process and values of 1 means a zero order kinetic process. The n values greater than 1 indicate that the release is highly retained by a strong barrier, so that the total dissolution of the solute to the medium occurs at an infinite time.[135] Despite the Rigter and Peppas equation has been normally used to explain the slow/controlled release of molecules hosted by polymeric spheres, it can be used in the present case as an indicative of the real solubility of the Hap nanoparticles when shielded by the Ur and TPS:Ur matrices. In fact, since the solubilization is a difusional process, Equation 5.1 estimates the effect of the host matrix on the phosphate release.

TABLE 5.1. Kinetic parameters of phosphate release obtained by the Rigter and Peppas model.

Materials	n	K (s^{-1})
Hap	2.200±0.326	0.000689
Ur/Hap 4:1	0.3350±0.051	18.3707
Ur/Hap 2:1	0.4508±0.084	6.9374
Ur/Hap 1:1	0.4729±0.087	4.9760
TPS:Ur/Hap4:1	0.0538±0.011	77.6700
TPS:Ur/Hap 2:1	0.3373±0.051	19.1463
TPS:Ur/Hap 1:1	0.1220±0.047	21.4819

The very low *K* value for pure Hap, along with the high n exponent is an indicative of low solubility of Hap under the experimental conditions. Despite the *n* value does not have a specific meaning, this can be interpreted as the high barrier for bare solubility in agglomerated powders, which was expected for Hap. For Ur/Hap nanocomposites, the *n* values approached 0.5, which indicates a classical diffusion mechanism, expected for freestanding nanoparticles (as proposed here). The *K* values were in accordance with the Hap content, i.e., higher Hap contents indicate lower release rates, as expected. On the other hand, the TPS:Ur/Hap nanocomposites showed much higher *K* values, which can be interpreted as a faster phosphate release when compared with the Ur/Hap nanocomposites. However, the lower *n* values (below 0.5 and without a clear tendency) show that the TPS played a role in prolonging the phosphate release time, which is probably associated with the swelling of the TPS:Ur matrix after some period of immersion into water. In fact, this is possible because the porous structure of the TPS:Ur/Hap nanocomposites can facilitate the release of phosphate at short times, but the structure is likely to be modified by swelling, obstructing the water transport over longer times. In this case, it is noticeable that the TPS:Ur/Hap 4:1 sample presented a *n* value close to zero, which is interpreted as a zero-order dissolution mechanism – close to that expected for very soluble phosphate sources.

5.5.   *Conclusions*

In summary, our experiments showed the role played by the agglomeration of mineral phosphate powders on the effective solubilization of phosphate (i.e., phosphate release), demonstrating that it is possible to tailor a nanocomposite by finely dispersing hydroxyapatite (assumed here as a model for mineral phosphate fertilizers) within two matrices with different levels of hydrosolubility. The matrix solubility was found to be less important than the water accessibility in the nanocomposite structure, since the porous TPS:Ur matrix exhibited better phosphate release when compared with a dense urea matrix. However, it is important to notice that both types of host matrices are innovative, since TPS:Ur/Hap nanocomposites may provide a very fast phosphate release, whereas Ur/Hap nanocomposites enable an appropriate phosphate release with a delayed urea solubilization. The Hap-loaded nanocomposites are also interesting coupled fertilizers, since both components have nutritional effect in agricultural crops (i.e., as a source of P

and N). These results could support the development of a new class of smart fertilizers, which can open new ways of applications for poorly soluble phosphate mineral phases.

6. Chapter IV: How Soil Intrinsic Features affect Nanocomposites Nutrient Availability

The content of this chapter is an adaptation of the article entitled **"Role of Slow-Release Nanocomposite Fertilizers on Nitrogen and Phosphate Availability in Soil"** by Amanda S. Giroto, Gelton G. F. Guimarães, Milene Foschini and Caue Ribeiro, published in Scientific Reports.

Reference: Sci. Rep., 2017, 7, 46032.

Role of Slow-Release Nanocomposite Fertilizers on Nitrogen and Phosphate Availability in Soil

Amanda S. Giroto[1,2], Gelton G. F. Guimarães[2], Milene Foschini[2] & Caue Ribeiro[2]

6.1. Abstract

Developing efficient crop fertilization practices has become more and more important due to the ever-increasing global demand for food production. One approach to improving the efficiency of phosphate and urea fertilization is to improve their interaction through nanocomposites that are able to control the release of urea and P in the soil. Nanocomposites were produced from urea (Ur) or extruded thermoplastic starch/urea (TPSUr) blends as a matrix in which hydroxyapatite particles (Hap) were dispersed at ratios 50% and 20% Hap. Release tests and two incubation experiments were conducted in order to evaluate the role played by nanocomposites in controlling the availability of nitrogen and phosphate in the soil. Tests revealed an interaction between the fertilizer components and the morphological changes in the nanocomposites. TPSUr nanocomposites provided a controlled release of urea and increased the release of phosphorus from Hap in citric acid solution. The TPSUr nanocomposites also had lower NH_3 volatilization compared to a control. The interaction resulting from dispersion of Hap within an urea matrix reduced the phosphorus adsorption and provided higher sustained P availability after 4 weeks of incubation in the soil.

6.2. Introduction

Nitrogen (N) and Phosphorus (P) are two important macronutrients responsible for the growth and yield of agricultural crops. Developing efficient fertilization practices has become more and more important due to the ever-increasing global demand for food products. About 40–70% of N and 80–90% of P applied as normal fertilizers are lost to the environment or chemically bound in the soil and are unavailable to plants.[132,136-139]. These losses come at a large economic and environmental cost. The low efficiency of P fertilizers is attributed to the formation of Fe- and Al-based oxides, especially in tropical soils. Most of the P released from organic matter and that added as fertilizer is rapidly scavenged by soil minerals and turned into fixed or insoluble inorganic compounds that are not susceptible to leaching[140]. Thus, soil PO_4^{3-} concentrations are typically very low (less than 0.01 to 1.00 ppm)[141,142]. On the other hand, high NH_3 volatilization due to a rapid hydrolysis of urea, leads to an accumulation of NH_4^+ and increase the soil pH.

Recently, the use of slow release fertilizers (SRF) has been considered to be a promising strategy to improve the utilization of macronutrients.[132,143,144] Slow-release fertilizers have many advantages over conventional fertilizers, confirmed in different cultures such as improved fertilizer use efficiency in potato,[145,146] better matching of nutrient demand in crops,[147] and increased P recovery in barley.[148] Many studies propose novel developments, such as attapulgite-based fertilizers[149,150] or urea-templated oxalate-phosphate-amine a novel slow-release fertilizer.[140] The overall effect is that less fertilizer is needed which lowers the potential negative effects from over-fertilization.[90,151] Beyond this, slow release fertilizers are designed to release their nutrient contents gradually in order to coincide with the nutrient requirement of plants. These fertilizers can be physically prepared using engineered matrices as a way to control their release rate.[21,143] Currently, degradability of attention towards environmental protection issues.[152] Furthermore, matrices must be compatible with the surface properties of fertilizers, i.e., they should be hydrophilic. As previously proposed by our group,[21] interesting candidate matrices for SRF are thermoplastic starch and urea. Urea is one of the most important synthetic fertilizers worldwide due to its low cost and high N content. On the other hand, starch is a cheap, largely available and biodegradable natural polymer that has been extensively used as an encapsulating matrix of agrochemicals. When plasticized by alcohols or even by urea, starch is known as thermoplastic starch (TPS). Composite materials made of starch and urea have not been successfully tested as a conventional urea-based fertilizer displaying a prolonged N release profile.

In addition to controlling the release of urea, the starch matrix could improve the efficiency of phosphate fertilization. The combination of urea and phosphate within a single matrix has the potential of decreasing P fixation in the soil.[141] The high pH created in the starch matrix from the conversion of urea to NH_4^+ may able to change the dynamic of chemical fixation of phosphorus in the soil.[153]. Therefore, the dispersion of phosphate-rich minerals into urea and thermoplastic starch as a nanocomposite produced by extrusion could provide control over the release of urea and increase the availability of P in soil.

In the present work, we report on a strategy to use nanocomposites produced from TPS, urea, and phosphate as a slow release fertilizer matrix. The synergistic roles played by the host matrices in preventing immobilization of phosphate and volatilization of nitrogen when in contact with soil were studied in detail.

6.3.   *Experimental*

Raw materials - The raw materials used in the nanocomposite formulations were: urea (Synth, Brazil), hydroxyapatite (Sigma-Aldrich, USA), Amidex 3001 (Corn Products, Brazil) citric acid (Synth, Brazil), and stearic acid (Vetec, Brazil). A commercial simple superphosphate (SSP) (Heringer, Brazil) was used for comparison purposes. Other materials were used as received.

Preparation of Nanocomposites - The nanocomposites having urea as a matrix were prepared by mixing urea (Ur) and hydroxyapatite (Hap) at 20 and 50 wt.% Hapratios (w.w^{-1} basis) using a urea mixed-melt processing method. The nanocomposites were produced on a torque rheometer (Polylab RHEODRIVE Rheomix mixer and OS4) under conditions of 60 rpm for 10 min at 100°C, and further dried at room temperature for 24 hours. These nanocomposites were designated as UrHap50 and UrHap20.The nanocomposites comprising thermoplastic starch (TPS) as a matrix were obtained from a physical mixture of corn starch, urea (Ur) and distilled water at a mass proportion of 56/24/20, respectively. Stearic acid 1% (w.w^{-1}) and 1% citric acid (w.w^{-1}) were added to this blend. This final formulation was processed on a co-rotating twin screw extruder (L/D = 40, ZSK-18 Coperion model) equipped with conveying and kneading elements. Six heating zones on the extruder were set at temperatures of 100, 110, 115, 120 and 120°C. The extruder was operated with a rotating speed of 150 rpm and the extrudated was extruded through a rod die to obtain TPSUr (TPS+Ur) blends in the form of rods that were subsequently pelletized. The TPSUr/Hap nanocomposites with Hap mass contents of 50 and 20 wt. % were produced by mixing and processing the powders (starch, urea, stearic acid, citric acid, and Hap) by extrusion using the same processing conditions used to obtain the pure TPSUr blend. These nanocomposites were designated as TPSUr/Hap50 and TPSUr/Hap20, respectively. Both types of materials have been previously described by Giroto et. al .(2015).[21]

Characterization of materials - Scanning electron microscopy (SEM) was performed on a JSM6510 microscope (JEOL) (Thermo Scientific NSS coupled or linked). Samples were previously fixed onto carbon stubs and coated with thin layer of gold in an ionization chamber (BALTEC Med. 020). SEM imaging was carried out using the secondary electron mode. Thermal degradation of samples was evaluated in the range 25 °C–600 °C using a Q500 analyzer(TA Instruments, New Castle, DE, USA)

under the following conditions: sample size of 10.0 ± 0.5 mg, synthetic air atmosphere (80% N_2 and 20% O_2) with flow of 60 mL.min^{-1}, and heating rate of 10 °C.min^{-1}.

Release Tests in solution - Determination of phosphorus content was based on the method reported by Murphy and Riley (1962)[122]. An apparatus was arranged by placing different mass of each sample into a beaker with capacity of 600 mL containing citric acid solution 2% (w.w^{-1}) in order to obtain the same final concentration (250 mg L^{-1}) of phosphorus for each material. The mixture was incubated at controlled temperature of 25 °C and agitation of 45 rpm (347 Fanem CD). Aliquot parts were collected at different time intervals up to 144 hours for phosphate quantification in triplicate. Concomitantly, quantifications were performed for tests involving pure Hap and SSP as a control experiment. Urea release experiments were performed parallel with phosphorus solubilization tests according to the method adapted from Tomaszewska and Jarosiewicz (2002)[55].The concentration of urea in solution was determined by UV-Vis spectrophotometer (Shimadzu-1601PC). Each measurement was done in triplicate under identical experimental conditions for each sample.[56] The final concentration of urea (1250 mg.L^{-1}) was also standardized in order to have the same final concentration of urea for all materials.

Release and transformation of Nitrogen in Soil - Release of urea from nanocomposites was evaluated in a Red-Yellow Oxisol which was collected at 20 cm depth at a pasture site in São Paulo. The soil was previously dried in air and sieved through a 2 mm screen. Physical-chemical characterizations provided the following soil parameters: 667 g kg^{-1} (sand), 19 g kg^{-1} (silt) and 314 g kg^{-1} (clay), according to soil texture analysis by the pipette method;[59] water-holding capacity[58] of 140 g kg^{-1}; pH (H_2O) 5.3; organic C content of 7.5 g kg^{-1} by the Walkley-Black method;[57] available P content of 1.9 mg kg^{-1}, total N content of 1.06 g kg^{-1} by Kjeldahl method;[154]; cation-exchange capacity (CEC)[58] of 4.77 cmolc kg^{-1}, remaining phosphorus (P-rem)[155] content of 20 mg L^{-1}, potential acidity[15] (H + Al) of 3.8 cmolc kg^{-1}and urease activity of 9.63 mg urea N hydrolyzed kg^{-1} soil h^{-1} by a modified Tabatabai and Bremner (1972)[60] buffer method. The incubation system used was similar in design to the unit described by Bremner and Douglas (1971)[156] with the modifications proposed by Guimarães et. al. (2016)[78]. Samples of soil (10 g sample) were incubated with urea or nanocomposite at a soil:N ratio of 1000:1 (g.g^{-1}) in polyethylene bottles com capacity of 125 mL. The samples were weight with this amounts (Ur: 21.32 mg.g^{-1}; UrHap20 26.60 mg.g^{-1}; UrHap50 41.70 mg.g^{-1}; TPSUr/Hap20 87.34 mg.g^{-1} and TPSUr/Hap50 118.80 mg.g^{-1}).

Samples were incorporated into the soil which was humidified to 80% of its water retention capacity with the addition of deionized water. A container with 5 mL of 4% boric acid solution was added to the polyethylene bottles for scavenging the volatilized ammonia (NH_3) during the incubation period. Incubation was performed for 0, 1, 3, 7, 14, 25 days under controlled temperature and relative humidity.

Volatilized NH_3 was quantified by titration of boric acid with HCl (0.01 $molL^{-1}$). Mineral N produced during incubation was extracted by shaking the soil sample with 100 mL of KCl ($lmol.L^{-1}$)containing phenylmercuric acetate (5 $mg.L^{-1}$) as a urease inhibitor (soil:solution ratio of 1:10). Afterwards, the suspension was kept under stirring for 1 hour and filtered with slow filter paper (diameter 12.5 cm).The resulting soil extract was stored in 100 mL polyethylene bottles at 5 °C.

The ammonium (NH_4^+) and nitrate (NO_3^-) levels in the soil extracts were determined by the colorimetric methods of Kempers and Zweers (1986)[61] and Yang et. al. (1998)[62], respectively. The contents recovered in each N fraction were expressed as percentages in relation to the N added to soil in the form of urea or nanocomposite. Replicate data of NH_3 were adjusted to the *Logistic model*, which allowed estimating the total content of volatilized N and the time required to volatilize 25% of the N added to the soil. Recovery of N as NH_4^+ in soil was adjusted to the *Rational model*, which permitted estimating the maximum recovery of NH_4^+, time of maximum NH_4^+ recovery, curve tangent at 6 days and the NH_4^+ recovery at the end of the incubation. The adjusted models were presented by their average values and respective standard deviations. Differences between means values were determined by analysis of variance (ANOVA). Duncan´s multiple comparison test was used to compare all pairs of treatments previously determined as significant by the F test. The significance level was set at 0.05.

Release and Availability of Phosphorus in Soil - The release of phosphorus to soil was evaluated using the Red-Yellow Oxisol described in the previous section. Soil samples (50 g $sample^{-1}$) were incubated with Hap, SSP or nanocomposites at soil:P ratio of 5000:1 (g g^{-1}) in 300 mL capacity transparent plastic bags. Distilled water was then added to raise the soil moisture to 80% of its moisture holding capacity. Samples were incubated for 42 days at controlled temperature and relative humidity. Soil moisture was monitored throughout all experiment and distilled water was added to maintain the moisture at 80% when necessary.

After the incubation period, the soil samples were dried in air sieved through a 2 mm screen. The available P was extracted with water and anionic resin as

proposed by Quaggio and Raij (2001).[157] The extraction of P with water was performed at water:soil rate of 1:5). 5 g of soil were stirred in 25 mL of water for 30 min in 50 mL capacity Falcon tubes. After stirring, the suspension was centrifuged at 3000 rpm for 15 min and the supernatant (extract) was collected for available P determinations. This extraction procedure was repeated three times. The contents of P (P-water) and (P-resin) were measured by molecular absorption spectrometry. The available P content of the soil at the initial time of incubation (0 day) was also determined. The pH (H_2O) of soil was measured (soil:water ratio, 1:2,5) with a glass electrode of samples at initial time (0 day) and 42 days after incubation.

Available P contents were expressed as a percentage of the total P applied to the soil. The percentages of P extracted with water were expressed as a sum of three successive extractions. Differences between means values were determined by analysis of variance (ANOVA) and F test. Differences between pairs of treatment means were determined by Duncan-test at significance level of 0.05.

6.4. *Results and discussion*

TABLE 6.1 shows the content of P and N in the pure urea, single superphosphate (SSP), hydroxyapatite (Hap) and in the nanocomposites. The nanocomposites presented reduced of nutrient contents in relation to the original materials due to incorporation of Hap in urea or TPSUr polymer. Their N and P contents were verified to fall between 3 and 8% and from 8.4 to 38%, respectively, which are amounts comparable to those comprised in commercial fertilizers.

TABLE 6.1.The content of P and N in the nanocomposites.

Composites Fertilizers	P (g Kg^{-1})	N (g Kg^{-1})
Urea	-	450
SSP	100	-
Hap	150	-
UrHap50	80	240
UrHap20	40	380
TPSUr/Hap50	50	84
TPSUr/Hap20	30	115

FIGURE 6.1 shows SEM images of the nanocomposites, as well as the morphologies of pure Hap and SSP (materials used in control experiments). As observed in FIGURE 6.1a, Hap powder is comprised of nanometric particles with agglomerate sizes around 100 – 300 nm. SSP powder is characterized by micrometric

agglomerates, FIGURE 6.1b. However, careful observation of FIGURE 6.1b reveals the nanometric structure of SSP which is characterized by many small particles in the agglomerate. These features may influence the solubilizing profile of both materials since the dissolution dynamics is dependent on the surface accessibility – which is related to particle size. In FIGURE 6.1(c), the characteristic morphology of urea appeared crystallized as platelets with sizes larger than 100 μm. The SEM micrograph of TPSUr in FIGURE 6.1d exhibits a relatively homogeneous surface, indicating the efficiency of urea in plasticizing starch.
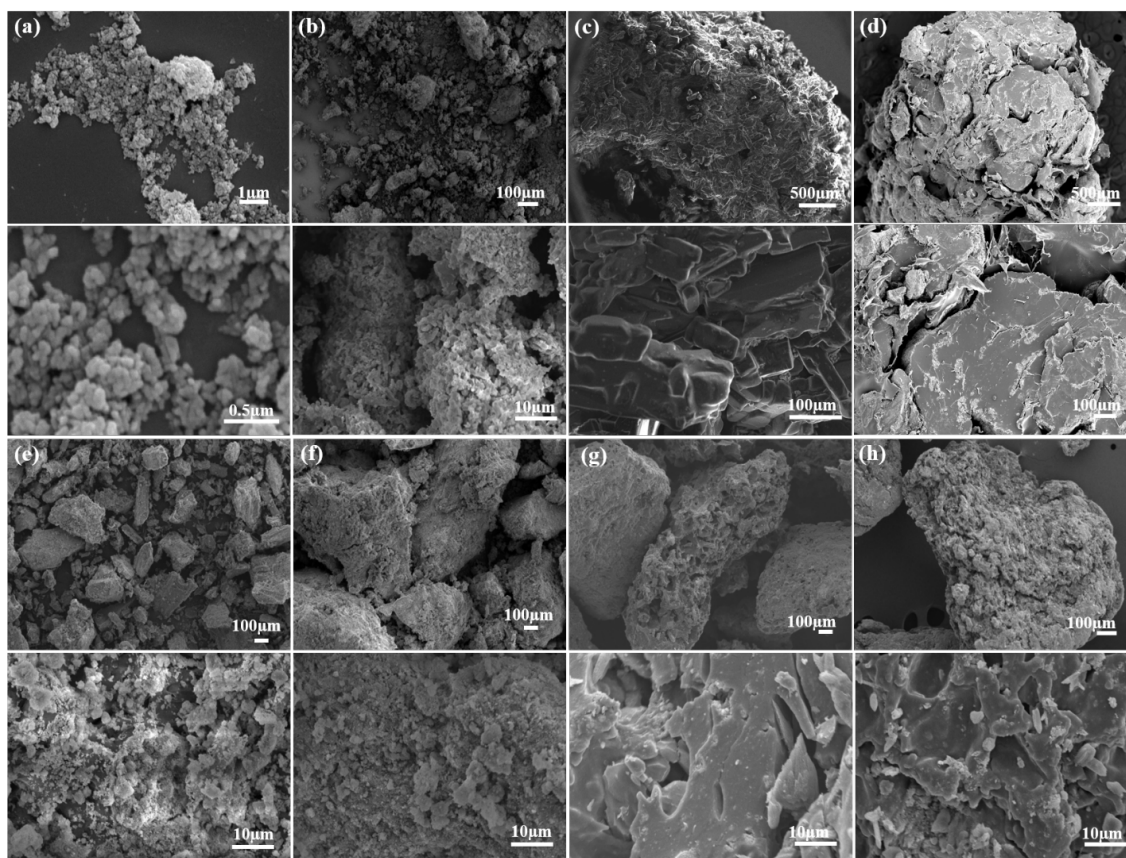
FIGURE 6.1.SEM images of the materials precursors (a) Hap, (b) SSP, (c) Urea, (d) TPSUr, (e) UrHap20, (f) UrHap50, (g) TPSUr/Hap20 and (h) TPSUr/Hap50.

All nanocomposites showed a complex structure, which is clearly seen in FIGURES 6.1e, f, g, and h. TPSUr and urea matrices produce a continuous phase in which Hap nanoparticles are embedded, and generally, phase separation is not observed. In this case, the nanocomposite samples can be assumed to be homogeneous, although TPSUr is characterized by a continuous, porous structure, whereas urea produces a more granular, friable matrix – as seen by the small particle sizes obtained.
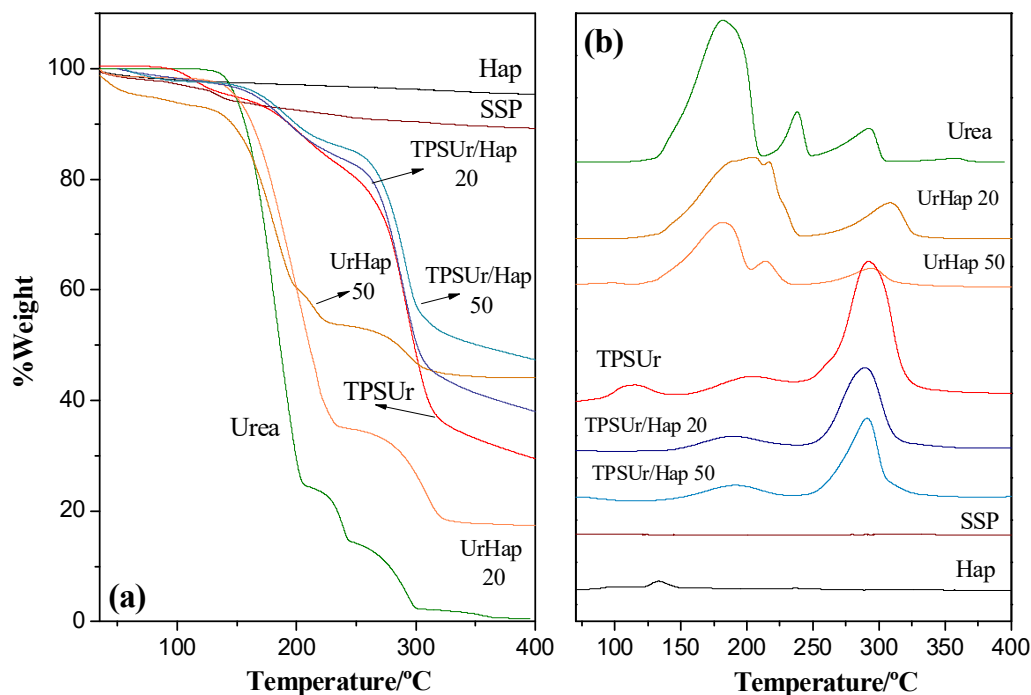
FIGURE 6.2.(a) Thermogravimetric analysis of materials and (b) derivate.

FIGURE 6.2 shows the thermogravimetric profiles of the precursors materials and nanocomposites. It is possible to see that Hap presents a weight loss of only 5% while SSP has a maximum weight loss of 10%.[26] These thermal events are related to elimination of physically bonded and structural water molecules (FIGURE 6.2a). TPSUr shows the typical degradation curve of urea-plasticized starch with appearance of a final residue content of 30%, possibly due to strong interaction between urea and starch.[34,35]. Four of the most significant decomposition stages of pure urea were identified by Chen and Isa (1998).[98] The first weight loss starts at 118 °C before the urea melting point (133 °C) until complete urea oxidation at around 380 °C. The nanocomposite UrHap50 shows a thermal degradation behavior largely represented by the urea degradation, thus showing the same degradation temperatures. The nanocomposite UrHap20 comprised the lowest Hap content but presented the highest dispersion of urea within the matrix. This proves that high Hap dispersion accounted for the increased thermal stability of the nanocomposites, as seen from the changes in the temperature of the first urea degradation stage, at about 20 °C, in FIGURE 6.2(b). This behavior is due to strong interactions between Hap nanoparticles and urea, as signs of degradation related to free urea are not observed in the thermal profiles of the nanocomposites. TPSUr/Hap 50 and 20 have a thermal degradation behavior mainly represented by degradation of the TPSUr polymer matrix. A decrease of about 8 °C was

observed in the thermal stability of starch phase of TPSUr/Hap20 when compared with the degradation peak of the pure polymer network (FIGURE 6.2b). This is probably because of small polar molecules inside the structure that would accelerate the breakdown of starch chains, as reported by Giroto et. al. (2014).[129] The final residue in all nanocomposites refers to the Hap phase when present.
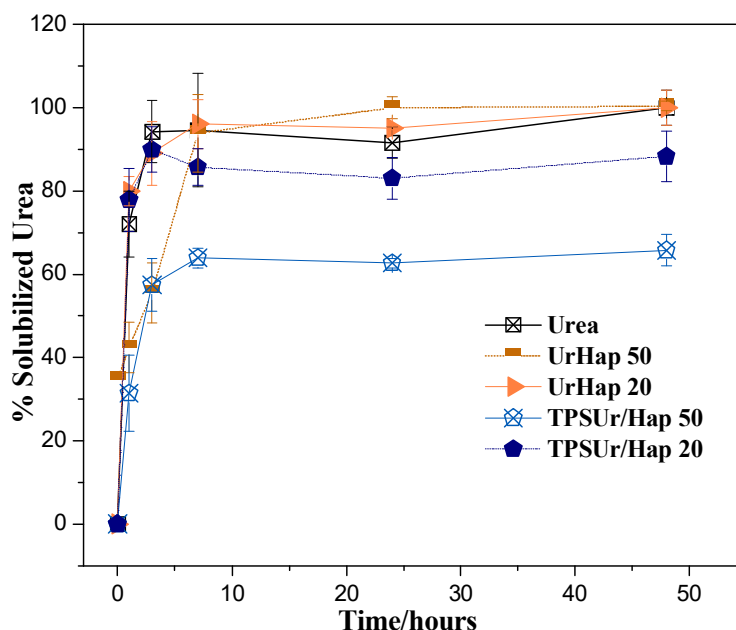
FIGURE 6.3.The release rate of urea as a function of time for pure urea and each of the composites at pH 7 and 25ºC.

The use of urea as dispersing matrix for Hap was an interesting choice since urea is highly water soluble and is of great agronomic importance. Release rates (produced in FIGURE 6.3) were then determined to assess the functionality of the nanocomposites on urea solubilization. It can be observed rapid dissolution of pure urea within only two hours. The nanocomposites UrHap50 and UrHap20 displayed solubilizing behavior very similar to that of pure urea, and reached equilibrium between 10-15 h. A slower urea release behavior was observed for the nanocomposites based on TPSUr matrix. The nanocomposite containing 50% Hap (TPSUr/Hap50) provides a solubilizing urea extent of only 55%. Additionally, it was possible to verify a different behavior for the nanocomposite TPSUr/Hap20. The presence of Hap induced the formation of pores throughout the nanocomposite granule structure. These pores allowed the solution to flow out, which facilitated solubilizing of urea comprised in the

polymer matrix. It can be seen that part of urea used to plasticize starch ended up being encapsulated by the TPSUr matrix, thereby reducing its contact with water.
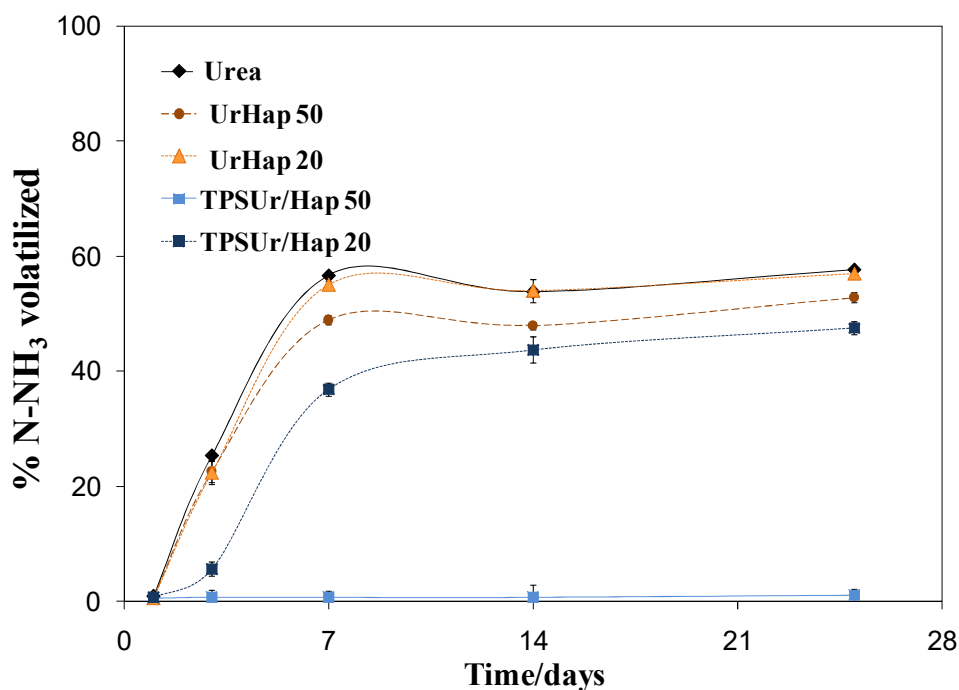
FIGURE 6.4.Percentage of volatilized ammonia (NH_3) during the aerobic incubation of urea or composites applied to the soil. Data are shown as a mean of triplicate incubations with bars to indicate the standard deviation of the mean.

FIGURE 6.4 shows ammonia volatilization results from urea or nanocomposites in soil incubation experiments. The rapid N-release from urea or nanocomposites UrHap50 and UrHap20 in soil can be observed by the intense NH_3 volatilization that occurred over 7 days of incubation, with values of N loss equal or higher than 50 % in relation to the total N applied as urea. In contrast, NH_3volatilization losses for nanocomposites TPSUr/Hap20did not exceed 46 % until the second week of incubation, indicating a slower N-release behavior. This finding can be attributed to the controlled release of urea by the thermoplastic starch (TPS), the amended urea TPSUr/Hap50 presented the higher controlled behavior with inexpressive NH_3volatilization during the incubation period. As evidenced in FIGURE 6.3, the urea encapsulated by the TPS matrix had reduced contact with the solution. Moreover, the highest rate of TPSUr/Hap50 compared to TPSUr/Hap20 processed by extrusion promoted a greater control over the NH_3 volatilization by the lower N-release extent or by some interaction between ammonium and phosphates in soil. A little advantage was evidenced for the nanocomposite UrHap50with respect to N losses in relation to the

unamended urea, which may be attributed to the same interaction. The high NH_3 volatilization rate (about 50 % of the N-urea applied) in this soil could be attributed to the rise of pH caused by urea hydrolysis, combined with the low soil CEC and buffer capacity, which created conditions favorable for NH_3 volatilization. This behavior was also observed for Guimarães et. al. (2016).[78] The authors worked with similar chemical-physical characteristics to the soil used in this work and using the similar incubation system. They observed a N losses from unamended urea ultimately exceeded 50% for the Assis soil (CEC of 3.5 cmolc kg^{-1} and pH 5.3), as compared to more than 70% for the Bloomfield soil that was lower in CEC (1.2 cmolc kg^{-1}) and higher in pH 6.9.In addition, the incubation system utilized can be intensified the NH_3 volatilization due to the limited diffusion of N in the small sample of soil used this incubation experiments.

The volatilization model of ammonia was well adjusted to all nanocomposites, except for TPSUr/Hap50 which showed inexpressive N losses over the incubation intervals (TABLE 6.2). Following a Logistic model – $y = A. (1+B.e^{-C.t})^{-1}$, where A is the maximum NH_3 volatilization expected (or total N volatilized); C is a recovery factor and B is the weight of delayed release on the total volatilization. In this model, when C > 1, the release tends to the conventional release, whereas when 0 < C < 1 the delays are more representative on the total profile.

TABLE 6.2. Model adjusted for volatilization of ammonia (NH_3), total nitrogen volatilized in the incubation period, and time spent to volatilize 25% (Time 25%) of the N applied to the soil from urea or composites.

Treatment	Logistic Model	Total N volatilized	Time 25 %
		%	days
Ur	$\hat{y} = 56.1/ (1 + 640.4\ e^{\ (-2.08\ t)})$	56.1 d[1]	2.9 a
UrHap50	$\hat{y} = 50.0 / (1 + 513.2\ e^{\ (-2.01\ t)})$	50.0 c	3.1 a
UrHap20	$\hat{y} = 55.4 / (1 + 840.6\ e^{\ (-2.03\ t)})$	55.4 d	3.1a
TPSUr/Hap50	-	1.0 a	-
TPSUr/Hap20	$\hat{y} = 45.6 / (1 + 133.3\ e^{\ (-0.87\ t)})$	45.6 b	5.5 b

[1]Mean values reported from triplicate incubations. Values within a column followed by the same letter do not differ significantly by the Duncan's test at a significance of 0.05.

The unamended urea sample exhibited the highest loss of total N as NH_3 volatilization and it differed from the other composites, UrHap50 and TPSUr/Hap20. However, it is similar to that of nanocomposite UrHap20. The nanocomposite TPSUr/Hap20 showed a reduction of 10 % of the N loss compared with urea. Moreover, the NH_3 losses occurred more gradually from TPSUr/Hap20, requiring

5.5 days to volatilize 25% of the total N added to soil, whereas unamended urea required 2.9 days to reach the same volatilization extent. Further evidence of controlled volatilization is the lower C recovery factor for the nanocomposite TPSUr/Hap20 in relation to the other treatments. The latter finding shows that TPS was effective in controlling the urea release, however, this process was influenced by the rate of Hap, as evidenced in the nanocomposite TPSUr/Hap50, which showed only 1 % of the N volatilized due to the very low urea release extent. The advantage of the UrHap50 nanocomposite, cannot be attributed to the control urea release, since both treatments volatilized 25% of the total N incubated in the soil in same time.
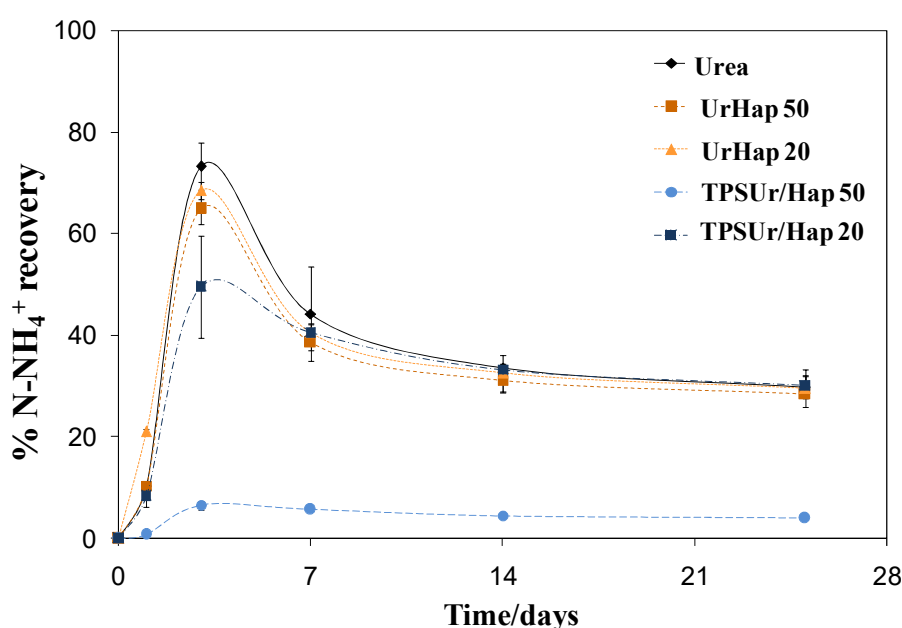
FIGURE 6.5. N recovery as ammonium (NH_4^+) during the aerobic incubation of urea or nanocomposites applied to the soil. Data shows as a mean of triplicate incubations with bars to indicate the standard error of the mean.

FIGURE 6.5 compares the five treatments in terms of N recovered as exchangeable NH_4^+ before and after incubation intervals. N recoveries values reported in FIGURE 6.5 indicate production of NH_4^+ through urea hydrolysis after release of unamended urea or nanocomposites, and consumption by NH_3 volatilization. The NH_4^+ levels had maximum accumulation until the third day of incubation. However, the increase in NH_3 volatilization after 3 to 7 days (FIGURE 6.4) led to a gradual decrease in NH_4^+ recovery continued throughout the incubation period. When compared to pure urea, the nanocomposite TPSUr/Hap20 exhibited significantly lower exchangeable NH_4^+ content after 1 and 3 days of incubation, but this difference became insignificant after

the first week of incubation. The lower NH_4^+ content of the nanocomposite TPSUr/Hap50 may be attributed to its very low urea release. It is noteworthy that the recovered N as NH_4^+ for samples Ur, UrHap50 and UrHap20, are consistent with the final NH_3 volatilization: in general, the unrecovered N corresponds approximately to the volatilized content. On the other hand, the sample TPSUr/Hap20 presented a final N recovery of 30% and a volatilized NH_3 content of 45%. This indicates that a significant N amount still remains into the nanocomposite structure, and could be released over longer times. In fact, this result is consistent with the lower recovery factor of this sample (C = 0.87), as shown in TABLE 6.2. Finally, the very low N recovery values for the nanocomposite TPSUr/Hap50, associated with the negligible NH_3 volatilization, strongly suggests that this sample is still undergoing the N releasing process.

TABLE 6.3. Model adjusted for N recovery as ammonium, maximum recovery NH_4^+ (max NH_4^+), time that occurred the max NH_4^+ (t max), tangent curve in 6 days (tg 6), and recovery NH_4^+ in the final incubation period (Final NH_4^+) of urea or nanocomposites in soil.

Treatment	Rational models	max NH_4^+	t max	tg 6	Final NH_4^+
		%	days		%
Ur	$\hat{y} = (0.5t^2)/(1 - 0.71t + 0.19t^2)$	77 c[1]	2.9ab	-0.46 c	29.8 b
UrHap50	$\hat{y} = (0.81t^2)/(1 - 0.92t + 0.32t^2)$	76 c	2.2 a	-0.31 b	28.3 b
UrHap20	$\hat{y} = (0.83t^2)/(1 - 0.92t + 0.32t^2)$	79 c	2.2 a	-0.33 b	29.6 b
TPSUr/Hap50	$\hat{y} = (0.05t^2)/(1 - 0.54t + 0.14t^2)$	07 a	3.8 c	-0.04 a	4.0 a
TPSUr/Hap20	$\hat{y} = (0.5t^2)/(1 - 0.59t + 0.19t^2)$	52 b	3.5bc	-0.25 b	30.2 b

[1] Mean values reported from triplicate incubations. Values within a column followed by the same letter do not differ significantly by the Duncan's test at a significance level of 0.05.

Owing to ammonium content in soil is a result of urea hydrolysis and ammonia volatilization process, kinetics parameters of NH_4^+ recovery were estimated to study the N transformation within the soil (TABLE 6.3). The samples Ur, UrHap20 and UrHap50 presented similar maximum recovery of NH_4^+, which exceeded 75% of the total N incubated in the soil, and occurred at the same time, between 2.2 and 2.9 days. However, the nanocomposite TPSUr/Hap20 showed a lower maximum NH_4^+ recovery and delayed the formation of ammonium in the soil in relation to unamended urea. The nanocomposite TPSUr/Hap50 showed the lowest formation of NH_4^+, indicating that TPS and Hap prevent the urea release. The values below the tangent curve at 6 days indicate that the slowed transformation of ammonium to ammonia in the soil and the

NH_4^+content was more homogeneous over the incubation period. The ammonium contents after the incubation period (25 days) were similar, between 28.3 to 30.2% of the N applied to soil, except for the nanocomposite TPSUr/Hap50, which had a low urea release profile. The latter finding may be attributed to the little soil ability to retain ammonium as its CEC and buffer capacity are low, which standardized the ammonium content in the soil. Although the nanocomposite TPSUr/Hap20 presented ammonium content similar after the incubation period, the control over the urea release provided a smaller N loss by volatilization and maintained a more constant NH_4^+ content in the soil.

The rational model can be interpreted as a balance of a solubilizing curve (from fertilizer), which is the only source of NH_4^+, and volatilization – as shown in FIGURE 6. In fact, the content at equilibrium is a soil characteristic, and may vary over time. Then, during 3 – 7 days, all the samples presented a metastable feature, i.e., this NH_4^+ remained available to the soil but started to volatilize because it was not used in any fixation process.

TABLE 6.4.Recovery of N as exchangeable nitrate (N-NO$_3^-$) during aerobic incubation of urea or nanocomposites in soil.

Treatment	Recovery of NO$_3^-$ after incubation period (days)/ %				
	1	3	7	14	25
Ur	$0.64 \pm (0.05)^1$	$0.83 \pm (0.10)$	$1.57 \pm (0.03)$	$1.56 \pm (0.05)$	$0.80 \pm (0.03)$
UrHap50	$0.78 \pm (0.02)$	$1.77 \pm (0.01)$	$1.33 \pm (0.06)$	$1.68 \pm (0.04)$	$1.83 \pm (0.05)$
UrHap20	$0.45 \pm (0.04)$	$1.12 \pm (0.05)$	$0.84 \pm (0.01)$	$1.36 \pm (0.10)$	$0.80 \pm (0.04)$
TPSUr/Hap50	$0.73 \pm (0.07)$	$1.41 \pm (0.05)$	$1.25 \pm (0.03)$	$1.03 \pm (0.09)$	$1.16 \pm (0.06)$
TPSUr/Hap20	$0.60 \pm (0.04)$	$1.11 \pm (0.04)$	$1.61 \pm (0.03)$	$1.65 \pm (0.05)$	$1.63 \pm (0.03)$

[1]Mean values reported from three replicate soil cores, with standard deviations in parentheses

TABLE 6.4 shows the recovery of NO$_3^-$during aerobic incubation of urea or nanocomposites in soil. The low nitrate level during incubation can be attributed to limited nitrification of NH_4^+, which did not exceed 2% from N-urea incubation soil and did not present a consistent profile in evaluated period. No definite explanation can be offered for the latter finding. However, the low nitrification in coarse-textured soils was also reported by Guimarães et. al. (2016),[78] using the similar incubation system. The authors report that nitrification was limited by the extensive loss of urea-derived NH_4^+-

N through volatilization. The high concentration of ammonia (NH_3) inhibits the activity of bacteria of the genus *Nitrobacter* responsible for nitrification from NO_2^- to NO_3^{-}[158].
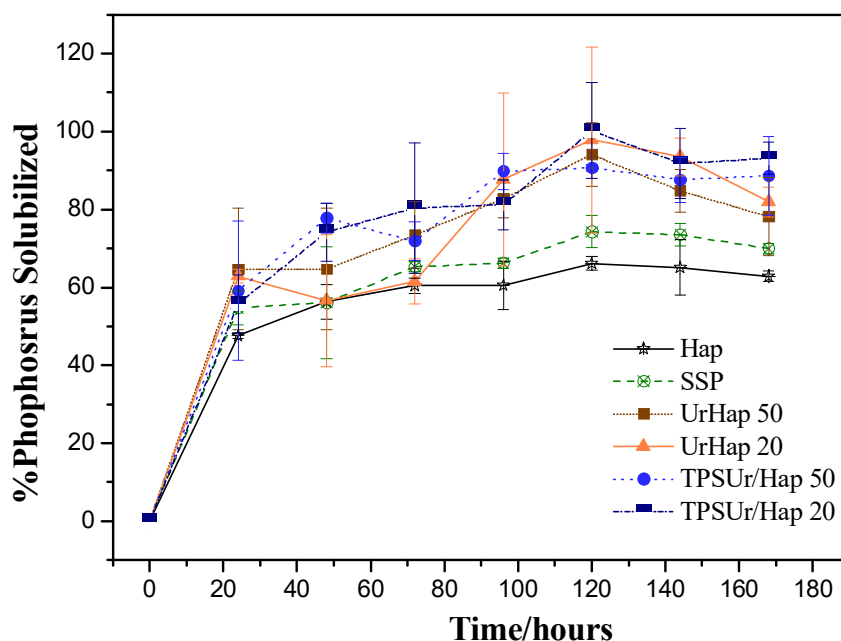
FIGURE 6.6.The release rate of phosphorus as a function of time for Hap, SSP and each of the nanocomposites at pH 4 and 25 ºC.

The solubilizing curves of Hap for the nanocomposites were compared with those of Hap and SSP, as represented in FIGURE 6.6. Analyzing the behavior of the nanocomposites, it can be noticed that all samples presented a higher Hap release compared to pure Hap and SSP. This means was increase of over 40% for all composite total release time for Hap and SSP, which both released at the same time only 60 and 68% Hap respectively. It can be proved that the morphology of all nanocomposites before grinding was effectively responsible for the phosphate solubilization. The nanocomposite matrix containing urea had a dense structure in which the solubilization of Hap occurred only after complete solubilization of the urea structure. On the other hand, the TPSUr/Hap nanocompositespresented faster releases of phosphate and ureathan the Ur/Hap nanocomposites, which is probably due tothe water accessibility through their highly porous matrices. In fact, this is possible because the porous structure of the TPSUr/Hap nanocomposites could facilitate the release of phosphate at short times, but the structure is likely to be modified by swelling, obstructing the water transport over longer times.[21] The original structures of the materials were modified by grinding and therefore their release profiles were modified as well. As can be seen from

FIGURE 6.6, there is no significant difference between the total amounts of Hap released for each nanocomposite.

The P-source release from Hap, SSP or nanocomposites applied to soil was evaluated after 42 days of aerobic incubation with controlled temperature and humidity. The fraction of available phosphorus (labile) in the soil after the incubation period and at the start of incubation (0 day) was extracted in water and anionic resin. The availability of P in the soil showed a similar behavior for both extractors, but with different extents. The anion exchange resin promoted a large extraction of the available P fraction, with values between 44 and 97% of the total P applied to the soil, whereas water extracted a small part of the available P fraction, with values between 1 and 26%.

TABLE 6.5.Available P in soil fraction extracted with water (P-water) and extracted by anion resin (P-resin) after the aerobic incubation period SSP of Hap and nanocomposites compared to the P applied to the soil.

Treatment		% P available				
		0 day	42 days		0 day	42 days
Hap		21.0 ab[1]	2.9 c		96.2 a	44.1 d
SSP		25.9 a	3.4 c		91.8 a	49.1 d
UrHap20	P-water	19.6 b	25.6 a	P-resin	97.5 a	87.3 a
UrHap50		19.9 b	22.3 a		81.9 a	88.6 a
TPSUr/Hap20		11.4 c	0.7 d		76.0 a	62.6 bc
TPSUr/Hap50		4.6 d	10.6 b		69.2 a	73.8 ab

[1]Mean values reported from triplicate incubations. Values within a column followed by the same letter do not differ significantly by the Duncan's test at a significance level of 0.05.

TABLE 6.5 shows the fraction of available P in the water at the start (0 day) and after incubation period (42 days), relative to the total P incubated in soil. The SSP and Hap had similar water solubility at the start of incubation, an average of 26 and 21% of the total P, respectively. The dispersion of Hap within the urea matrix, as in the nanocomposites UrHap50 and UrHap20, did not increase the release of P compared with pure Hap. Conversely, the TPSUr matrix decreased the release of P from Hap. This result could be attributed to the high water solubility of Hap, similar to that of SSP, which did not reflect to the effect of dispersion of the soluble matrix as urea, when applied to the soil. The TPSUr array can be assigned to the retention effect and control of release provided by the polymer. It acted as a physical barrier, retarding release of P

to soil, different from that observed in the release solution of 2% citric acid (FIGURE 6.6).

After the incubation period (42 days), there was a reduction of the labile fraction of P in soil extracted with water for SSP and Hap, in comparison with the P available at the start of the incubation. This reduction can be attributed to the P adsorption by soil colloids. The Oxisol used in the incubation experiment has favorable characteristics that are indicative of high adsorption of P in soil, such as low pH, low available P content, low P remaining and high acidity potential[159]. Additionally, the prevalence of Fe and Al oxides in Oxisol makes them more effective with regard to adsorption of phosphoros.[160]

Nanocomposites UrHap50 and UrHap20 showed greater P availability after the incubation period, showing a decreased adsorption of P by the soil compared with SSP and Hap. This result can be explained by two factors: the first is related to raise of pH of the soil around the particles due to urea hydrolysis, which can reach pH between of 8 to 9.[161-163] The second factor is the interaction between the NH_4^+ ions formed during the hydrolysis of urea and anion P release from Hap, providing a reduction in the adsorption of phosporus.[153]

TABLE 6.6.pH value after aerobic incubation period of soil, SSP, Hap and nanocomposites in soil.

Treatment	pH after incubation period		Δ pH [2]	
	0 day	42 days	0 day	42 days
Soil	$5.19 \pm (0.04)$[1]	$4.94 \pm (0.03)$	-	-
Hap	$6.09 \pm (0.04)$	$4.85 \pm (0.02)$	0.90	- 0.08
SSP	$4.91 \pm (0.02)$	$5.24 \pm (0.04)$	- 0.28	0.30
UrHap20	$6.36 \pm (0.03)$	$7.20 \pm (0.01)$	1.17	2.26
UrHap50	$7.09 \pm (0.05)$	$7.90 \pm (0.05)$	1.90	2.97
TPSUr/Hap20	$5.84 \pm (0.01)$	$6.30 \pm (0.06)$	0.65	1.37
TPSUr/Hap50	$6.31 \pm (0.02)$	$7.58 \pm (0.06)$	1.12	2.65

[1] Mean values reported from three replicate soil cores, with standard deviations in parentheses.[2]Difference in pH of each treatment relative to soil.

TABLE 6.6 shows the pH change after the incorporation of the fertilizers or nanocomposites in the soil at the initial time (0 day) and 42 days after the incubation. The soil pH increased for Hap and composites treatments at the initial time, that can be attributed to the higher pH of these sources (pH $\approx$ 6 for Hap and 7 for urea) compared to

the initial soil pH (pH = 5,19). On the other hand, it was observed a small decrease in the soil pH after SSP incorporation, related to its acid character. After 42 days of incubation, the pH of the soil fertilized with Hap or SSP remained close to the pH of the soil without fertilization, with pH around 5.However, in this same period, the soil fertilized with the nanocomposites preserve higher pH in relative of the soil without fertilization, with values between6.30 to 7.90. The latter findings are to be expected due the high hydrolyses of urea in the soil with low CEC and buffer capacity.

Thus, the results indicate that the interaction between urea and Hap, both nanocomposites UrHap50 and UrHap20, provided a more homogeneous phosphorus availability during the incubation period. On the other hand, nanocomposites TPSUr/Hap that have lower urea content and control of P release had lower availability of P and greater heterogeneity.

As previously mentioned, the available P estimated by anionic resin showed the same behavior of P extracted by water of different treatments, however, the resin provided the extraction of a larger fraction of P-labile (TABLE 6.5). After 42 days of incubation of Hap and SSP in soil, the P availability decreased by 42 and 52%, respectively, demonstrating the high adsorption P in the soil under these conditions, as discussed above. On the other hand, nanocomposites containing Ur/Hap showed little variation during the same period and presented a high availability of P with values between 82 and 97% relative to the total P applied to the soil. Similarly, the nanocomposites containing TPSUr/Hap also had the most homogeneous phosphorus availability during the incubation period, but with lower values ranging between 62 to 76%.

6.5. *Conclusions*

The control over the nutrient release and homogenous availability of nutrients in soil are desirable characteristics of fertilizers that have promoted increasing interest in research. The strategy involving dispersion of mineral phosphate sources into urea and thermoplastic starch (TPSUr) have great potential, allowing the control N-release and increasing P-availability in soil. In the conditions tested in this work, the interaction between Hap and urea are probably the responsible factors that reduced phosphorus immobilization and consequently provided greater P availability in soil during the incubation period.

7. General Conclusions

In this thesis, it was demonstrated the produce of different nutrient matrices for dispersion of phosphate particles. In accordance with the results shown and based on proposed goals, it can be concluded that the dispersion of the particles in these matrices provides the viable alternative for improving the performance fertilizers. Also, other remarks may be highlighted:

- The results showed that by this simple method (melt-mixing process using precursors in form powders) it was possible to obtain dense urea: urea-formaldehyde composites, and with very high N contents and with nutrient release easily controlled by the composition;

- The insertion of the melamine in the TPSUr matrix was fundamental in the substitution of the urea bonds directly with the starch. The presence of melamine and the processing conditions were the key roles for the production of more homogeneous and compact materials. According to the greenhouse trials, melamine did not present a nutritional role in short periods of experimentation but created a favorable environment for a greater availability of urea;

- The results demonstrated that it was possible to tailor a nanocomposite by finely dispersing hydroxyapatite (within two matrices with different levels of hydrosolubility. The matrix solubility was found to be less important than the water accessibility in the nanocomposite structure, since the porous TPS:Ur matrix exhibited better phosphate release when compared with a dense urea matrix;

- The strategy involving dispersion of mineral phosphate sources into urea and thermoplastic starch (TPSUr) have great potential, allowing the control N-release and increasing P-availability in soil. In the conditions tested in this work, the interaction between Hap and urea are probably the responsible factors that reduced phosphorus immobilization and consequently provided greater P availability in soil during the incubation period.

8. References

1.   RABELLO, W. S. "Sorção e lixiviação de herbicidas." 2011. 27p. Monografia (graduação em ciências Agrárias) - Universidade Federal dos Norte Fluminense Darcy Ribeiro, Campos dos Goytacazes, RJ.

2.   ISHERWOOD, K. F. "O uso de fertilizantes minerais e o meio ambiente." ANDA, São Paulo, 2000, 63p.

3.   GOMES, A. S.; FERREIRA, L. H. G.; BENDER, R. R.; "Uso do fosfato natural no cultivo de arroz, soja e milho em rotação, no sistema plantio direto." Pelotas: Embrapa – Clima Temperado, 2005, 37p.

4.   LOUREIRO, F. E. V. L.; MELAMED, R.; O fósforo na agricultura brasileira: uma abordagem minero-metalúrgica. Rio de Janeiro: CETEM – Centro de Tecnologia Mineral, 2006, 76p.

5.   FERREIRA, L. H. G.; GOMES, A. S.; POSSER, C. A.; Fosfatos naturais na adubação de sistema de culturas de verão com ênfase no arroz irrigado. Pelotas: Embrapa – Clima Temperado, 2008, 8p.

6.   FAO (Food and Agriculture Organization).World Agriculture: Towards 2015/2030 an FAO Perspective. BRUINSMA, J (Ed.). Rome, Earthscan Publications Ltd., 2003. 97p.

7.   CONAB; Insumos fertilizantes entregues ao consumidor. 2013. Disponível   em: http://www.conab.gov.br/OlalaCMS/uploads/arquivos/13_03_15_19_02_02_0605_fe rtilizantes _entregues.pdf . Acessado em: Maio 2013.

8.   FERNANDES, E.; GUIMARÃES, B. A. & MATHEUS, R. R. "Principais empresas e grupos brasileiros do setor de fertilizantes." In: BNDES setorial, Rio de Janeiro, n. 29, 2009. p. 203-228.

9.   LANA, R. M. Q.; ZANÃO JUNIOR, L. A.; LUZ, J. M. Q & SILVA, J. C. "Produção da alface em função do uso de diferentes fontes de fósforo em solo de cerrado." Horticultura Brasileira, **22**(3): 525, 2004.

10.   BENEDITO, D. S. "Eficiência agronômica de fontes alternativas de fósforo e modelo de predição do uso de fosfatos naturais." Tese (doutorado). Escola superior de Agricultura Luiz de Queiroz, Piracicaba, 2007, 121p.

11.   NARDI, A.; BARBOSA, A. C.; FIORAVANTE, E. F.; CÂMARA, F. O.; SILVEIRA, I. L. Proposição de limites máximos de emissão de poluentes

atmosféricos de fontes fixas para a indústria de fertilizantes em nível nacional. 2004. Disponível em: http://www.mma.gov.br/port/conama/processos/198FC8A8/EmendaFertilizantes7oG T.doc . Acessado em: 07 out. 2015.

12. RIEDER, J. H. "Destinação racional dos jazimentos fosfáticos nacionais. In: Encontro nacional de rocha fosfática", 1986, Brasília. Anais. São Paulo:IBRAFOS, 1986. cap. 3, p.135-172.

13. REIS, N. P. "Pespectivas para o fósforo". In: Simpósio Nacional do Setor de Fertilizantes, 2, 2002, São Paulo. Palestra. São Paulo: ANDA, 2002, 364p.

14. HOROWITZ, N.;MEUER, E. J. "Eficiência de dois fosfatos naturais farelados em função do tamanho de partícula." Ciência Rural, **33(**1):. 41, 2004.

15. CANTARELLA, H. "Nitrogênio." In: NOVAIS, R. F.; ALVAREZ V., V. H.; CANTARUTTI, R. B.; NEVES, J. C. L. (Ed.). "Fertilidade do solo." Viçosa: Sociedade Brasileira de Ciência do Solo, 2007. p.375-470.

16. SNYDER, C. S.; BRUULSEMA, T. W.; JENSEN, T. L. & FIXEN, P. E. "Review of greenhouse gas emission from crop production systems and fertilizer management effects". Agr. Ecosyst. Environ., **133**: 247, 2009.

17. PEREIRA, E. I. "Estudo do processo de liberação lenta de fertilizantes a partir de nanocompósitos de matriz de ureia." São Carlos, Programa de Pós-Graduação -UFSCar, 2014. Tese de doutorado, 95p.

18. MARTHA JÚNIOR, G. B.; CORSI, M.; TRIVELINI, P. C. O.; VILELA, L.; PINTO, T. L. F.; TEIXEIRA, G. M.; MANZON, C. S. & BARIONI, L. G. "Perda de amônia por volatilização em pastagem de capim-tanzânia adubada com ureia no verão." R. Bras. Zootec., **33**(6): 240, 2004.

19. PEREIRA, E. I.; MINUSSI, F. B.; DA CRUZ, C. C. T.; BERNARDI, A. C. C. & RIBEIRO, C. "Urea– montmorillonite-extruded nanocomposites: a novel slow-release material." J. Agric. Food Chem., **60**(21): 5267, 2012.

20. PEREIRA, E. I. DA ; CRUZ, C. C. T.; SOLOMONC, A.; LED, A.; CAVIGELLID, M. A. & RIBEIRO, C. "Novel slow release nanocomposite nitrogen fertilizers: the impact of polymers on nanocomposite properties and function." Ind. Eng. Chem. Res., **54**(14): 3717, 2015.

21. GIROTO, A. S.; FIDÉLIS, S. C. & RIBEIRO, C. "Controlled release from hydroxyapatite incorporaded into biodegradable soluble host matrixes." RSC Adv., **5**: 104179, 2015.

22.	GIROTO, A. S.; GUIMARÃES, G. F. G.; FOSCHINI, M. & RIBEIRO, C. "Role of Slow-Release Nanocomposite Fertilizers on Nitrogen and Phosphate Availability in Soil." Sci. Rep., **13**(7): 46032, 2017.

23.	RYCHTER, A.; KOT, M.; BAJER, K.; ROGACZ, D.; SISKOVÁ, A. & KAPUSNIAK, J. "Utilization of starch films plasticized with urea as fertilizer for improvement of plant growth." Carbohyd. Polym., **137**: 127, 2016.

24.	ATKINS, P. & DE PAULA, J. Físico-Química Volume 1. LTC Editora, São Paulo, 2008, 8ª edição. 592 p.

25.	KLAIC, R.; PLOTEGHER, F.; RIBEIRO, C.; ZANGIROLAMI, T. C. & FARINAS, C. S. "A novel combined mechanical-biological approach to improve rock phosphate solubilization." Int. J. Miner. Process., **161**: 50, 2017.

26.	PLOTEGHER, F. & RIBEIRO, C. "Preparação e Caracterização de Compósitos Poliméricos Baseados em Amido Termoplástico e Materiais de Alta Área Superficial: Zeólita ZSM-5 e Sílica Coloidal." Polímeros, **23**(2): 236, 2013.

27.	PEREIRA, E. I.; NOGUEIRA, A. R. A.; CRUZ, C. C. T.; GUIMARÃES, G. G. F.; FOSCHINI, M. M.; BERNARDI, A. C. C. & RIBEIRO, C."Controlled Urea Release Employing Nanocomposites Increases the Efficiency of Nitrogen Use by Forage." ACS Sustainable Chem. Eng., **5**(11): 9993, 2017.

28.	DE ROSA, M. C.; MONREAL, C.; SCHNITZER, M.; WALSH, R. & SULTAN, Y. "Nanotechnology in fertilizers." Nat. Nanotechnol., **5**: 91, 2010.

29.	WANG, K. H.; CHOI, M. H.; KOO, C. M.; CHOI, Y. S. & CHUNG, I. J. "Synthesis and Characterization of mateated polyethylene/clay nanocomposites." Polymer, **42**: 9819, 2001.

30.	MAXIMO, E.; BENDASSOLLI, J. A.; TRIVELIN, P. C. O.; ROSSETE, A. L. R. M.; OLIVEIRA, C. R & PRESTES, C. V. "Produção de sulfato de amônio duplamente marcado com os isótopos estáveis 15n e 34s." Quim. Nova, **28**(2): 211, 2005.

31.	CORRADINI, E.; CARVALHO, A. J. F.; CURVELO, A. A. S.; AGNELLI, J. A. M. & MATTOSO, L. H. C. "Preparation and characterization of thermoplastic starch/zein blends." Mater. Res., **10**: 227, 2007.

32.	AOUADA, F. A.; MATTOSO, L. H. C. & LONGO, E. "New strategies in the preparation of exfoliated thermoplastic starch-montmorillonite nanocomposites." Ind. Crop. Prod., **4**: 1502, 2011.

33.   MA, X. & YU, J. "The plastcizers containing amide groups for thermoplastic starch." Carbohyd. Polym., **57**: 197, 2004.

34.   MA, X. F.; YU, J. G. & WAN, J. J. "Urea and ethanolamine as a mixed plasticizer for thermoplastic starch." Carbohyd. Polym., **64**: 267, 2006.

35.   MA, X. F. & YU, J. G. "The effects of plasticizers containing amide groups on the properties of thermoplastic starch." Starch, **56**: 545, 2004.

36.   CORRADINI, E.; MEDEIROS, E. S.; CARVALHO, A. J. F.; CURVELO, A. A. S. & MATTOSO, L. H. C. "Mechanical and morphological characterization of starch/zein blends palsticized with glycerol." J. Appl. Polym. Sci. 101: 4133, 2006.

37.   CURVELO, A. A. S; CARVALHO, A. J. F. de& AGNELLI, J. A. M. "Thermoplastic starch±cellulosic fibers composites: preliminary results." Carbohyd. Polym., 45: 183, 2001.

38.   CARVALHO, A. J. F. de; CURVELO, A. A. S. & AGNELLI, J. A. M. "A first insight on composites of thermoplastic starch and kaolin." Carbohyd. Polym., **45**: 189, 2001.

39.   LARA-CABEZAS, W. A. R.; KORNDORFER, G. H. & MOTTA, A. "Volatilização de N-NH$_3$ na cultura de milho: II. avaliação de fontes sólidas e fluidas em sistema de plantio direto e convencional." Rev. Bras. Ciênc. Solo, **21**: 481, 1997.

40.   MELO JR., H. B.; DUARTE, I. N.; SILVA, A. A. & LANA, R. M. Q. "Uso de fontes revestidas com polímeros de liberação gradual e ureia convencional." Enc. Bio., **6**: 1, 2011.

41.   SUHERMAN, I. & ANGGORO, D. D. "Producing Slow Release Rate Urea by Coating with Starch/Acrylic Acid in Fluid Bed Spraying." Int. J. Eng. Technol., 11:62,2011.

42.   ZAREI, A. & GHAFFARIAN, V. "Preparation and characterization of biodegradable cellulose acetate-starch membrane." Polym. Plast. Techn., **52**: 387, 2013.

43.   VIEIRA, B. A. R. M. & TEIXEIRA, M. M. "Adubação de liberação controlada chega como solução." Revista Campo e Negócios, **41** (3): 4, 2004.

44.   YAMAMOTO, C. F.; PEREIRA, E. I.; MATTOSO, L. H. C.; MATSUNAKA, T. & RIBEIRO, C. "Slow release fertilizers based on urea/urea-formaldehyde polymer nanocomposites". Chem. Eng. J., **287**: 390, 2016.

45. TRENKEL, M. E. Slow- and Controlled-Release and Stabilized Fertilizers: An Option for Enhancing Nutrient Use Efficiency in Agriculture IFA, International Fertilizer Industry Association, Paris, 2010. 163p.

46. DAVE, A. M.; MEHTA, M. H.; AMINABHAVI, T. M.; KULKARNI, A. R. & SOPPIMATH, K. S. "A review on controlled release of nitrogen fertilizers through polymeric membrane devices." Polym. Plast. Technol. Eng., **38**: 675, 1999.

47. NEYMAN, G. B. & DERR, E. A. (2002) Homogeneous granules of slow-release fertilizer and method of making the same. Patent US 011087 A1 31 Jan 2002

48. JAHNS, T.; EWEN, H. & KALTWASSER, H. "Biodegradability of urea-aldehyde condensation products." J. Polym. Environ., **11**: 155, 2003.

49. GABRIELSON, K. D.; EPLING, M. L. (2011) Reaction products and methods for making and using the same cross-references to related applications. Patent WO 2011137393-A1, 03 Nov 2011

50. SUTTON, A. R.; CASE, M. & HEALEY, T. J. (2010) Urea formaldehyde polymer additive for odor control of unmanipulated manure. Patent WO 2010093462-A1, 19 Aug 2010

51. PHILLIPS, J. C.(2008) Extended-release urea-based granular fertilizer. Patent US 2008141747-A1, 19 Jun 2008

52. PHILLIPS, J. C.; WERTZ, S. L.; COTHRAN, A. K.; GABRIELSON, K. D.; PHILLIPS, Y. A. C. (2006) High nitrogen liquid fertilizer. Patent US 2006196241-A1, 07 Sep 2006

53. PHILLIPS, J. C.; PACE, C. B.; HOLT, T. G. & COCHRAN, K. D. (2005) Extended-release nitrogen-containing granular fertilizer. Patent US 2005144997-A1, 7 Jul 2005

54. KIERNAN, J. A. "Formaldehyde, formalin, paraformaldehyde and glutaraldehyde: What they are and what they do." Microsc. Today, **1**: 8, 2003.

55. TOMASZEWWSKA, M. & JAROSIEWICZ, A. "Use of Polysulfone in Controlled-Release NPK Fertilizer Formulations." J. Agric. Food Chem., **50**: 4634, 2002.

56. WITH, K.; PETERSEN, T. D. & PETERSEN, B. "Simple spectrophotometric method for the determination of urea in blood and urine." J. Clin. Pathol., **14**: 202, 1961.

57.   NELSON, D. W. & SOMMERS, L. E."Methods for the Determination of Total Organic Carbon (TOC) in Soils and Sediments". In D. L. SPARKS, A. L. PAGE, P. A. HELMKE, R. H. LOEPPERT, P. N. SOLTANPOUR, M. A. TABATABAI, C. T. JOHNSTON AND M. E. SUMNER (ed) Methods of Soil Analysis, Part 3. SSSA Books Series, Madison, pp 961-1010.

58.   Empresa Brasileira de Pesquisa Agropecuária (1979) Manual de métodos de análise de solo. Embrapa Solos, Rio de Janeiro.

59.   KILMER, V. J. & ALEXANDER, L. T. "Method of making mechanical analyses of soils." Soil Sci., **68**: 15, 1949.

60.   TABATABAI, M. A.; BREMNER, J. M. "Assay of urease activity in soils." Soil Biol. Biochem., **4**: 479, 1972.

61.   KEMPERS, A. J. & ZWEERS, A. "Ammonium determination in soil extracts by the salicylate method."Commun. Soil Sci. Plant. Anal., **17**: 715, 1986.

62.   YANG, J. E.; KIM, J. J.; SKOGLEY, E. O. & SCHAFF, B. E. "A simple spectrophotometric determination of nitrate in water, resin, and soil extracts." Soil Sci. Soc. Am. J., **62**: 1108, 1998.

63.   ROUMELI, E.; PAPADOPOULOU, E.; PAVLIDOU, E.; VOURLIAS, G.; BIKIARIS, D.; PARASKEVOPOULOS, K. M. & CHRISSAFIS, K. "Synthesis, Characterization and thermal analysis of urea-formaldehyde/nanoSiO2 resin."Thermochim. Acta, **527**: 33, 2012.

64.   LUNDSTRÖM, A.; ANDERSSON, B. & OLSSON, L. "Urea thermolysis studied under flow reactor conditions using DSC and FT-IR." Chem. Eng. J., **150**: 544, 2009.

65.   LIU, Y.; TIAN, Y.; ZHAO, G.; SUN, Y.; ZHU, F. & CAO, Y. "Synthesis of urea-formaldehyde resin by melt condensation polymerization." J. Polym. Res., **15**: 501, 2008.

66.   CHRISTJANSON, P.; SIIMER, K.; PEHK, T. & LASBN, I. "Synthesis of urea-formaldehyde resin by melt condensation polymerization." Holz. Roh. Werkst. **60**:379, 2002.

67.   TAYLOR, R.; FRAGNELL, R. J.;MCLAREN, J. V. & SNAPE, C. E. "Evaluation of NMR Spectroscopy for the Quantitative Characterization of Urea-Formaldehyde Resins." Talanta, **29**: 489, 1982.

68.   HE, G. & YAN, N. "^{13}C NMR study on structure, composition and curing behavior of phenol–urea–formaldehyde resole resins." Polymer, **45**: 6813, 2004.

69.   HOONG, Y. B.; PIZZI, A.; CHUAH, L. A. & HARUN, J. "Phenol–urea–formaldehyde resin co-polymer synthesis and its influence on Elaeis palm trunk plywood mechanical performance evaluated by ^{13}C NMR and MALDI-TOF mass spectrometry." Int. J. Adhes. Adhes., **63**: 117, 2015.

70.   FAN, D.; CHANG, J.; LI, J.; MAO, A. & ZHANG, L. "^{13}C-NMR Study on the Structure of Phenol-Urea Formaldehyde Resins Prepared by Methylolureas and Phenol." J. Appl.Polym. Sci., **112**: 2195, 2009.

71.   TOMITA, B.; OHYAMA, M. & HSE C-Y. "Synthesis of Phenol-Urea-Formaldehyde Co-condensed Resins from UF-Concentrate and Phenol." Holzfoncbung, **48**(6): 522, 1994.

72.   EDOGA, M. O. "Comparative study of synthesis procedures for urea–formaldehyde resins Part I." Leonardo El. J. Pract. Tehnol., **9**: 63, 2006.

73.   SAMARZIJA-JOVANOVIC, S.; JOVANOVIC, V.; KONSTANTINOVIC, S.; MARKOVIC, G. & MARINOVIC-CINCOVIC, M. "Thermal behavior of modified urea–formaldehyde resins." J. Therm. Anal. Calorim., **104**: 1159, 2011.

74.   JADA, S. S. "The structure of urea–formaldehyde resins." J. Appl. Polym. Sci., **35**: 1573, 1988.

75.   MATTOS, E. C.; VIGANÓ, I.; DUTRA, R. C. L.; DINIZ, M. F. & IHA, K."Aplicação de metodologias FTIR de transmissão e fotoacústica à caracterização de materiais altamente energéticos: parte II." Quim. Nova, **25**(5): 722, 2002.

76.   ZHONG, R.; GU, J.; GAO, Z.; TU, D. & HU, C. "Impacts of urea-formaldehyde resin residue on recycling and reconstitution of wood-based panels." Int. J. Adhes. Adhes., **78**: 60, 2017.

77.   GUIMARÃES, G. G. F.; MULVANEY, R. L.; KHAN, S. A.; CANTARUTTI, R. B. & SILVA, A. M."Comparison of urease inhibitor N-(n-butyl) thiophosphorictriamide and oxidized charcoal for conserving urea-N in soil." J. Plant. Nutr. Soil Sci., **179**: 520, 2016.

78.   NI, B.; LIU, M. & LÜ, S."Multifunctional slow-release urea fertilizer from ethylcellulose and superabsorbent coated formulations." Chem. Eng. J., **155**: 892, 2009.

79.   AZEEM, B. S.; KUSHAARI, K.; MAN, Z. B.; BASIT, A. & THANH, T. H. "Review on materials & methods to produce controlled release coated urea fertilizer." J. Control. Release, **181**: 11, 2014.

80.   YAN, D. & ZHENG-YIN, W. "Release Characteristics of Different N-Forms in an Uncoated Slow/Controlled Release Compound Fertilizer." Agric. Sci. China, **6**(3): 330, 2007.

81.   XIAO, X.; YU, L.; XIE, F.; BAO, X.; LIU, H.; JI, Z. & CHEN, L."One-step method to prepare starch-based superabsorbent polymer for slow release of fertilizer." Chem. Eng. J., **309**: 607, 2017.

82.   POURJAVADI, A.; HARZANDI, A. M. & HOSSEINZADEH, H."Synthesis of a novel polysaccharide-based superabsorbent hydrogel via graft copolymerization of acrylic acid onto kappa-carrageen an in air." Eur. Poly. J., **40** :1363, 2004.

83.   GUILHERME, M. R.; AOUADA, F. A.; FAJARDO, A. R.; MARTINS, A. F.; PAULINO, A. T.; DAVI, M. F. T.; RUBIRA, A. F. & MUNIZ, E. C. "Superabsorbent hydrogels based on polysaccharides for application in agriculture as soil conditioner and nutrient carrier: a review." Eur. Polymer J., **72**: 365, 2015.

84.   CHANG, C.; DUAN, B.; CAI, J. & ZHANG, L. "Superabsorbent hydrogels based on cellulose for smart swelling and controllable delivery." Eur. Polymer J., **46**: 92, 2010.

85.   RASHIDZADEH, A.; OLAD, A.; SALARI, D. & REYHANITABAR, A. "On the preparation and swelling properties of hydrogel nanocomposite based on Sodium alginate-g Poly (acrylic acid-co-acrylamide)/Clinoptilolite and its application as slow release fertilizer." J. Polym. Res., **21**: 344, 2014.

86.   TANG, J.; HONG, J.; LIU, Y.; WANG, B.; HUA, Q.; LIU, L. & YING, D. "Urea Controlled-Release Fertilizer Based on Gelatin Microsphere." J. Polym. Envirom., doi 10.1007./s10924-017-1074-6, 2017.

87. NIU, Y. & LI, H."Controlled Release of Urea Encapsulated by starch-g-poly(vinyl acetate)." Ind. Eng. Chem. Res., **51**: 12173,2012

88.   HAO, A.; GENG, Y.; XU, Q.; LU, Z. & YU, L. "Study of different effects on foaming process of biodegradable PLA/starch composites in supercritical/compressed carbon dioxide." J. Appl. Polym. Sci., **109**: 2679, 2008.

89.   ZHONG, K.; LIN, Z. T.; ZHENG, X. L.; JIANG, G. B.; FANG, Y. S.; MAO, X. Y. & LIAO, Z. W. "Starch derivative-based superabsorbent with

integration of water-retaining and controlled-release fertilizers." Carbohydr. Polym., **92**: 1367, 2013.

90.   EL-SAYED, W. S.; EL-BAZ, A. F. & OTHMAN, A. M."Biodegradation of melamine formaldehyde by Micrococcus sp. strain MF-1 isolated from aminoplastic wastewater effluent. " Int. Biodeter. Biodegr., **57**: 75, 2006.

91.   NOVAIS, R. F. & MELLO, J. W. V. Relação solo-planta in Fertilidade do solo. (EDS NOVAIS, R. F., ALVAREZ, V. H., BARROS, N. F. FONTES, R. L. F., CANTARUTTI, R. B., Neves, J. C. L., Eds) 276–374 (Sociedade Brasileira de Ciência do Solo, 2007).

92.   CHEN, X.; GUO, L.; DU, X.; CHEN, P.; JI, Y.; HAO, H. & XU, X. "Investigation of glycerol concentration on corn starch morphologies and gelatinization behaviours during heat treatment." Carbohyd. Polym., **176**: 56, 2017.

93. WANG, J.; CHENG, F. & ZHU, P."Structure and properties of urea-plasticized starch films with different urea contents."Carbohyd. Polym., **101**: 1109, 2014.

94.   CORREA, A. C.; CARMONA, V. B.; SIMÃO, J. A.; MATTOSO, L. H. C. & MARCONCINI, J. M."Biodegradable blends of urea plasticized thermoplastic starch (UTPS) and poly(-caprolactone) (PCL): Morphological, rheological, thermal and mechanical properties."Carbohyd. Polym., **167**: 177, 2017.

95.   IVANIČ, F.; JOCHEC-MOŠKOVÁ, D.; JANIGOVÁ, I. & CHODÁK, I."Physical properties of starch plasticized by a mixture of plasticizers." Eur. Polym. J., **93**: 843, 2017.

96.   WANG, D.; HUI, S. & LIU, C. "Mass loss and evolved gas analysis in thermal decomposition of solid urea." Fuel, **207**: 268, 2017.

97.   BRACK, W.; HEINE, B. BIRKHOLD, F.; KRUSE, M.; SCHOCH, G.; TISCHER, S. & DEUTSCHMANN, O. "Kinetic modeling of urea decomposition based on systematic thermogravimetric analyses of urea and its most important by-products." Chem. Eng. Sci., **16**: 1, 2014.

98.   CHEN, J. P. & ISA, K. "Thermal decomposition of urea and urea derivatives by simultaneous TG/(DTA)/MS." J. Mass Spectromet. Soc. Jpn., **46**: 299, 1998.

99.   CARVALHO, K. T. G.; NOGUEIRA, A.E.; LOPES, F. L.; BYZYNSKI, G. &RIBEIRO, C. "Synthesis of g-C3N4/Nb2O5 heterostructures and their application in the removal of organic pollutants under visible and ultraviolet irradiation." Ceram. Int., **43**: 3521, 2017.

100.   JURGENS, B.; IRRAN, E.; SENKER, J.; KROLL, P.; MULLER, H. & SCHNICK, W. "Melem (2,5,8-Triamino-tri-s-triazine), an Important Intermediate during Condensation of Melamine Rings to Graphitic Carbon Nitride: Synthesis, Structure Determination by X-ray Powder Diffractometry, Solid-State NMR, and Theoretical Studies." J. Am. Chem. Soc., **125**: 10288, 2003.

101.   HARRIS, R. K. "Applications of solid-state NMR to pharmaceutical polymorphism and related matters."vJ. P. N. J. Pharmacol., **59** (2): 225, 2010.

102.   MUTUNGI C.; PASSAUER, L.; ONYANGO, C.; JAROS, D. & ROHM, H. "Debranched cassava starch crystallinity determination by Raman spectroscopy: Correlation of features in Raman spectra with X-ray diffraction and 13C CP/MASNMR spectroscopy." Carbohyd. Polym., **87**: 598, 2012.

103.   MARCHESSAULT, R. H. & TAYLOR, M. G."Solid-state ^{13}C-C.P.-M.A.S. N.M.R. of starches." Carbohyd. Res., 144:1, 1985.

104.   PARIS, M.; BIZOT, H.; EMERY, J.; BUZARE, J. Y. & BULEON, A. "Crystallinity and structuring role of water in native and recrystallized starches by ^{13}C CP-MASNMR spectroscopy 1: Spectral decomposition." Carbohyd. Polym., **39**: 327, 1999.

105.   TAN, I.; FLANAGAN, B. M.; HALLEY, P. J.; WHITTAKER, A. K. & GIDLEY, M. J."A Method for Estimating the Nature and Relative Proportions of Amorphous, Single, and Double-Helical Components in Starch Granules by ^{13}C CP/MAS NMR." Biomacromolecules, **8**: 885, 2007.

106.   ZHU, F. "NMR spectroscopy of starch systems." Food Hydrocolloid., **63**: 611, 2017.

107.   TAYLOR, R. E.; BACHER, A. D. & DYBOWSKI, C. "^{1}H NMR Relaxation in Urea."J. Mol. Strut., **846**(1): 147, 2007.

108.   KRISTENSEN, J. H.; BAMPOS, N. & DUER, M. "Solid state ^{13}C CP MAS NMR study of molecular motions and interactions of urea adsorbed on cotton cellulose." Phys. Chem. Chem. Phys., **6**: 3175, 2004.

109.   MERCER, L. P.; FLODIN, N. W. & MORGAN, P. H. "New methods for comparing the biological efficiency of alternate nutrient sources." J Nutr., **108** (8):1244, 1978.

110.   HASANAEEN, M. N. A.; ABDEL-AZIZ, H. M. M.; EL-BIALY, D. M. A. & OMER, A. M. "Preparation of chitosan nanoparticles for loanding with NPK fertilizer." Afr. J. Biotechnol., **13**: 3158, 2014.

111.   CORRADINI, E.; DE MOURA, M. R. & MATTOSO, L. H. C. "A preliminary study of the incorporation of NPK fertilizer into chitosan nanoparticles." Express Polym. Lett., **4**: 509, 2010.

112.   LIU, R. & LAL, R. "Potentials of engineered nanoparticles as fertilizers for increasing agronomic productions." Sci. Total Environ., **514**: 131, 2015.

113.   XIAO, C. -Q.; CHI, R. -A.; HUANG, X. -H.; ZHANG, W. -X.; QIU, G. -Z. &WANG, D. -Z. "Optimization for rock phosphate solubilization by phosphate-solubilizing fungi isolated from phosphate mines." Ecol. Eng., **33**: 187, 2008.

114.   MITTAL, V.; SINGH, O.; NAYYAR, H.; KAUR, J. & TEWARI, R. "Stimulatory effect of phosphate-solubilizingfungal strains (Aspergillus awamori and Penicillium citrinum) on the yield of chickpea (Cicerarietinum L. cv. GPF2)." Soil Biol. Biochem., **40**:718, 2008.

115.   ALSTON, M. & CHIN, K. W. "Response of subterranean clover to rock phosphates as affected by particle size and depth of mixing in the soil." Aust. J. Exp. Agric. Anim. Husb., **14**: 649, 1974.

116.   KHASAWNEH, F. & DOLL, E. "The use of phosphate rock for direct application to soils." Adv. Agron., **30**: 159, 1979.

117.   WATKINSON, J. "Dissolution rate of phosphate rock particles having a wide range of sizes." Soil Res., **32**: 1009, 1994.

118.   MONTALVO, D.; MCLAUGHLIN, M. J. & DEGRYSE, F. "Efficacy of hydroxyapatite nanoparticles as phosphorus fertilizers in Andisols and Oxisols." Soil Sci. Soc. Am. J., **79**: 551, 2015.

119.LIU, R. Q. & LAL, R. "Synthetic apatite nanoparticles as a phosphorus fertilizer for soybean (Glycine max)." Sci. Rep., **4**: 5686, 2014.

120.   WANG, D.; BRADFORD, S. A.; HARVEY, R. W.; GAO, B.; CANG, L. & ZHOU, D. "Humic acid facilites the transport of ARS-labeled hydroxyapatite nanoparticles in iron oxyhydroxide-coated sand." Environ. Sci. Technol., **46**: 2738, 2012.

121.   MURPHY, J. & RILEY, J. P."A Modified Single Solution Method for the Determination of Phosphate in natural waters." Anal. Chim. Acta, **27**: 31, 1962

122.   WU, C. C.; HUANG, S. -T.;TSENG, T. -W.; RAO, Q. -L.& LIN, H. -C. "FT-IR and XRD investigations on sintered fluoridated hydroxyapatite composites." J. Mol.Struct., **979**: 72, 2010.

123.   SADAT-SHOJAI, M.; KHORASANI, M.-T. & JAMSHIDI, A. "Hydrothermal processing of hydroxyapatite nanoparticles—A Taguchi experimental design approach." J. Cryst. Growth, **361**: 73, 2012.

124.   ZUO, G.; WAN, Y.; MENG, X.; ZHAO, Q.; REN, K.; JIA, S. & WANG, J. "Synthesis and characterization of a lamellar hydroxyapatite/DNA monohybrid." Mater. Chem. Phys., **126**: 470, 2011.

125.   YE, F.; GUO, H. & ZHANG, H. "Biomimetic synthesis of oriented hydroxyapatite mediated by nonionic surfactants." Nanotechnology, **19**: 245605, 2008.

126.   ZUO, G.; LIU, C.; LUO, H.; HE, F.; LIANG, H.; WANG, J. & WAN, Y. "Synthesis of Intercalated Lamellar Hydroxyapatite/Gelatin Nanocomposite for Bone Substitute Application." J. Appl. Polym. Sci., **113**: 3089, 2009.

127.   GIROTO, A.; DE CAMPOS, A.; PEREIRA, E. I.; RIBEIRO, T. S.; MARCONCINI, J. M. & RIBEIRO, C. "Photoprotective effect of starch/montmorillonite composites on ultraviolet-induced degradation of herbicides." React. Funct. Polym., **93**: 156, 2015.

128.   GIROTO, A.; DE CAMPOS, A.; PEREIRA, E. I.; CRUZ,C. C. T.; MARCONCINI, J. M. & RIBEIRO, C. "Study of a nanocomposite starch-clay for slow-release of herbicides: Evidence of synergistic effects between the biodegradable matrix and exfoliated clay on herbicide release control." J. Appl. Polym. Sci., **131**: 41188, 2014.

129.   KOTTEGODA, N.; MUNAWEERA, I.; MADUSANKA, N. & KARUNARATNE, V."A green slow release fertilizer composition based on urea-modified hydroxyapatite nanoparticles encapsulated wood." Curr. Sci., **101**: 73, 2011.

130.van Raij, Fertilidade do solo e adubação. Piracicaba: Ceres (1991) 180-203.

131.   WU, L. & LIU, M. "Preparation and properties of chitosan-coated NPK compound fertilizer with controlled-release and water-retention." Carbohyd. Polym.,**72**: 240, 2008.

132.   AVEROUS, L. "Biodegradable multiphase systems based on plasticized starch: A review." J. Macromol. Sci.-Polym. Rev., **44**: 231, 2004.

133.   RITGER, P. L. & PEPPAS, N. A. "A simple equation for description of solute release I. fickian and non-fickian release from non-swellable devices in the form of slabs, spheres, cylinders or discs." J. Control. Release, **5**: 26, 1987.

134.   RITGER, P. L. & PEPPAS, N. A."A simple equation for description of solute release II. Fickian and anomalous release from swellable devices." J. Control. Release, **5**: 37:1987.

135.   LARA-CABEZAS, W. A. R.; TRIVELIN, P. C. O.; BENDASSOLLI, J. A. & GASCHO, G. J. "Calibration of a semi-open static collector for determination of ammonia volatilization from nitrogen fertilizers." Commun. Soil Sci. Plant Anal., **30**: 389, 1999.

136.   JAROSIEWICZ, A. & TOMASZEWSKA, M. "Controlled-release NPK fertilizer encapsulated by polymeric membranes." J. Agr. Food Chem., **51**: 413, 2003.

137.   GUO, M. Y.; LIU, M. Z.; ZHAN, F. L. & WU, L. "Preparation and properties of a slow-release membrane-encapsulated urea fertilizer with superabsorbent and moisture preservation." Ind. Eng. Chem. Res., **44**: 4206, 2005.

138.   EL-AILA, H. I.; EL-SAYED, S. A. A. & YASSEN, A. A. "Response of Spinach Plants to Nanoparticles Fertilizer and Foliar Application of Iron." Int. J. Environ., **4**: 181, 2015.

139.   ANSTOETZ, M.; ROSE, T. J.; CLARK, M. W.; YEE, L. H.; A. RAYMOND, C. A. & VANCOV, T. "Novel Applications for Oxalate-Phosphate-Amine Metal-Organic-Frameworks (OPA-MOFs): Can an Iron-Based OPA-MOF Be Used as Slow-Release Fertilizer?" PLoS ONE, **10**: 144, 2015.

140.   JUO, A. S. R. & FOX, R. L. "Phosphate sorption capacity of some benchmark soils in West Africa." Soil Sci., **124**: 370, 1977.

141.   BORGGAARD, O. K.; JORGENSEN, S. S.; MOBERG, J. P. & RABEN-LANGE, B. "Influence of organic matter on phosphate adsorption by aluminium and iron oxides in sandy soils." Eur. J. Soil Sci., **41**: 443, 1990.

142.   LI, X.; LI, Q.; XU, X.; SU, Y. YUE, Q. &GAO, B."Characterization, swelling and slow release properties of a new controlled release fertilizer based on wheat straw cellulose hydrogel." J. Taiwan Inst. Chem. Eng., **60**: 564, 2016.

143.   AKELAH, A. "Novel utilizations of conventional agrochemicals by controlled release formulations." Mater. Sci. Eng., **4**: 83, 1996.

144.   SHOJI, S.; DELGADO, J.; MOSIER, A. & MIURA, Y. "Use of controlled release fertilizers and nitrifcation inhibitors to increase nitrogen use efficiency and to conserve air and water quality." Commun. Soil Sci. Plant. Anal., **32**:1051, 2001.

145.	HUTCHINSON, C.; SIMONNE, E.; SOLANO, P.; MELDRUM, J. & LIVINGSTON-WAY, P. "Testing of controlled release fertilizer programs for seep irrigated Irish potato production." J. Plant. Nutr., **26**: 1709, 2002.

146.	NELSON, K. A.; PANIAGUA, S. M. & MOTAVALLI, P. P. "Effect of polymer coated urea, irrigation, and drainage on nitrogen utilization and yield of corn in a clay and soil." Agron. J., **101**: 681, 2009.

147.	NYBORG, M.; SOLBERG, E. D. & PAULY, D. G. "Controlled release of phosphorus fertilizers by small, frequent additions in water solution." Can. J. Soil Sci., **78**: 317, 1998.

148.	NI, B., LÜ, S. & LIU, M. "Novel multinurient fertilizer and its effect on slow release, water holding, and soil amending." Ind. Eng. Chem. Res., **51**: 12993, 2012.

149.	GUAN, Y.; SONG, C.; GAN, Y. & LI, F.-M. "Increased maize yield using slow-release attapulgite-coated fertilizers." Agron. Sustainable Dev., **34**: 657, 2014.

150.	GUO, M. Y.; LIU, M. Z.; LIANG, R. & NIU, A. Z. "Granular urea-formaldehyde slow-release fertilizer with superabsorbent and moisture reservation." J. Appl. Polym. Sci., **99**: 3230, 2006.

151.	SHAVIT, V.; REISS, M. & SHAVIV, A. "Wetting mechanisms of gel-based controlled-release fertilizers." J. Control. Release, **88**: 71, 2002.

152.	SHAHEEN, S. M.; CHRISTOS, D. T. & ESKRIDGE, K. M. "Effect of common ions on phosphorus sorption and lability in greekalfsols with different pH. "Soil Sci. **174**: 21, 2009.

153.	BREMNER, J. M. Nitrogen Total in Methods of soil analysis, Part 3. (eds Sparks, D. L. et al.) 1085–1121 (SSSA and ASA, 1996).

154.	ALVAREZ, V. V. H.; NOVAIS, R. F.; DIAS, L. E. & OLIVEIRA, J. A. "Determinação e uso do fósforo remanescente." Bol. Inf. Soc. Bras. Ci. Solo, **25**: 27, 2000.

155.	BREMNER, J. M. & DOUGLAS, L. A. "Inhibition of urease activity in soils." Soil Biol. Biochem., **3**: 297, 1971.

156.	QUAGGIO, J. A. & RAIJ, B. van. "Determinação do pH em cloreto de cálcio e da acidez total in Análise química para avaliação da fertilidade de solos tropicais (edsRaij, B. van, Andrade, J. C., Cantarella, H. & Quaggio, J. A.) 181–188, 2001.

157.   FIRESTONE, M. K. Biological denitrifcation in Nitrogen in agricultural soils (eds Stevenson, F. J., Bremner, J. M., Hauck, R. D., & Keeney, D. R.) 289–326 (Madison, American Society of Agronomy), 1982.

158.   NOVAIS, R. F. & MELLO, J. W. V. Relação solo-planta in *Fertilidade do solo*. (eds Novais, R. F., Alvarez, V. H., Barros, N. F. Fontes, R. L. F., Cantarutti, R. B., Neves, J. C. L., Eds) 276–374, 2007).

159.   MOTTA, P. E. F.; CURI, N.; SIQUEIRA, J. O.; VAN RAIJ, B.; FURTINI NETO, A. E. & LIMA, J. M. "Adsorção e formas de fósforo em latossolos:influência da mineralogia e histórico de uso. "R. Bras. Ci. Solo, **26**: 349, 2002.

160.   OVERREIN, L. N. & MOE, P. G. "Factors affecting urea hydrolysis and ammonia volatilization in soil. "Soil Sci. Soc. Am. J., **31**: 57, 1967.

161.   KISSEL, D. E.; CABRERA, M. L. & FERGUSON, R. B. "Reactions of ammonia and urea hydrolysis products with soil." Soil Sci. Soc. Am. J., **52**: 1793, 1988.

162.   RODRIGUES, M. B. & KIEHL, J. C. "Distribuição e nitrifcação da amônia proveniente da uréia aplicada ao solo. "Rev. Bras. Ciênc. Solo, **16**: 403, 1992.